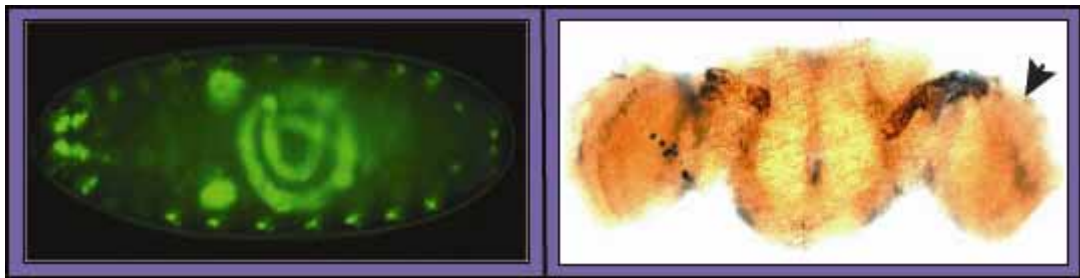




***optomotor-blind* and the Horizontal and Vertical System cells of the *Drosophila* optic lobes: Molecular and laser ablation studies**



Dissertation

zur Erlangung des Grades
Doktor der Naturwissenschaften

am Fachbereich Biologie
der Johannes Gutenberg- Universität
in Mainz

Vorgelegt von
Aditya Sen
geb. in Burdwan, Indien

Mainz, January 2006

Table of Contents

Pages

1. Introduction

1 – 17

1.1	<i>Development of embryonic and larval visual system</i>	1
1.2	<i>Optic lobe (OL) and optic lobe anlagen (OLA)</i>	3
1.3	<i>HS/VS neurons in the fly visual system</i>	4
1.4	<i>Identification of cell lineages in the fly visual system</i>	5
1.5	<i>Laser ablation and laser heat shock: physical principles</i>	5
1.6	<i>Laser ablation and laser heat shock: applications in C. elegans, Drosophila and Musca</i>	9
1.7	<i>Characterization of OMB target site specificity in vitro</i>	12
1.8	<i>Genetic and molecular characterisation of lethal optomotor blind (omb) mutants</i>	14
1.9	<i>Objectives of the study</i>	17

2. Materials and Methods

18 - 37

2.1	<i>Chemicals, enzymes, and kits</i>	18
2.2	<i>Buffers and stock solutions</i>	18
2.3	<i>Laser ablation .</i>	19
2.4	<i>Larval olfactory tests</i>	21
2.5	<i>Whole mount X-gal staining of Drosophila larva and embryo</i>	23
2.6	<i>Whole mount X-gal staining of eye-brain complex (EB) of Drosophila</i>	24
2.7	<i>Drosophila melanogaster stocks and crosses</i>	24
2.8	<i>Purification (recombination) of the stock l(1)omb[12]/ FM7a,</i>	25
2.9	<i>Genomic DNA isolation</i>	26
2.10	<i>PCR amplification of omb locus</i>	27
2.11	<i>Sequencing of the amplified products</i>	27
2.12	<i>Introduction of a A508V mutation into the OMB T-domain</i>	28
2.13	<i>Cloning, expression, and purification of wild type and mutant OMB-T (T-domain from OMB) clones</i>	30

2.14 <i>In vitro</i> target site selection (SELEX)	34
2.15 Electrophoresis mobility shift assay (EMSA)	36

3. Results **38 – 74**

3.1 Ablation of larval olfactory organ and behavioural experiments	38
3.2 Bolwig's organ (BO) as a test system for the analysis of the specificity and efficiency of ablation	48
3.3 Ablations within the embryonic / larval optic lobe anlage	52
3.4 Standardization of SELEX for the determination of OMB target selectivity	60
3.5 Genetic and molecular characterization of lethal omb mutant lines	64

4. Discussion **75 – 82**

4.1 AMCs in larval olfaction	75
4.2 Presence of precursor cell(s) for HS/VS neurons in the embryonic optic lobe anlagen	75
4.3 Mutation in evolutionary conserved residues	76
4.4 Consequences for OMB DNA binding affinity of the <i>l(1) omb¹³</i> mutation	78
4.5 Mutation in the lethal <i>l(1) omb¹⁵</i> allele	81
4.6 Cause of lethality in <i>l(1) omb¹¹</i> and <i>l(1) omb¹²</i> lethal omb mutants	82

5. Summary-Zusammenfassung **83-86**

6. References **87-94**

7. Appendix **95-119**

Appendix 1: Set up and specifications of laser unit	95
Appendix 2: Locations of primers in genomic DNA fragment covering omb region	97
Appendix 3: Detail about the primers used for amplification and/or sequencing of the omb locus	100
Appendix 4: Detail about the primers used for different experiments	101
Appendix 5: Suspected mutations in four lethal omb mutant lines	102
Appendix 6: Fly stocks used in the experiments	104

<i>Appendix 7: Established fly stocks of lethal omb mutant containing duplication over the In(2LR) Gla,Bc-chromosome</i>	107
<i>Appendix 8: Genetic characterization of lethal omb mutants</i>	108
<i>Appendix 9: Alignment of OMB with other T-box proteins</i>	110
<i>Appendix 10: Sequence of omb cDNA along with the translated protein sequence</i>	117
8. Acknowledgements	120
9. Curriculum vita	121
10. Erklärung	122

1. Introduction

1.1 Development of the embryonic and larval visual system in *Drosophila*

The complex mechanism and pathways by which the *Drosophila* visual system develops was described well by electron-microscopic and BrdU incorporation studies (Green, Hartenstein et al. 1993). The studies on the identification of the larval visual system of Dipteran flies started at the beginning of the 20th century where the dorsal organ was confused as larval eye. But the identification of the real larval eye came from Bolwig's study in house fly larvae (Bolwig 1946). The larval eye in *Drosophila* today is named as Bolwig's organ (Steller, Fischbach et al. 1987). The development of larval visual system significantly varies from that of central and peripheral nervous system. In CNS and PNS, development of axon tracks are determined by axonal growth and selective migration, whereas Bolwig's Organ (BO) makes its initial contacts of the pioneer axons by relocating itself near to the target cells. The optic lobe and Bolwig's organ develop by invagination from the posterior procephalic region (PPR). At stage 11, the cells of the lateral part of PPR form the optic lobe placode which subsequently invaginates during stage 12 and 13. During these stages, the invaginated optic lobe placode forms a pouch containing about 85 cells and loses contact with the outer surface of the embryo and becomes attached to the lateral part of the developing brain as optic lobe. Until early stage 13, the cells which will subsequently form Bolwig's organ are morphologically distinguishable at the ventral tip of the optic lobe placoid and can be detected by expression of Krüppel protein (Hartenstein 1988; Schmucker, Taubert et al. 1992; Green, Hartenstein et al. 1993) and form a cluster of 12 cells located in one plane. In later stages, cells in Bolwig's organ start differentiation and during head involution the whole group of differentiated neurons slides out of the head epidermis and attach themselves to the dorsal pouch arching over the pharynx. But the relation between relocation of BO to the anterior position and the process of head involution are not clear. Analysis of mutations, which affects the anterior relocation of BO, suggested that head involution and migration of BO may be separable from each other (Holmes, Raper et al. 1998). A schematic diagram of the whole process of visual system development is shown in figure 1.1.

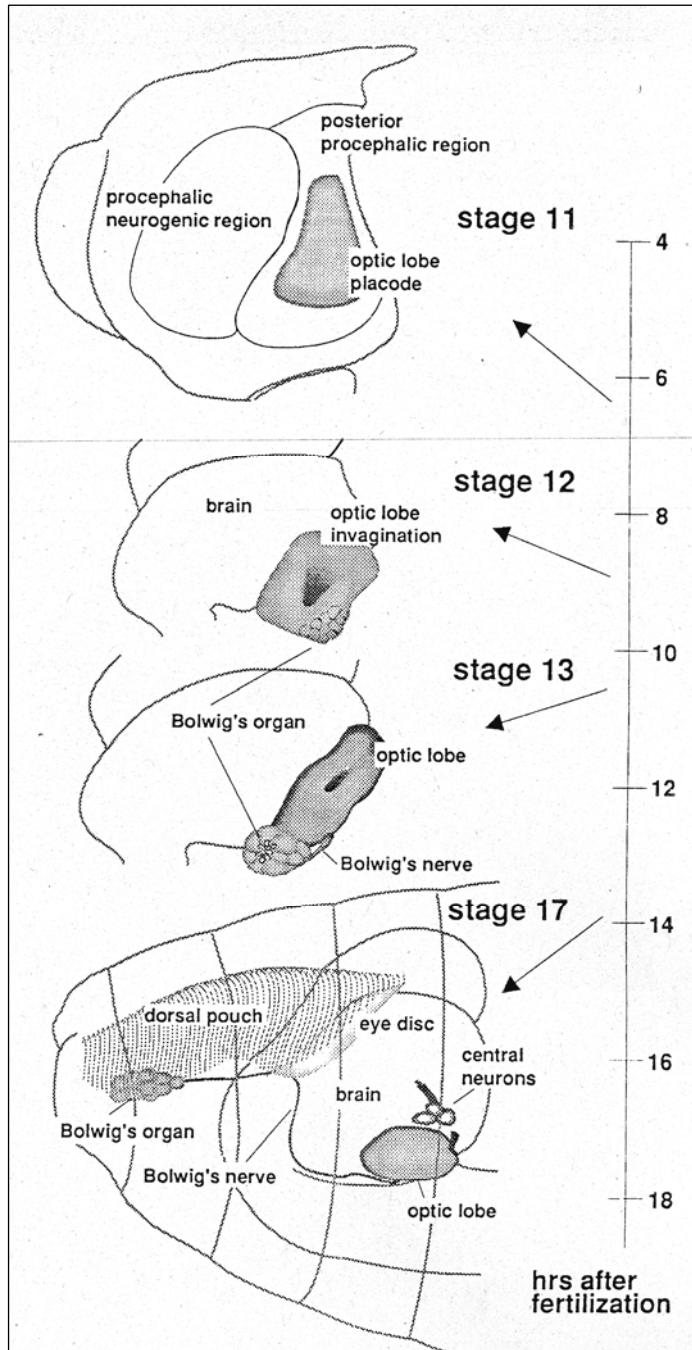


Figure 1.1: Schematic representation of embryonic development of the *Drosophila* visual system. Lateral views of the anterior end are shown in four different stages (time scale on the right hand side of the figure). (Green, Hartenstein et al. 1993)

1.2 Optic lobe (OL) and optic lobe anlagen (OLA):

The structural complexity of the visual system of *Drosophila melanogaster* starts at the very early stages of development. Each of the compound eyes in the adult fly consists of about 800 ommatidia and each ommatidium contains 8 photoreceptor cells. These photoreceptor cells project in a retinotopic manner to deeper neuropil areas. These photoreceptor cells receive the image information from external visual field and transduce them to neurons present in the corresponding neuropil areas. The outermost neuropil, the lamina, is situated just below the retina. The lamina is followed by the medulla and lobula complex. The innermost neuropil i.e., lobula complex, is split into two distinct neuropils, the lobula and lobula plate. The total number of neurons as well as the types varies within the neuropil regions (Pflugfelder and Heisenberg 1995). A schematic diagram of the *Drosophila* brain representing different retinula cells and optic neuropils is shown in figure 1.2.

The embryonic origin of all the components of the adult visual system is the embryonic optic lobe placode which gives rise to the larval eye imaginal disc as well as the larval optic lobe (Jurgens, Lehmann et al. 1986; Meinertzhagen and Hanson 1993). The optic lobe anlagen (OLA), a group of about 70 cells, is derived from the embryonic optic lobe at hatching. A small group of cells, which detaches from the main body of the optic lobe, forms the inner optic anlagen and the main body itself forms the outer optic anlagen (Green, Hartenstein et al. 1993).

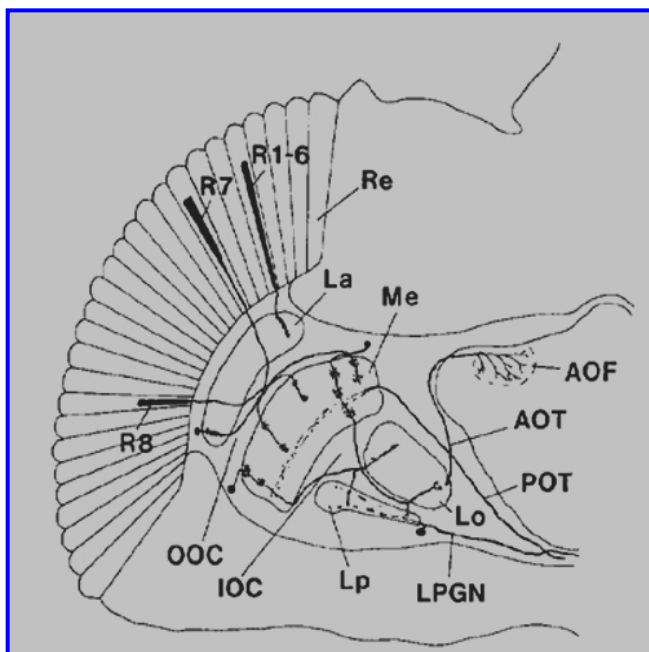


Figure 1.2: Schematic representation of a horizontal section through a *Drosophila* brain (left half). Three types of retinula cells, e.g. R1-6, R7 and R8 receive visual information from the retina (Re) and pass them to the neuropils. R1-6 go upto lamina (La) whereas, R7, R8 and other interneurons pass through the outer optic chiasm (OOC) to the inner neuropils [medulla (Me), lobula (Lo) and lobula plate (Lp)] which are connected by inner optic chiasm (IOC). Anterior optic tract (AOT) connects lobula to the anterior optic focus (AOF) and each lobula plate giant neuron (LPGN) project from Lp to the central brain [Adopted from (Pflugfelder and Heisenberg 1995)]

1.3 HS/VS neurons in the fly visual system:

The lobula plate tangential cells in the fly visual system are critical constituents of the visual information centre in the fly brain. The total number of about 60 individual tangential cells was grouped into a number of families of which three groups, i.e. CH (centrifugal horizontal), HS (horizontal system) and VS (vertical system) have been well studied regarding their arborisation patterns in the lobula plate and their specific response to visual field motion (Pierantoni 1976). Based on the dendritic arborisation patterns in the lobula plate, the HS system was divided into HS north (HSN), HS equatorial (HSE), and HS south (HSS) [see figure 1.3]. In recent years, the visual response properties of these tangential neurons were studied using intracellular recordings and computer simulations (Krapp and Hengstenberg 1996; Haag, Theunissen et al. 1997; Haag, Vermeulen et al. 1999; Scott, Raabe et al. 2002) and these studies clearly show that the CH as well as the HS cells preferentially respond to horizontal image motions and VS cells plays role in vertical motion detection. The role of HS and VS cells in visual orientation behaviour were initially evident from the abnormal optomotor behaviour of the H31 mutant from *Drosophila* which lacks a set of giant fibres in the lobula plate (Heisenberg 1972; Heisenberg 1975). Further evidence came from the studies by Geiger and Nässel in the house fly (Geiger and Nassel 1981) where unilateral ablation of precursor cells of adult HS/VS cells at an early developmental stage by laser microbeam altered the visual orientation behaviour. The complex overlapping patterns of the HS and VS cells were visualized in individual clones by the MARCM technique (Scott, Raabe et al. 2002).

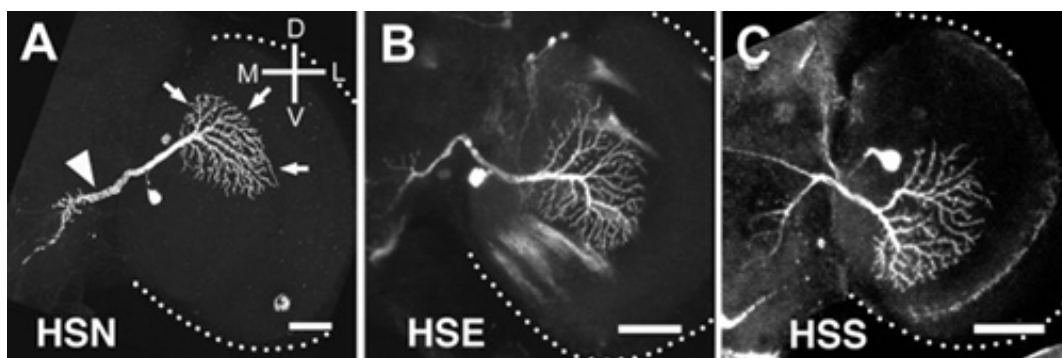


Figure 1.3: Single cell clones of HS neurons. HSN (A), HSE (B) and HSS (C) show dendritic arborisation patterns to the dorsal, dorso-ventral and ventral sides of the lobula plate respectively (Scott, Raabe et al. 2002).

1.4 Identification of cell lineages in the fly visual system:

The historical background of the study of cell lineages development have been described by Stent (Stent 1987; Stent 1998). The studies began in the 1870s with Ernst Haeckel's controversial 'biogenetic law' which implies that in animal development the cells of early embryos recapitulate the non-differentiated tissues of a remote, sponge-like ancestor. But this hypothesis was contradicted by other scientists who suggested that differentiated properties that characterize a given cell of post-embryonic animal are causally linked with the cell's developmental line of descent (Maienschein 1972). In the 1970s, the interest in the developmental role of cell lineage revived. Introduction of novel techniques such as direct observation of embryogenesis using differential interference optics (Sulston, Schierenberg et al. 1983; White, Amos et al. 1987), generation of mosaic embryos (Garcia-Bellido and Merriam 1969), laser ablation techniques (Sulston, Albertson et al. 1980) and embryonic cell labelling with intracellular lineage tracer (Weisblat, Sawyer et al. 1978; Weisblat, Harper et al. 1980) helped in revealing the line of descent of single cells. Use of these novel techniques showed that the developmental process is highly determinate in simple invertebrates whereas it is indeterminate in the early stage of embryonic development in vertebrates.

1.5 Laser ablation and laser heat shock: physical principles:

1.5.1 Laser: its nature and action in the cell

The word Laser stands for "Light Amplification by Stimulated Emission of Radiation." Stimulated emission of radiation occurs when an electron is already present in an excited state, and then an incoming photon for which the quantum energy is equal to the energy difference between the excited level and the ground level of that of the existing electron can stimulate a transition of the electron to the ground level by producing a second photon of the same energy. When the number of excited electron present at the time of stimulation is high, stimulated emission of multiple photons having definite phase relationship is possible and which in turn produce a coherent, collimated and monochromatic amplified light called 'LASER'. A schematic outline of laser production is depicted in figure 1.4.

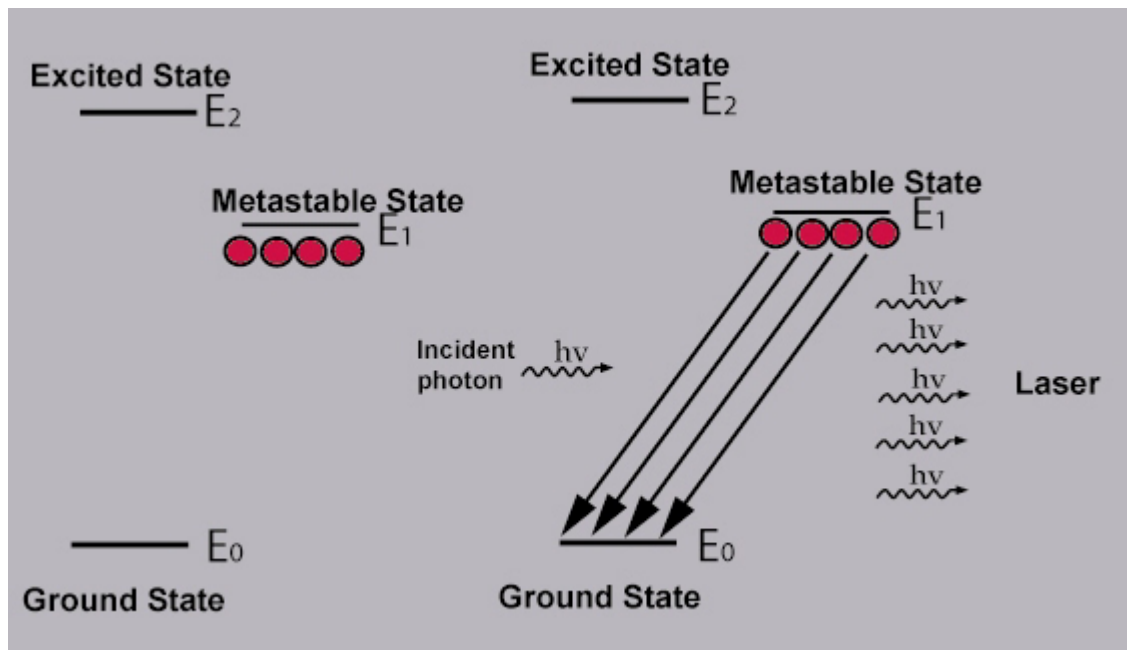


Figure 1.4: The principle of laser. Population inversion mechanism helps to maintain a substantial amount of molecule in metastable state. When the energy of a incident photon, $E_n = E_1 - E_0$, stimulated emission of coherent radiation is produced.

The main difference between laser light and normal light lies in the unique method of generation of light which confers the unique properties of laser light being a **coherent** i.e., phase relationship is maintained over long enough time to be useful; **monochromatic**, i.e. light consists of one wavelength; and **collimated**, i.e., beams are very narrow and spread very less and hence, the energy density of laser light is much more than that of the normal light. The wavelength of laser may vary from UV to infrared region and one can choose the wavelength according to the need.

The principle behind laser ablation and laser heat shock is that the energy carried out by the laser beam is transferred to a particular cell or a group of cells causes them either to be destroyed (ablated) or to be heated enough to undergo a 'heat shock'. But the occurrence of these two events, i.e., 'heat shock' and 'ablation' depends on the nature of the laser and its application. For instance, high energy laser might not be able to produce a heat shock when it is applied in quick pulses and it was reported that an attenuated dose of laser is able to induce *lacZ* expression by activating a heat shock promoter, but a quick and high energy laser is not able to do the same (Stringham and Candido 1993). Results also suggest that

sensitivity to laser may be cell-type dependent e.g., laser treatment for 8 to 10 minutes is required to induce *lacZ* in PC71ubIn4 cells, whereas treatment for 4 minutes is sufficient for the equivalent level of induction in PC72ubIn5 cells. In a typical cell ablation experiment it was found that an unattenuated laser can damage a cell quickly without being lethal to the whole organism (Stringham and Candido 1993). So, during laser ablation a number of factors, e.g. laser energy, frequency of pulse, number of pulse, cell type etc., should be taken into account. A proposed pathway depicting how laser ablation works is presented in figure 1.5.

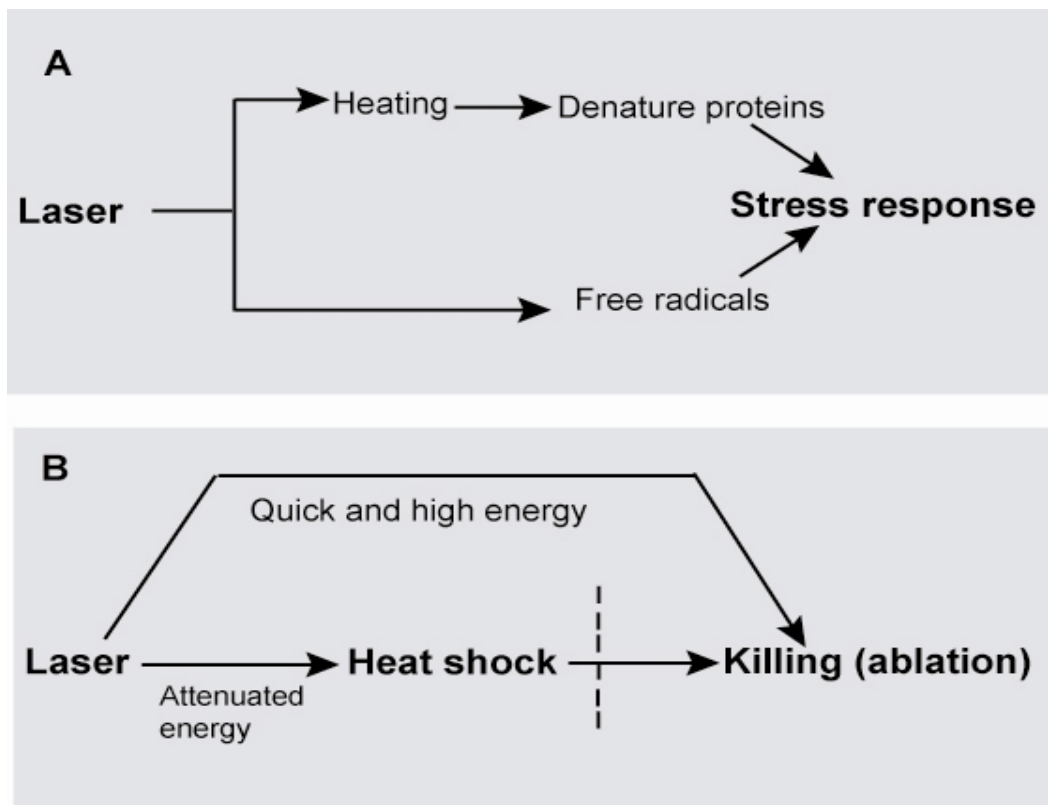


Figure 1.5: Proposed pathways of laser ablation. A: Laser might induce stress response by denaturation of protein or by production of free radicals in the cell as proposed by (Ananthan, Goldberg et al. 1986). B: Laser heat shock vs. laser ablation

1.5.2 How laser ablation works:

Bargmann and Avery (Bargmann and Avery 1995) have described the physical principle and theory behind laser ablation. When a laser microbeam is fired at a cell, three main events happen in a sequence: **energy deposition** in the cell, followed by **transport** of energy to the surrounding cells, followed by energy-induced **damage**. Although the

mechanisms of energy deposition and transport are known to some extent, very little is known about how laser energy damages the cells.

Energy deposition:

The deposition of energy occurs in two major ways. The first and most obvious mechanism of energy deposition is the direct absorption of laser energy. The light enters the specimen from above in a broad symmetrical cone. The Energy deposition in the specimen depends, firstly, on the linearity of absorption, e.g. if source is 440nm and specimen absorb better at 220, then two photons will be absorbed at sufficient light intensities, and as the **two-photon absorption** (in the above case) goes as the square of the light intensities, energy deposition by this mechanism goes down as the inverse fourth power of distance from the focus. The second mechanism for energy deposition is mechanical and this is due to the refractive index gradients within the cell nucleoplasm and cytoplasm which actually convert the momentum of light into mechanical twist within the particles.

The final effect of either direct absorption of photon or **refractive compression** is increased pressure and temperature and the mechanisms are based on the thermodynamic principles. The absorption of photon directly increases the temperature which in turn increase the pressure and on the other hand refractive compression increases the pressure and work done in compression is partially converted into heat

Transport:

This event is not at all desired from the preciseness (of ablation) point of view. In this process, the energy deposited in the targeted area moves away to the surrounding cells and causes damage to them. The mechanical energy is transported away from the beam of focus either by sound waves or by supersonic shock waves and these waves may be spherical (for symmetrical waves) or pressure jet (for nonsymmetrical waves). Heat energy is transported by diffusion. The rate of diffusion and temperature elevation depends on the mode of heat deposition. When heat is deposited for a long time, heat diffusion away from the point of source will reach a steady state and the temperature increase is inversely proportional to distance from the source. On the other hand, in case of quick pulse, the heat diffusion won't be steady and the temperature at a distance will reach a peak and then decrease and the peak temperature increase is proportional to the inverse cube of distance from the source.

1.6 Laser ablation and laser heat shock: applications in *C. elegans*, *Drosophila* and *Musca*:

1.6.1 An overview:

Applications of laser ablation and laser heat shock have become an uprising era in modern developmental biology. These two techniques have been used to explore some eminent fields in modern cell biology which includes cell lineage tracing, individual cell function, cell-cell interaction, cell signalling, somatic mosaicism etc. In the field of developmental biology of both animal and plants, transgenic organisms have also played a vital role. The tissue- or cell- or time-specific expression of transgenes is limited by certain factors like availability of tissue specific promoters or other regulatory elements. The induction of these genetic elements is, sometimes, governed by external cues like temperature, nutrients etc. The laser heat shock technique has not only advanced the existing scope and method of ectopic transgene expression (Gibson, Golub et al. 1991; Brand, Manoukian et al. 1994), it also may increase the preciseness of the application which allows us to target a particular cell or a group of cells without affecting the others. In standard heat shock experiments, where expression is not targeted by a tissue specific promoter, expression throughout the organism is the prominent feature (Figure 1.6). But introduction of laser heat shock among the experimental approaches has helped to overcome that barrier. In the following subsections we will discuss how laser ablation and laser heat shock were applied to understand different developmental processes and molecular mechanisms in different organisms.

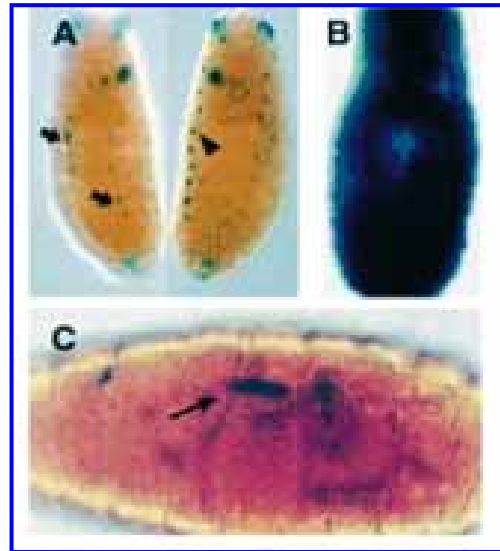


Figure 1.6: Induction of heat shock in *hsp26-lacZ* embryos. A: control embryos, maintained at 18°C without heat shock; dorsal view (right) shows expression along the tracheal trunk (arrow head); ventral view (left) shows expression along the edge of CNS, but not within it (thick arrow). B: standard heat shock in incubator. C: laser heat shock ; β -galactosidase expression in a single ventral somatic muscle fibre (arrow) (Halfon, Kose et al. 1997)

1.6.2 Applications in *Caenorhabditis elegans*: The role of a cell can be studied by its elimination and the observation of the subsequent developmental and behavioural abnormalities in the organism. In *C. elegans*, this is usually done by selective killing of a cell or group of cells of interest by

applying laser microbeam. This technique has been used to infer the developmental role of cells in embryos and larvae and was also very useful to determine the functions of different cell types, including neurons involved in locomotion, feeding, mechanosensation, and chemosensation (Chalfie, Sulston et al. 1985; Avery and Horvitz 1989; Bargmann and Horvitz 1991; Bargmann 1993) in the adults.

Laser ablation can be used to learn how cells interact with each other during development. Signalling and inductive interactions can be

examined by killing the precursor cells at an early stage and observe the development of others in later stages. Working in this direction Kimble and White (Kimble and White 1981) showed that killing the distal tip cells of the somatic gonad causes premature differentiation of germ line and providing evidence for soma to germline cell-cell interaction for the first time. The precise **soma-germline cell** interactions in *C. elegans* hermaphrodite germline development has been well established by (McCarter, Bartlett et al. 1997) and they have shown that ablation of both sheath/ spermatheca precursor (SS) cells in a gonad arm at the L2/L3 molt eliminates the entire sheath as well as 18 spermathecal cells (figure 1.7) from the gonad arm.

Laser ablation has also been used in the study of **cellular morphogenesis**. In *C. elegans* the epithelial morphogenetic movements, which includes spreading, invagination, extension and fusion or detachments of epithelia, are accomplished by changes in cell shape. These

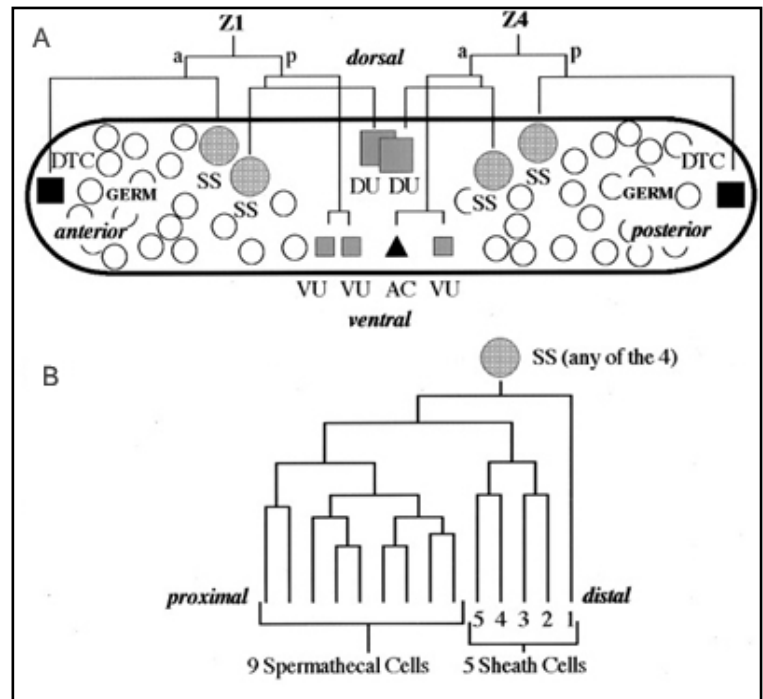


Figure 1.7: A: Schematic of the gonad somatic primordium after L2 reorganization. the lineage giving rise to each somatic cell from Z1 and Z4 is shown.

B: the lineage arising from each sheath/spermatheca (SS) precursor cell generates 9 spermathecal and 5 sheath cells (McCarter, Bartlett et al. 1997)

events in cellular morphogenesis are coordinated by the interactions among the cells and the surrounding matrix and cytoskeleton and have been described with single cell resolution. Roles of individual cells have been demonstrated by cell ablation experiments (Chin-Sang and Chisholm 2000).

As mentioned earlier, laser ablation is useful in the determination **of neuronal function in locomotion**. The function of some of the 26 GABAergic neurons in *C.elegans* has been determined by selective killing of these cells with a laser microbeam (McIntire, Jorgensen et al. 1993). In this study they have shown, for example, how the laser killing of DD and VD neurons affects the sinusoidal body wave during locomotion. The typical **feeding behaviour** of *C. elegans* has also been analyzed with laser ablation (Avery 1993). It has been shown that M3 and neuron 15 influence the timing of pharyngeal muscle motion. Laser killing can also assist in the **interpretation of mutant phenotype** and help to correlate the gene function with a particular phenotype. Genes that affects the cells may be identified by isolating mutants with phenotypes similar to cell killing (Ferguson and Horvitz 1985).

1.6.3 Laser ablation and laser heat shock in *Drosophila* and *Musca*:

Phenocopy induction:

The term ‘Phenocopy’, coined by Goldschmidt (Goldschmidt 1935), describes mutant-like morphological alterations that could be induced by stress inducing agents or conditions. Although, (Mitchell and Lipps 1978) did not used laser to induce the heat shock in their phenocopy induction studies, the research opened up a wide ranging scope for the use of laser as a condition to induce stress.

Study the Visual orientation behaviour of housefly (Geiger and Nässel, 1981):

In their study they have shown that laser ablation of the presumptive of HS / VS precursor cell in one of the adult optic lobes could change the visual orientation behaviour in adult flies. They also studied different structural abnormalities in the ablated side as compared to the normal side of the lobular plate in the brain section and established the specific role of HS and VS giant neurons in background motion detection rather than playing role in orientation towards single objects.

Induction of site specific recombination and generation of mosaic:

The process of site-directed homologous recombination has been studied intensively using yeast as a model system. This process, after modifications, has been used for genetic manipulation in many higher eukaryotes. In *Drosophila melanogaster*, the inducible site specific recombination using the conventional yeast FRT-FLP system has been used to produce somatic mosaics (Golic and Lindquist 1989) In this study, FLP recombinase (FLP) was expressed under the control of the hsp70 promoter and the recombination process was induced by heat shock. Laser may be a way of providing a localized heat shock.

Targeted gene expression without tissue specific promoter:

The scope of laser ablation in this regard has been already mentioned at the beginning of this section. In their studies, (Halfon, Kose et al. 1997) showed 1 to 2 minutes of laser treatment of individual cell from a varieties of tissues was able to induce heat shock (Figure 1.8) and that could be measured by β -galactosidase expression of a *hsp26-lacZ* reporter construct or by of UAS target gene expression after induction of *hsGal4*.

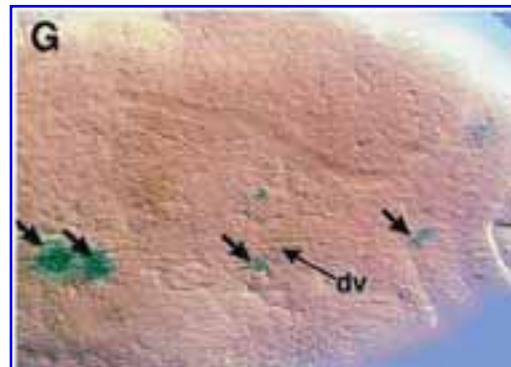


Figure 1.8: Laser heat shock induction of UAS-lacZ target gene in specific single cell: cells in the dorsal vessel were targeted (thick arrows) (Halfon, Kose et al. 1997)

1.7 Characterization of OMB target site specificity *in vitro*

T-domain proteins are important developmental regulatory transcription factors. To obtain a better understanding of their action, knowledge of their target genes is highly desirable. Three different general approaches can be taken. One starts with the elucidation of target site specificity, the other tries to identify genes whose expression is affected by loss- or

gain-of-function of the relevant transcription factor. Lastly, chromosomal binding positions can be identified.

In the first approach, either the regulatory regions of candidate target genes are carefully analysed ("promoter crunching") or it is attempted to identify the binding site preference in a more global way (SAAB). In the second approach, gene transcription is followed individually or globally (e. g. by Northern blot, qRT-PCR, subtractive hybridization, differential display, serial analysis of gene expression (SAGE), microarray hybridization). In the third approach, chromosomal binding sites of transcription factors can be identified at a resolution of a few kb [Chromatin Immune Precipitation (ChIP) or Dam methylase identification (DamID)]. While the first approach directly identifies potential target sites (without information on target genes), the latter two identify potential target genes (without information on target sites). In all three approaches, bioinformatic tools are required to identify target sites AND target genes (Taverner, Smith et al. 2004).

B. Herrmann and colleagues were the first to identify potential T-domain target sites *in vitro* using a SAAB protocol and the mouse Brachyury protein (Kispert and Herrmann 1993). SAAB (selected and amplified binding site analysis) was introduced under various acronyms by several authors in the early 1990s (Blackwell and Weintraub 1990; Pollock and Treisman 1990; Thiesen and Bach 1990). Kispert et al. identified a target consensus in which two slightly degenerate half sites were combined to form a palindrome. S. Grimm (1997) performed a similar analysis for OMB and selected targets that were related to the Bra consensus palindrome in that the same half sites were selected. They occurred, however, preferentially as direct repeats or as everted palindromes with a central 4 bp spacer (Grimm 1997).

In both cases, the selection experiment was performed with oligonucleotides containing a 26 bp degenerate core. Given the fact that a half site encompasses already 10 bp, other arrangements of half sites (e. g. with an 8 bp central spacer would be excluded from the analysis). I, therefore, established a selection system based on DNA fragments containing a 46 bp degenerate core. This should allow the selection of more spacious arrangements than was previously possible. Following the SAGE-like strategy of Roulet et al. (2002), the region of degeneracy was flanked by restriction sites such that degenerate cores could be excised from the selected fragments, concatenated *in vitro*, cloned, and sequenced (Roulet, Busso et al. 2002) (see Materials and Methods).

1.8 Genetic and molecular characterisation of lethal *optomotor blind* (*omb*) mutants

1.8.1 An overview of the *omb* gene:

The *optomotor blind* (*omb*) gene plays vital roles in different developmental processes in *Drosophila melanogaster*. The pleiotropic nature of *omb* is evident from the occurrence of several defects in different developmental processes in *omb* mutants. The defects due to mutations in *omb* range from altered brain morphology, specially in optic lobe development, altered wing morphology [bifid (*bi*)] and increased abdominal pigmentation [Quadroon(*Qd*)] (Pflugfelder and Heisenberg 1995) to complete lethality. Recently, it has also been found that variations in *omb* nucleotide sequence contribute to abdominal pigmentation variations in *D. polymorpha*. It has been found that nucleotide variations, which includes length variation due to asparagines (N) runs as well as amino acid change, in N-terminal region of *omb* in *D. polymorpha* is responsible for abdominal pigmentation variations (Brisson, Templeton et al. 2004). These wide ranges of phenotypic abnormalities in *omb* mutants depict its vital role in complex developmental network in *Drosophila melanogaster* and related species. The first molecularly characterized mutant *In(1)omb^{H31}*, a recessive and viable allele, exhibits aberrant optomotor behaviour in adult flies and structural defects in the brain. These defects include an apparent loss of a subset of lobula plate giant neurons (LPGNs) called HS and VS neuron along with loss of M-fibres and a reduction in volume of the lobula plate (Heisenberg 1978). A number of lethal *omb* alleles have been isolated (Pflugfelder, unpublished). To understand the reasons for their insufficiency, one needs to know the underlying molecular defects.

1.8.2 Optomotor blind gene locus:

1.8.2.1 Cytological localization of *omb*:

The complex nature of *optomotor blind* gene was described by Pflugfelder et al. (Pflugfelder, Schwarz et al. 1990). The *omb* gene locus is located in chromosome region 4BC in the genome of *Drosophila melanogaster*. It was first localized with respect to seven other genes in that region (Banga, Bloomquist et al. 1986) and further specific studies on that region set up the proximal and the distal limit for *omb* (Oliver, Perrimon et

al. 1987). *Ruby*, a *Drosophila* gene involved in photoreceptor pigment granule morphogenesis, has been placed proximal to *omb* and on the other hand molecular studies placed *no receptor potential A (norpA)*, which is associated with the calcium-mediated signalling pathway, on its distal side. Lethal mutations in the *omb* complementation unit uncovered three other mutations affecting wing morphology (*bi*), wing reflectance (*lac*) and abdominal pigmentation (*Qd*).

1.8.2.2 Structure of *omb* locus:

A schematic diagram of the *omb* locus is shown in figure 1.9. The transcription unit of *omb* is flanked by upstream and downstream regulatory elements. Several P-element insertions are present in the upstream regulatory region. The entire downstream regulatory region, the optic lobe regulatory region (OLR), is divided into three subdomains based on deletion and inversion breakpoints. They are designated as OLR1, OLR2 and OLR3. The first isolated *omb* mutant line *In(1)omb^{H31}* which lacks the HS/VS cells in the adult optic lobe is an inversion mutant devoid of OLR2 and OLR3. But the heteroallelic combination (*Df(1)rb5/In(1)omb^{H31}*), where OLR3 is absent, shows a reduced number of fibres in the anterior tract (Brunner, Wolf et al. 1992; Pflugfelder and Heisenberg 1995). Loss of entire OLR leads to more severe abnormality in the optic lobe.

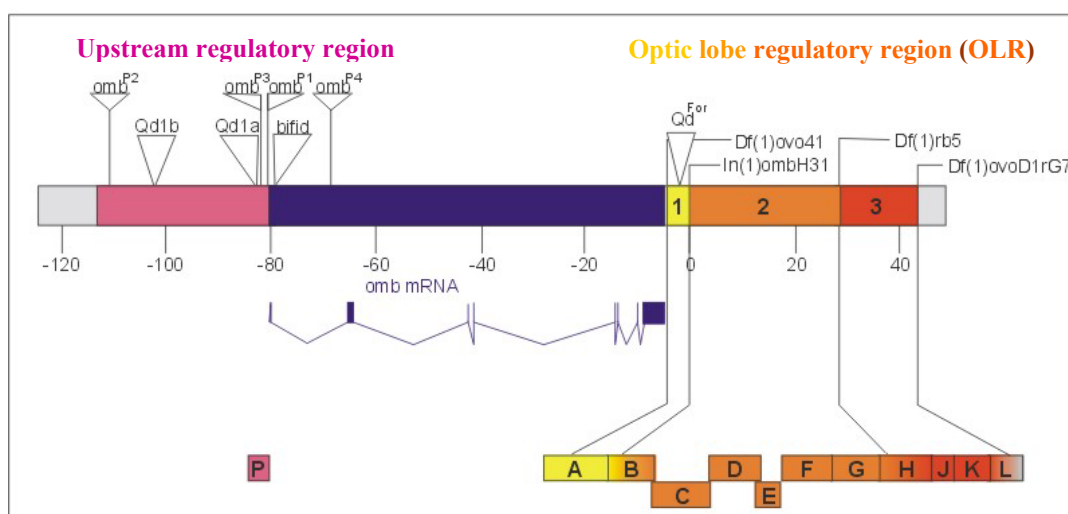


Figure 1.9: Schematic diagram of the *omb* locus. P-element insertion sites, breakpoints of inversions and deficiencies are indicated. Transcription unit was labelled in Blue, upstream regulatory region labelled in pink adopted from (Hofmeyer 2001)

1.8.2.3 Omb lethal alleles:

Lethal mutations in optomotor blind [*l(l)omb*], a complementation unit at the core of the *omb* locus, cause larval and pupal lethality. Phenotype adults rescued from hemizygous lethal male pupal case show severe malformation in optic lobe development. *l(l)omb* alleles e.g. *l(l)omb*²⁸², *l(l)omb*³¹⁹⁸, *l(l) bi*^{D4} etc. fail to complement the viable *In(l)omb*^{H31} and also do not complement the viable mutants *bi* and *Qd* (Pflugfelder, Roth et al. 1992).

1.8.3 The T-box gene family and the Optomotor blind Protein (OMB):

The T-Box genes encode a family of transcriptional regulators which play an important role in a wide range of biological functions in vertebrate as well as invertebrate organisms. The first gene discovered in this family, mouse *Brachyury (Bra)* also called *T* plays a crucial role in mesoderm and notochord development. So far a total number of about 50 T-box genes have been identified from a wide range of organisms [mammals (18 members), *Drosophila* (11 members), *C. elegans* (14 members), annelid to cnidarians (Herrmann and Kispert 1994; Papaioannou and Silver 1998; Smith 1999; Haworth, Putt et al. 2001; Papaioannou 2001). The functional diversity of T-box genes with regard to development depends on the spatio-temporal expression patterns of the gene and hence, abnormalities in this regard often alter the normal developmental course. A variety of developmental anomalies due to improper differentiation and organogenesis have been revealed by clinical as well as animal studies in T-box gene mutants. It has been demonstrated that mutations in the T-box genes are associated with human diseases, e.g. Holt-Oram-Syndrome (HOS; associated with mutations in TBX5), Ulnar-Mammary-Syndrome (UMS; associated with mutations in TBX3), DiGeorge Syndrome (DGS; associated with mutations in TBX1) (Li, Newbury-Ecob et al. 1997; Bamshad, Le et al. 1999; Gong, Gottlieb et al. 2001) etc. From the structural and functional analysis of OMB it was evident that OMB is a member of T-box gene families. The T-domain is located in the middle of the protein, from amino acid number 299 to 513 within the total 974 residues.

1.9 Objectives of the study:

The purpose of this dissertation was twofold.

One goal was to identify the embryonic precursor cell(s) of the HS and VS (horizontal and vertical system) cells of the optic lobes in the adult *Drosophila* brain. These cells fulfill an essential role in the processing of large-field visual motion stimuli. Lack of these cells causes flies to be blind with regard to this kind of visual stimulus, they are "optomotor-blind".

The other was to characterize mutants in the gene *optomotor-blind* (*omb*). Both their brain developmental phenotype and their molecular defects were to be determined. Flies hemi- or homozygous for particular alleles of *omb* are optomotor-blind because they lack the HS/VS cells.

No markers are currently known which label the lineage of the HS/VS cells from the presumptive embryonic precursor(s) to the adult stage. Several markers are, however, known which mark the adult HS/VS cells (e. g. the enhancer trap inserin A122). If one were able to identify the embryonic precursor, it might be possible to reproducibly label the lineage by a combination of genetic and non-genetic (namely laser heat shock) tools. As a means to identify the precursor(s) laser ablation was to be used. Does laser allow to selectively ablate cells in the interior of the fly embryo without obvious consequences for overall organismic development? This was first to be tested using fly sensory organs as model systems. Subsequently, the method should be applied to the HS/VS precursor(s).

Lethal mutants in *omb* generally are null for all functions that have been recognized in the *omb* gene. However, preliminary evidence suggested that, with regard to HS/VS development, this might not be true for all known *l(1)omb* alleles. Therefore, HS/VS development was to be re-analyzed in these mutants and their molecular *omb* lesions were to be identified.

2. Materials and Methods

2.1 Chemicals, enzymes, and kits:

Chemicals and enzymes used for the experiment have been ordered from the following companies: Amersham, Applichem, Biorad, Boehringer, Fluka, Gibco-BRL, Merck, MBI Fermentas, New England Biolabs (NEB), Promega, Pharmacia, Roth. PCR purification kit, Gel extraction kit and Plasmid purification kit were purchased from Qiagen

2.2 Buffers and stock solutions:

Different stock solutions and buffers required for molecular work were prepared according to the instruction of laboratory manual (Sambrook 1989) with modifications as needed. Compositions of some common buffer solutions and solutions required in histochemical studies are given in table 2.1.

Buffers/solutions	composition
TE (pH 8.0)	10mM Tris-Cl, pH 8.0 and 0.2mM EDTA, pH 8.0.
5x TBE (per liter)	Tris base 60.55gm, Boric acid 30.9gm and Na ₂ EDTA 9.3gm
Ringer's solution	130 mM NaCl, 4.7 mM KCl, 0.74 mM KH ₂ PO ₄ , 0.35 mM Na ₂ HPO ₄ , 1.8 mM MgCl ₂ ; pH 7.0).
10x PBS (per liter)	NaCl 75.55gm, Na ₂ HPO ₄ , 2H ₂ O 12.45gm, NaH ₂ PO ₄ , H ₂ O 8.3gm
X-gal Staining solution:.	7mM Na ₂ HPO ₄ , 3mM NaH ₂ PO ₄ , 150mM NaCl ,1 mM MgCl ₂ , 3mM K ₃ [Fe(CN) ₆],3mM K ₄ [Fe(CN) ₆] .
PBT:	1x PBS +0.5% Triton X-100
0.2M Cacodylate buffer (per litre)	Sodium cacodylate trihydrate 42.8 gm ; adjust pH with HCl to 7.3;

2.3 Laser ablation:

2.3.1 Microscopic Setup:

A Zeiss Axioplan 2 imaging fluorescence microscope was connected to the ablation unit (Laser Science Inc.). This microscope has the important feature of allowing laser and fluorescence light to come through the same port to the ablation head and allows the viewer to visualise the targeted cell(s) by a compatible filter. The relevant features of this microscope are a high performance digital camera (AxioCam), a turret for 8 different filters and a set of ICS (Infinity Color-corrected System) objectives (Plan-Neofluar Objectives). The microscopic setup during the laser ablation experiments is as follows. Before turning on the ablation unit, one should check the microscopic setup, like filter position and the imaging system.

Filter number '1' was placed in the filter turret.

1. Fluorescent light was put on with the GFP filter in position.
2. All the required shutters were open to allow the light to come to the specimen.
3. Now the specimen was brought into focus using the appropriate objective and the desired cell or group of cells were positioned at the centre of the ablation head cross.
4. Now the filter was changed from '1' to '4'.
5. We could, if required, take images of the specimen using the AxioCam digital camera assisted by the required software. After photography, the path to the camera was blocked by the shutter and this is a very necessary step.
6. The laser unit was turned on now and at this point we should check position of all filters and shutters thoroughly.
7. Now the laser could be triggered manually or by automatic mode.

2.3.2 Immobilization of Drosophila embryos and larvae in halocarbon oil by a clinical volatile anesthetic-‘Forane’:

For the effective immobilization experiments on mature embryos as well as first instar larvae, we used ‘Forane’ (Isoflurane, USP; Baxter Healthcare Corporation) as an anaesthetic. Forane (1-chloro-2,2,2-trifluoroethyl difluoromethyl ether) a non flammable, nonexplosive inhalation anesthetic. Our main objective of this experiment is to transiently stop muscular motion in the mature embryo as well as in L1 larvae.

Preparation of anaesthetic solution:

The whole process of making anaesthetic solution was done in the exhaust hood. Before starting to make the solution, the small glass vials were kept in ice for few minutes. Required amount of halocarbon oil (‘VOLTALEF 10S’, Lehmann & Voss & Co.) was aliquot into a vial and the vial was kept on ice. In lower temperature the oil will be solidified. So, the oil should be melted just before use by rubbing the vials in the hands. Now the appropriate amount of anaesthetic was transferred into the chilled vials and oil was added immediately. The contents were mixed properly by shaking vigorously. 5%, 10%, 15% and 20% anaesthetic solutions were prepared for immobilization experiments.

Anaesthetisation of embryos and larvae:

L1 larvae and dechorionated embryos were transferred into a drop of anaesthetic solution. Larvae and embryos were inspected for internal muscle movement under the microscope in every 5 minutes interval for 30 minutes. Treatment was done in different batches for different anaesthetic concentrations. Time was noted for each concentration when larvae and embryos were completely immobilized. Finally, 15 % anaesthetic solution was used for experimental purpose. Incubation time was 5-7 minutes.

2.3.3 Laser ablation:

Embryos were collected from 3hrs egg lays and dechorionated manually on a double stick tape (Tesa). The embryos were then arranged in a certain pattern (see figure 2.1) on the

slide and mounted under a coverslip (Manzel-Glaser, Germany; thickness 0.13-0.16mm) in halocarbon oil ('VOLTALEF 10S', Lehmann & Voss & Co.). The embryos were then focused in Zeiss Axioplan 2 imaging fluorescence microscope using the fluorescent light. The respective target cells were observed using the same filter (in our case filter 4 was used) which is to be used for the laser light. After examining the target cells the laser unit was turned on. The ablation was performed using a Laser Sciences (Cambridge, MA) VSL-337 ND-S Nitrogen dye laser, coupled to a dual mirror dye cell module emitting at 440 nm (with Coumarin 440) with peak pulse energy of 300 μ J and peak power of 75 kW

A short description and list of specifications of the laser unit is given in Appendix 1. Laser light was focused with a 40x, 20x or 10x objective. During the ablation, laser light was focused after attenuation using the slide attenuator plate. 2-6 pulses, depending on the extent of ablation, of 4ns pulse were delivered in each area at a frequency of 3-4 Hz. After ablation the slide containing the embryos was transferred to 18°C and was allowed to recover for 3-4 hours.

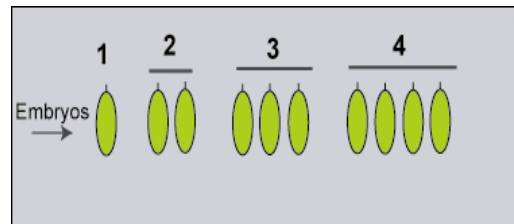


Figure 2.1: Arrangement of embryos on microscope slide during laser ablation. Embryos were arranged in groups, which were separated by longer space than the space between the embryos within a group. Each group is recognised the number of embryos present in that group, i.e., 4th group contains 4 embryos.

2.4 Larval olfactory tests:

The olfactory tests of third instar larvae were performed using the protocols of Heimbeck et al. (1999) with slight modification. Third instar larvae of control flies and the ablated flies were collected from the food vial after 4-5 days using concentrated sucrose solution. Larvae were selected not solely based on their age in days, but depending on the crawling of larvae. When the larvae starts to come out from the media and few of them try to crawl on the filter paper on the media, they were collected by using concentrated sucrose solution. The solution was poured into the food vial containing the larvae. After a few minutes, most of the larvae came out of the food and floated on top of the sucrose solution.

Then the larvae were collected by trapping them inside an inoculating loop. They were washed in water to remove the residual sucrose from the body surface. Around 15- 20 larvae were picked and placed on the centre of the plate (Sarstedt AG & Co.) containing 1.2% agarose (AppliChem GmbH). The plates were dried, by keeping the lid open for few hours after pouring the agarose, before use. After placing the larvae in the middle, the test solution, e.g. butanol, ethyl acetate and propionic acids, were applied on a small circular membrane of about 5mm diameter made from filter paper and immediately covered the lid of the Petri dish. All the chemicals were used in undiluted form and 1 μ l in each case. Water (deionised) was used as control. Now the larvae were counted every minute inside the source semicircular area (S), the opposite identical control side and in the rest area of the plate (Figure 2.2).

The Response index was then calculated using the following formula: Response Index (RI) = $(N_s - N_o) / (\text{total number of animals})$, where N_s is the number of larvae at the source area, N_o is the number of animals at the opposite identical control area. The whole experiment was done inside a dark chamber.

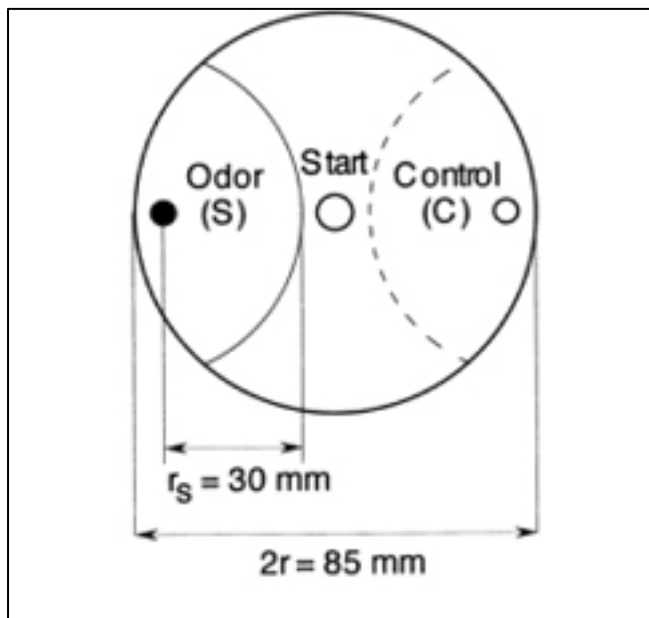


Figure 2.2: Olfactory larval plate assay. Schematic representation of the test set up. Small filter disks containing test chemical (S) and control diluent (C) are placed on opposite sides of a Petri dish covered with a layer of agarose. Animals were transferred to the start point and counted every minute. (Heimbeck, Bugnon et al. 1999)

2.5 Whole mount X-gal staining of *Drosophila* larva and embryo:

2.5.1 X-gal Staining in embryo

Embryos were bleached with 5% Na-hypochlorite (in PBT). After washing two times in PBT, embryos were incubated (fixed) in a mixture containing 5 ml of 2.5% glutaraldehyde (in PBS) and 3 ml of heptane for 10 min in a vial and the vial was shaken vigorously throughout the incubation time. Embryos were then transferred into a new vial containing 3 ml of heptane. Cold (-20°C) methanol was added and the vial was vigorously shaken for 15 seconds. Embryos should sink to the bottom. Methanol was exchanged and the vial was shaken vigorously until most of the embryos come to the bottom. Methanol was removed as much as possible and then 80% ethanol was added and was kept for 2 min. Ethanol was removed and embryos were washed 3 times in PBT (5 ml each). Embryos could be kept in PBT for 2 hrs, if needed. Staining was performed at room temperature (in dark) for few hours to overnight in staining solution (see table 2.1) containing X-gal (one volume of 2% X-gal was added to 29 volumes of pre-warmed (37°C) staining solution). Staining was stopped after incubation with 0.5 % glutaraldehyde for 5 min. Embryos were washed three times in PBT, each for 5 min. if traces of X-gal crystal remained after washing with PBT, embryos should be washed with 70% ethanol. Embryos were finally washed in 1x PBS and were incubated overnight in 80% glycerol (in PBS).

2.5.2 Whole mount X-gal staining of larva:

Larvae were dissected in ice cold Ringer solution (see table 2.1). The larvae were held in the middle with a forceps and the mouth hook was pulled up with another forceps. This technique is useful for our purpose of obtaining Bolwig's Organ and the larval brain hemisphere along with the mouth hook. They were then transferred to Ringer solution in a microtiter plate and the samples can be stored up to 2 hrs on ice until all the dissection was finished. The dissected parts were then incubated for 15 minutes in 100 µl of fixative (1% glutaraldehyde in 0.1 M NaCacodylate buffer, pH 7.3). Fixative was removed and tissues were rinsed with 1x PBS. One volume of 2% X-gal was added to 29 volumes of pre-

warmed (37°C) staining solution and the larval tissues were incubated few hours to overnight at 37°C in dark. After staining was over, larval tissues were washed three times in 1x PBS and incubated again in 50% glycerol. Unwanted tissue parts were removed carefully and the desired parts were placed on the slide with 80% glycerol (in PBS) and covered with cover slip. Specimens were sealed by nail polish and were photographed.

2.6 Whole mount X-gal staining of eye brain complex (EB) of *Drosophila*:

Whole mount X-gal staining was performed on adult eye brain complex (EB) of *Drosophila*. Adult flies, two to four days old, were anaesthetised with ether for 5 minutes. Flies were then placed onto a silicon plate and were pinned firmly by needles in thorax and abdomen. Flies were then submerged in ice cold Ringer's solution. With the help of forceps, the proboscis was removed and air sacks were removed as much as possible. The head capsule was removed carefully so that brain remained attached to the body. Remaining air sacks and other tissue were cleaned off from the brain. The Brain was then removed from the body and was stored in ice cold Ringer's solution up to 2 hours until all the preparations were done. Brains were fixed for 20-25 min in fixative (0.05% PBT, 1% glutaraldehyde) and subsequently washed two times, each for 10 minutes, in 1x PBS. Staining was done in staining solution containing 1/30th volume of 2% X-gal up to 20 hrs depending on the staining. Tissues were washed once with 0.3% PBT and twice with 1xPBS. Washed samples were then incubated in PBS-Glycerine mix (1:4) for another 24 hrs at room temperature and were subsequently mounted in the same solution.

2.7 *Drosophila melanogaster* stocks and crosses:

The genotypes of omb lethal mutant [*l(l)omb*] stocks used for the studies are described in Table 2.2. Four mutant lines, alleles in three lines were tagged with yellow(y) and y-tagged alleles were maintained as balanced stocks over FM-GFP. One allele was

maintained over FM7a. For the genetic complementation experiments, the duplication DpA1125 was introduced into each mutant line by crossing them individually with line 395 [*l(1)omb^{D4}, w; DpA1125/In(2LR)Gla, Bc*] and stable stocks containing the duplication were also established (see appendix 6) for all mutant lines except one (line 1041). Males containing the duplication over Glazed balancer chromosome from these stocks were crossed with the females from the deficiency mutant line *w Df(1)rb5 A122/FM6* to test the effect on HS/VS cell

GOP stock number	relevant genotype	Type of stocks
1039	<i>l(1) omb^{I1}/FM-GFP</i>	Lethal mutant
171	<i>l(1) omb^{I2}/FM7a</i>	Lethal mutant
1041	<i>l(1) omb^{I3}/FM-GFP</i>	Lethal mutant
1042	<i>l(1) omb^{I5}/FM-GFP</i>	Lethal mutant
143	<i>w Df(1)rb5 A122/FM6</i>	Deficiency mutant
145	<i>lacZ A122</i>	Adult shows HS/VS neurons
395	<i>l(1)omb^{D4}, w; DpA1125/In(2LR)Gla, Bc</i>	Stock containing duplication over Glazed marker.

development. A detailed outline of different crosses made is given in appendix 8. Fly stocks used in different experiments are listed in appendix 6.

2.8 Purification (recombination) of the stock *l(1)omb[12]/ FM7a*:

The *omb* lethal mutant line *l(1)omb[12]/FM7a* (171) was purified from a suspected second lethal mutation. To achieve the purified stock, females from this line were first crossed with males of line *w omb^P/Y; II* (82). Females having red and round eye phenotype within the F1 progeny were selected [*v l(1)omb[12]/w omb^P; II*]. In the second step the balancer chromosome was reintroduced by crossing those females with line *FM7a, vw/Y* (334). Bar eye females from the F1 progeny were the balanced one. But these females are either parental or recombinant. First we had to establish stable stocks from each individual female. Individual females from F1 were crossed with male *FM7a, vw/Y* (334) and stable stocks were maintained. These crosses were named as E3¹, E3², E3³, E3ⁿ. Stocks producing red round eye females were discarded and stocks having Bar eye phenotype were tested for positive purification. So, in the last step we set up a series of test crosses, named as E4¹, E4², E4³, E4ⁿ, using virgins from each of selected E3 crosses and males from line *l(1)omb^{D4}, w; Dp/In(2LR)Gla, Bc*. Progeny from each of the test cross were

counted based on their eye phenotype and prospective purified stocks were identified from the E3 stable stocks based on the production of round vermilion eye females in the F1 progenies of test crosses. An outline of different crosses associated with the purification steps is depicted in Box 2.1.

Box 2.1: Outline of genetic crosses made for purification of line *l(1)omb[x]/FM-GFP; II (171)*

E1 cross :

$v\ l(1)omb[12]/FM7a,vw; II (171) \times w\ omb^P/Y; II (82)$

F1..... $v\ l(1)omb[12]/w\ omb^P; II$ These female have round red eye

Cross E2 (recombination cross):

$v\ l(1)omb[12]^*/omb^P; II \times FM7a,vw/Y (334)$

F1..... $v\ l(1)omb[12]/FM7a,vw$ These females are either parental or recombinant

Cross E3¹..... Cross E3¹⁷⁶(stock establishment):

$v\ l(1)omb[12]^*/FM7a,vw \times FM7a,vw/Y (334)$

Cross E4¹ cross E4^B (test cross):

$v\ l(1)omb[12]^*/FM7a,vw; II (171) \times w\ l(1)omb[D4]/Y; DpA1125/ln(2LR),GlaBc (395)$

F1..... Look for the lines (from E3 series) which produce *Gla*⁺ vermilion males in these tests crosses.

2.9 Genomic DNA isolation:

Genomic DNA was extracted from about 50 adult flies using the standard protocol used in the lab. Pre-frozen flies were homogenized in 0.5 ml homogenization buffer (100mM NaCl; 100mM Tris-Cl, pH 8.0, 50mM EDTA, pH 8.0 and 0.5% SDS) and incubated at 60°C for 30min. After the incubation, 75µl of potassium acetate was added to the homogenate and the components were mixed thoroughly, by inverting and finger tapping.

The mixture was then incubated on ice for 30 minutes and was centrifuged for 10 minutes. DNA present in the supernatant was precipitated by 2.5 volume of ethanol and was washed in 70% ethanol. The unpurified DNA pellet was dissolved in TE (10mM Tris-Cl, pH 8.0 and 0.2mM EDTA, pH8.0) and was treated with RNase. After RNase treatment the DNA was extracted with equal volume of phenol and subsequently purified by chloroform-isomyl alcohol mixture (24:1). Purified DNA was then precipitated and was dissolved in 50 μ l of TE (10mM Tris-Cl, pH 8.0 and 0.2mM EDTA, pH8.0). 2 μ l of genomic DNA was used for each of the 50 μ l PCR reaction.

2.10 PCR amplification of omb locus:

All eight exons, except part of the 3' end of exon VIII, as well as exon-intron junctions were amplified by sets of primer pairs. Locations of primers within the *omb* primary transcript are depicted in Figure 2.2 and locations of primers in the genomic DNA sequence are shown in Appendix 2. The sequences of PCR primers along with T_m values and respective annealing temperatures are shown in Appendix 3. All reactions were set up with *Pfu* polymerase (MBI Fermentas). PCR reactions were performed on Eppendorf Mastercycler gradient using the following amplification program: 94°C for 5 min followed by 30 cycles at 95°C for 1 min, 48-60 °C for 1 min, and 72°C for 1-3 min followed by final extension at 72°C for 7 min. Annealing temperature was set 4-8°C below the lowest T_m value of the primer pair used in the reaction and extension times were varied according to the lengths of fragments to be amplified, i.e. one minute extension times per 500 bp of PCR product.

2.11 Sequencing of the amplified products:

The PCR products were sequenced directly by SEQLAB, Göttingen. In most of the cases sequencing of PCR fragment was done by the same primers used for the amplification. In some instance, some internal primers were used as required to get full sequence.

2.12 Introduction of a A508V mutation into the OMB T-domain

Starting clone was the plasmid pBAT70-71 encoding the OMB T-domain (Grimm 1997, p42). Two complementary primers were designed which introduce the DNA mutation (in bold) that lead to the A508V conversion. A single transition suffices to introduce the desired translational change (the affected codons are shown in red)

translated wildtype sequence

c gat aac aat ccg ttt **gcg** aag ggc ttt cgt gat act gg

D N N P F **A** K G F R D T

translated mutant sequence

c gat aac aat ccg ttt **gtg** aag ggc ttt cgt gat act gg

D N N P F **V** K G F R D T

OMB-A508V-uppermutprimer: cgataacaatccgttt**gtg**aaggccttcgtgatactgg

OMB-A508V-lowermutprimer: ccagtatcacgaaagcccttc**acaa**acggattgttatcg

Using the Stratagene QuickChange Site Directed Mutagenesis Kit the entire vector was amplified with the mutagenic primers. The amplified DNA was digested with DpnI. DNA synthesized *in vitro* is not methylated, whereas the starting plasmid, which was isolated from conventional *dam*⁺ *E. coli*, contains adenosine methylation within the DpnI target site (GATC). DpnI only digests Dam-methylated DNA. Therefore, the starting DNA but not the mutagenized DNA amplified *in vitro* is digested. Only the latter should be able to transform *E. coli*.

PCR-reaction (50 μ l) (assembled on ice)

5 μ l 10x reaction buffer

1 μ l (6,6ng) pBAT 7071

1 μ l (125ng) primer #1

1 μ l (125ng) primer #2

1 μ l dNTP mix

1 μ l (2,5U) *Pfu* Turbo DNA Polymerase (STRATAGENE)

40 μ l ddH₂O

PCR-program on Mastercycler Gradient (Eppendorf)

temperature	time	cycles
95°C	30s	1
95°C	30s	12
55°C	60s	
68°C	300s	
4°C	∞	

Transformation protocol (following Stratgene kit instructions)

One aliquot XL1-Blue cells was thawed on ice and divided into 50 µl aliquots. One aliquot was added to a prechilled 14 ml BD-Falcon tube. To this, 2 µl of of pre-chilled PCR reaction were added. The suspension was incubated on ice for 30 min and subsequently heat-shocked for 45 sec in a 42°C water bath. After chilling for 2 min on ice, 750 µl SOC medium were added. The suspension was then incubated at 37°C under shaking (1200 rpm) for 60 min. 100 µl, 200 µl, and 500 µl were plated onto LB-Carbenicillin (50 µg/ml) plates and incubated overnight at 37°C.

The next day 10 colonies were individually inoculated into 4 ml liquid culture (in 14 ml BD-Falcon tubes) and grown overnight.

Analysis

Plasmid DNA was isolated using Eppendorf's FastPlasmid Mini Kit and eluted with 40 µl elution buffer. Two preparations were randomly chosen for sequencing.

sequencing reaction (7 µl):

0,7µl (600ng) plasmid-DNA

1µl (20µM) primer M13reverse

5,3µl ddH₂O

Sequencing was performed commercially at Seqlab (Göttingen). Both clones yielded the desired mutation and did not contain accidental additional mutations.

2.13 Cloning, expression, and purification of wild type and mutant OMB-T (T-domain from OMB) clones:

2.13.1. Insert and Vector preparation:

T-domain of wild type OMB was amplified from *omb* cDNA clone by *Pfu* polymerase using primer-pair SG-70-SalI/SG-71-SalI. *SalI* site (blue) was introduced in each primer for subsequent cloning.

SG-70-SalI (802): ACA CAG TCG ACG ACG TCG TCC TTG CC

SG-71-SalI (803): TGT GTG TCG ACT TAG CCG GCA CCA GTA TC

When the T-domain is amplified by SG-70-SalI/SG-71-SalI, additional amino acids (green) in N- and C-terminal to the T-domain are introduced. Numbering of aa residues follows the original OMB sequence numbering (see appendix 10).

```

301  SAVAHQLHPA MRPLRALQPE DDGVVDDPKV TLEGKDLWEK FHKLGTEMVI DVVLA
351  TKSGRQMFPQ MKFRVSGGLDA KAKYILLLDI VAADDYRYKF HNSRWMVAGK
401  ADPEMPKRMV IHPDSPTTGE QWMQKVVSFH KLKLTNNISD KHGFVSTTIL
451  NSMHKYQPRF HLVRANDILK LPYSTFRITYV FKETEFIAVT AYQNEKITQL
501  KIDNNPFAKG LRDTGAG

```

PCR-program on Mastercycler Gradient (Eppendorf)

temperature	time	cycles
95°C	5min	1
95°C	40s	25
62°C	60s	
70°C	85s	
4°C	∞	

T-domain containing the missense mutation A508V was amplified using the same pair of primers used for the wild type T-domain amplification; but the clone containing the mutated T-domain, pBAT-7071 with omb-T^{A508V}, was used as template (see figure 2.3). Amplified fragments were purified by PCR purification kit (Qiagen) and were, subsequently, digested with *SalI*. Fragments were purified again and concentrations were measured.

pMAL-cRI plasmid (NEB) was used as cloning and expression vector. The vector was digested with *SalI* and was gel purified. Purified digested vector was dephosphorylated by Shrimp Alkaline Phosphatase (MBI). Phosphorylated vector was then purified using PCR purification kit (Qiagen). The concentration of the linearised vector was estimated on an agarose gel.

2.13.2. Cloning and screening:

SalI digested vector and inserts were ligated at 1:3 molar ratio and ligated materials were transformed into DH-5 α competent cells (Invitrogen) following the suppliers protocol. Clones were screened by minipreps and subsequent restriction analysis was performed to check the orientation (see the following section). Steps involved in cloning of mutant and wildtype T-domain of OMB into pMAL-cRI vector are schematically represented in figure 2.3.

Restriction analysis to check the orientation:

The amplified DNA fragment contains unique (within pceT3-1) *ScaI* (1640) and *SspI* (1613) sites, corresponding to position 436 and 415, respectively within this fragment.

ScaI cuts pMal-cRI at 3706; *SspI* cuts at 1389 and 3382.

Position of *SalI* is 2695.

Length of vector is 6131 bp.

ScaI analysis:

Correct orientation should give a 1224 bp fragment plus the complementary fragment; the wrong orientation will give a 1426 bp fragment along with the complementary fragment.

SspI analysis:

Correct orientation should give a 917 bp fragment plus the complementary fragments; the wrong orientation will give a 1123 bp fragment along with the complementary fragment.

Appropriate candidate clones were selected after proper restriction analysis. Clones were transformed into BL21 (DE3) competent cells.

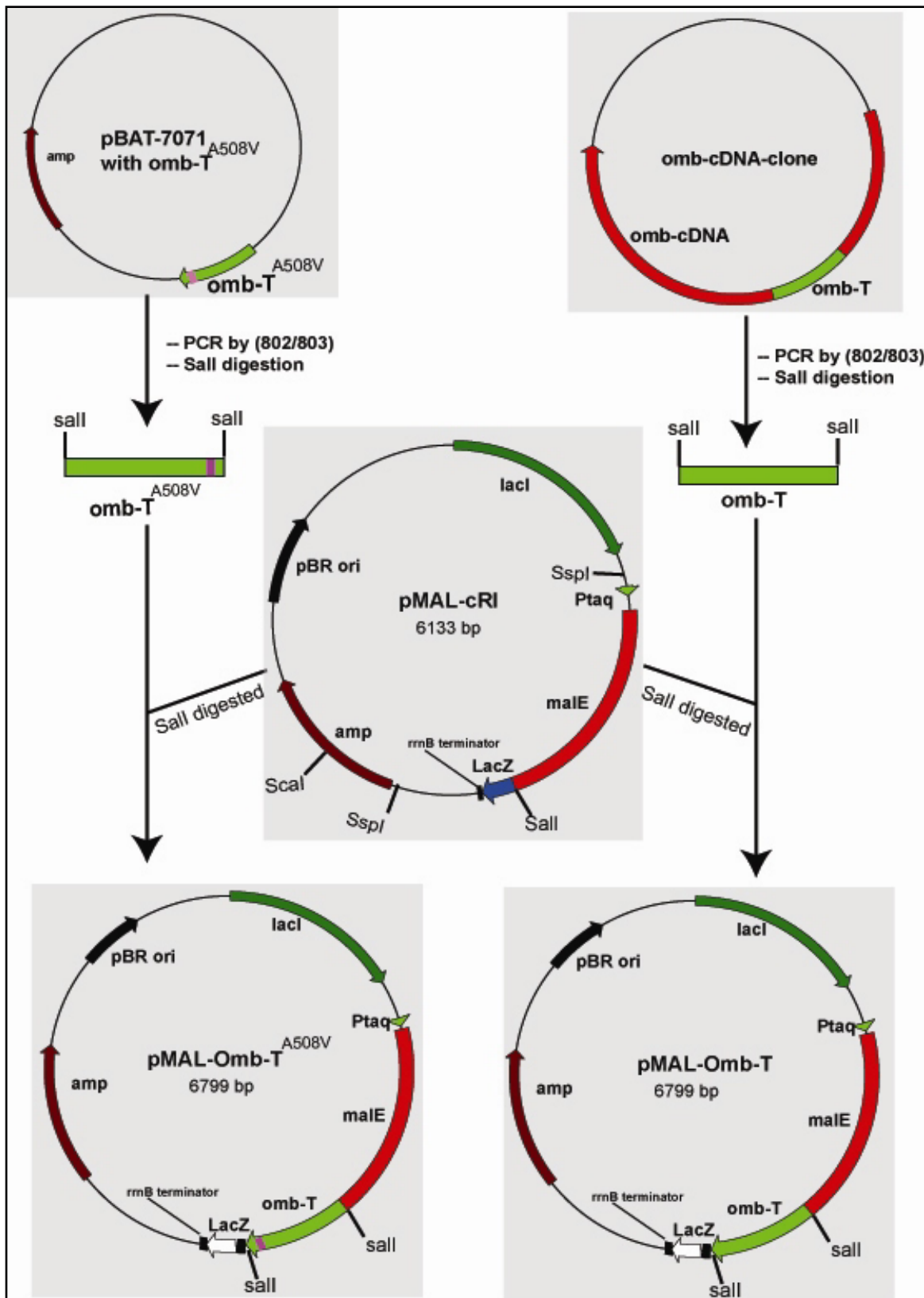


Figure 2.3: Cloning of mutant and wild type Omb T-domain into pMAL-cRI vector. Restriction sites are not to the scale.

2.13.3 Expression of wild type and mutant OMB-T domain:

Expression of OMB-T clones was performed following the protocol from pMAL protein fusion and purification system (NEB). Plasmid DNA from the OMB-T clones were transformed into BL21 (DE3) competent cells for expression. A single colony from the transformation plate was inoculated into 3 ml enriched medium (LB containing 0.2% glucose and 70µg/ml carbenicillin). 100 µl of overnight culture was inoculated into 20 ml of enriched medium and the culture was grown at 37°C with shaking at 180 rpm. Cells were induced with 0.7mM IPTG when the OD₆₀₀ reached about 0.9-1.0. Culture was incubated at 37°C at 180 rpm for another 6 hours. Samples of bacterial culture were collected before and after induction. Induced cells from 15 ml culture were collected after centrifugation at 5000rpm at 4°C for 15 minutes. Cells were resuspended in 1.5 ml column buffer (20 mM Tris-Cl, pH 7.5; 200 mM NaCl; 1 mM EDTA; 1 mM azide; 1 mM DTT) and were frozen overnight at -20°C. Next day, cells were ruptured by sonication (6-7 pulses of 20 second pulse with 30 second gap). After sonication, the suspension was centrifuged for 15 minutes at 9000g at 4°C. Supernatant (crude extract) was taken into a new tube and the pellet (insoluble matter) was resuspended into 1.5 ml column buffer. Protein samples were stored at 4°C.

2.13.4 Purification of MBP-OMB-T fusion protein:

Purification of MBP-OMB-T fusion protein was performed using the supplier's protocol (NEB). The whole process of purification was done at 4°C. 1.5 ml of amylose resin (NEB) was poured into an empty column (Qiagen; 1ml, disposable; No. 34924) and the column was equilibrated with 12 ml of column buffer (20 mM Tris-Cl, pH 7.5; 200 mM NaCl; 1 mM EDTA; 1 mM azide; 1 mM DTT). In the meantime, 1.5 ml of crude extract was diluted two times with column buffer. After equilibration, the diluted crude extract was loaded onto the column and the flow-through was collected. The column was then washed with 18 ml of column buffer. Elution of protein was done by 2ml of 10 mM maltose solution (in column buffer). 0.2 – 0.3 ml fractions were collected and absorbance of all fractions was measured at 280 nm. Fractions containing the protein were analysed on SDS-PAGE.

2.14 In vitro target site selection (SELEX):

a. Construction of vector containing HindIII but no BamHI site:

This was done for the cloning of selexHB-random-92 (Oligo 673) in pBluescript II KS (-) vector. The 40 nucleotide degenerate part (pink) of selexHB-random-92 is flanked by two *BamHI* sites (blue) has to be replaced by the standard Bra palindrome (see the following sections). Cloning vector pBluescript II KS (-) was linearized by digestion with *BamHI*. Linearized plasmid was then eluted and purified through Qiagen Gel Extraction kit. The protruding ends of the plasmid were Klenow filled-in and vector was then self-ligated. Klenow filled-in reaction should destroy the *BamHI* site on self-ligated vector. Self-ligated vector was redigested with *BamHI* to eliminate any cleavable plasmid. After this digestion plasmid was transformed into DH-5 α competent cells. The colonies from the transformation were screened for lack of *BamHI* site and presence of *HindIII* site. The isolated vector was named as pKS ^{Δ BamHI}.

b. Generation of random templates for in vitro selection experiments:

For the generation of random EMSA templates, three oligonucleotides were used. One of the three oligonucleotides, selexHB-random-92 (Oligo 673), contains the 40 nucleotide degenerate part (pink) flanked by two *BamHI* sites (blue). *HindIII* sites (red) were also incorporated at each end of this oligonucleotide to facilitate the cloning of the amplified products.

selexHB random-92 (oligo 673):

TCC AAGCTT TCTGTATGTCG GGATCC N40 GGATCC CCTAACCGACT AAGCTT ATT

This oligonucleotide served as a PCR template to make 40 bp random templates for selection experiment. selexHBfor (oligo 674: TCC AAGCTT TCTGTATGTCG) and selexHBrev (oligo 675: AAT AAGCTT AGTCGGTTAGG) were used as forward and reverse primers, respectively, for the amplification on selexHB-random-92. Details about the

oligonucleotides, mentioned here, are presented in Appendix 4. PCR was set up on selexHB random-92 using selexHBfor and selexHBrev using *Taq* polymerase.

PCR-program on Mastercycler Gradient (Eppendorf)

temperature	time	cycles
95°C	30s	1
95°C	30s	25
50°C	50s	
70°C	20s	
4°C	∞	

c. Generation of a single clone from the mixture of random PCR pool on degenerate oligonucleotide:

The 92 bp degenerate fragments were isolated from the gel and digested with *HindIII*. The resulting fragments were then cloned into *HindIII* digested and CIP (Calf intestinal phosphatase) treated pKS^{ΔBamHI} vector. No clone was obtained. The problem might have been the poor digestion of the 92bp fragment by *HindIII* sites because *HindIII* sites are present close to the ends of the fragment. So we decided to change our cloning strategy. The 92 bp PCR pool was first cloned into pDrive Cloning Vector (Qiagen). One of the clones was randomly selected and the 80 bp cloned fragment was excised by *HindIII* and was cloned back into *HindIII* digested pKS^{ΔBamHI} vector. The clone was designated as pKS^{ΔB-selex (H/H)}.

d. Construction of source clone for BraPal-92 fragment generation:

Two single stranded complementary oligonucleotides, selexB/B-BraPal-upper (oligo 676) and selexB/B-BraPal-lower (oligo 677), were annealed in 1x annealing buffer [10 mM Tris-Cl (pH 8.0), 50mM NaCl, 0.2mM EDTA (pH 8.0)] to make a DNA fragment containing Bra palindrome in it. These specific oligonucleotides were designed based on the

degenerate *BamHI* cassette of selexHB-random-92 (Oligo 673) (see section 2.14b), in which the 40 bp degenerate stretch was replaced by the standard Bra palindrome. The palindrome is flanked by 8 bp to make up a stretch of 40 bp. The *BamHI* sites are flanked by 3 bp to allow efficient cutting. oligo 676 and oligo 677 were annealed in 10 μ M concentration. The annealed product was digested with *BamHI* and was cloned into *BamHI* digested pKS ^{Δ B-selex (H/H)}. This BraPal clone was verified by restriction digestion with *StyI* enzyme which has a unique site in the BraPal fragment but no site in the vector. Subsequent sequencing has been done to confirm the clone. This clone will serve as a source for Bra palindrome to be used as control template for EMSA.

2.15 Electrophoresis mobility shift assay (EMSA):

Preparation of probe:

Single stranded complementary oligos were annealed in 10 μ M concentration in 1x annealing buffer [10 mM Tris-Cl (pH 8.0), 50mM NaCl, 0.2mM EDTA (pH 8.0)]. 5 pmoles of double stranded oligos were end-labelled with γ ATP³² (Amersham; 3000 Ci/mmol) by T4 polynucleotide kinase (NEB) using the supplier's protocol. Labelled probes were then purified using the Micro Bio-Spin 30 columns (Biorad). Sequence for the upper strand oligonucleotide containing Bra palindrome was selexB/B-BraPal-upper (5' TCG GGATCC AACTCAGT **AATTCACACCT AGGTGTGAAATT** TGA CTCAA GGATCC CCT 3').

1x GT top (5' GCGATACACTTGTGGAATGTGTTTGATTTGTTAGCC 3') and 1x GTbottom (complementary to 1xGTtop) were annealed together to make a fragment recognized by *Drosophila* Scalloped proteins.

EMSA:

Before the binding reaction was set up, a 5-6% polyacrylamid gel was cast and the gel was pre-run for 2hours at a temperature below 25°C. EMSA was performed using the protocols from various sources (Kispert and Herrmann 1993; Halder and Carroll 2001; White and Chapman 2005) after modifications in different parameters. About 1 μ g of bacterially expressed, both purified and unpurified, protein was incubated with 5 fmole of 5' end labelled probe in 20 μ l of binding buffer (20 mM HEPES, 100 mM KCl, 1 mM

DTT, 0.25 mM EDTA, 0.01%NP-40, 1 mM MgCl₂, 8%Glycerol, 100 µg/ml BSA, 0.1 mg/ml Poly (dI-dC)). The reaction mix without probe was pre-incubated for 10 minutes at room temperature and was re-incubated with probe for another 40 minutes on ice. After the binding reaction was over, 1µl of 6x loading dye was added and the reaction mix was loaded onto the gel. 6µl of 6x loading dye (0.25 % bromophenol blue plus 0.25% xylene cyalon XF in 30 % Glycerol) was loaded in one lane as a reference to the migration of probe into the gel. The Gel was run at 10V/cm at fixed current. After the gel run, the gel was fixed (20 ml methanol and 10 ml acetic acid in 70 ml deionized water) for 15 minutes. The gel was then transferred onto a piece of blotting paper (330 g/m²) [Hartenstein]. The gel was dried on a gel drier (Easy Breeze, Hoefer) for about 90 minutes and subsequently exposed to X-ray film (type: XBA; Fotochemische Werker, Berlin). The cassette was kept at -80°C for the desired time.

3. Results

3.1 Ablation of larval olfactory organ and behavioural experiments

The chemosensory organs in *Drosophila* larvae consist of the dorsal organ (DO), terminal organ (TO) and ventral organ (Stocker 1994). The DO and TO, which constitute the antennomaxillary complex (AMC), plays a major role in larval olfaction. Expression patterns of the P[*Gal4*] insertion line GH86 revealed that the AMC is composed of a total of 33-35 neurons, approximately equal number of neurons from each of the TO and DO (Heimbeck, Bugnon et al. 1999). In our experimental approach, we did the ablation of both AMC complexes by laser micro beam. The main objective of our experiment was to establish laser conditions sufficient to ablate a small set of cells. Successful ablation was verified by behavioural tests.

The *Gal4* driver line GH86, obtained from R. Stocker's lab, was used for the specific expression in the larval AMC. Reciprocal crosses were set up with the UAS responder line *UAS:GFPnls* (291). The *Gal4* driven targeted expression of GFP in the chemosensory neurons of the larval AMC visualises these cells. Before the ablation experiment was performed, we studied, first, the development of AMC in the late stages of embryogenesis. So, the first part of this experiment was to determine the embryonic stage when the AMCs are quite visible and the second part was the ablation. In the second part, we have studied the behavioural response of non-ablated and ablated flies.

3.1.1 Development of the AMCs :

Embryos were collected on apple juice plate and incubated at 25°C for different time intervals. Embryos were inspected 15h to 21h after egg deposition (in 1hr interval). The embryos were dechorionated manually and observed under the fluorescence microscope. Figure 3.1 shows the development of GH86-expression. It was observed that AMCs are quite prominent after 18h. So, for the ablation experiments embryos were selected at 18 hrs from the egg deposition time.

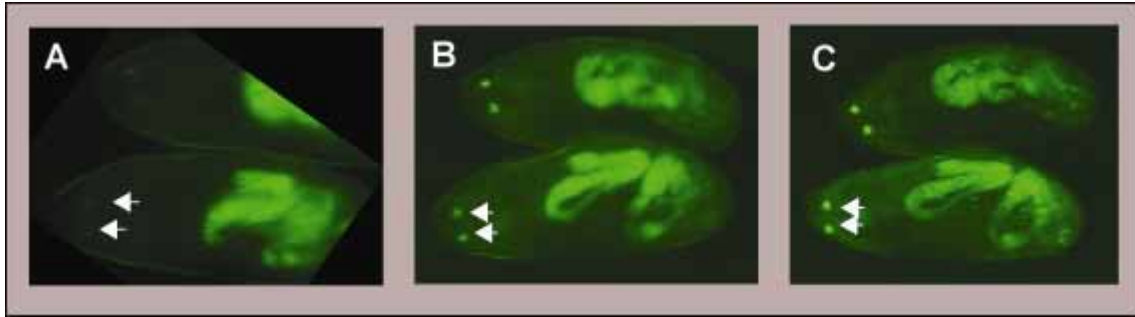


Figure 3.1: AMC development in different stages of embryos from the cross [*GH86-Gal4* (836) x *UAS:GFPnls* (291)]. Embryos are 16hrs (A), 17hrs (B) and 18hrs (C) from egg deposition time. The two AMCs are pointed out (arrow).

3.1.2 Ablation of AMCs:

Embryos from the cross *GH86-Gal4* x *UAS:GFP* were first dechorionated manually using double stick tape. Both AMCs were ablated by laser microbeam (Figure 3.2). The parameters of each ablation experiments are summarized (Table 3.1) and survival rates were determined for each set of experiment.

Table 3.1: Specimen score sheet for laser ablation experiments on AMC complex

Exp. No.	Line/Cross	Targeted area	Laser setting		Laser mode		Magnification	No. of embryos ablated	No of embryos survived	Survival rate, %
			S	L	F	P				
1	<i>GH86 (line836)</i> x <i>UAS:GFP</i> (291)	Both AMC	-1	Max	NA	2	20x	18	8	44.44
2	<i>GH86 (line836)</i> x <i>UAS:GFP</i> (291)	Both AMC	-1	Max	NA	2-3	20x	62	15	24.19
3	<i>GH86 (line836)</i> x <i>UAS:GFP</i> (291)	Both AMC	-1	Max	NA	4-5	10x	28	13	46.42
4	<i>GH86 (line836)</i> x <i>UAS:GFP</i> (291)	Both AMC	-1	Max	NA	2	10x	26	19	73.07

Note: S : Position of slide attenuator; L : Position of lever attenuator ; F : Frequency; P : Pulses ; NA : Not applicable

3.1.3 The Olfactory Test for Control Flies:

A detailed description of the larval plate olfactory tests is given in the Material and Methods section. To test the odour-induced behaviour, the larvae were subjected to a choice assay on agarose plates (Fig 4.1, Heimbeck et al., 1999). In our experiments, we used three chemicals, widely used for olfaction study, e.g. butanol, ethyl acetate and propionic acid as strong elicitors. One microlitre of each chemical in undiluted form was used in each case. Wild type larvae were first tested for their response to these chemical. The responses of larvae to different chemicals are summarized in Table 3.2.

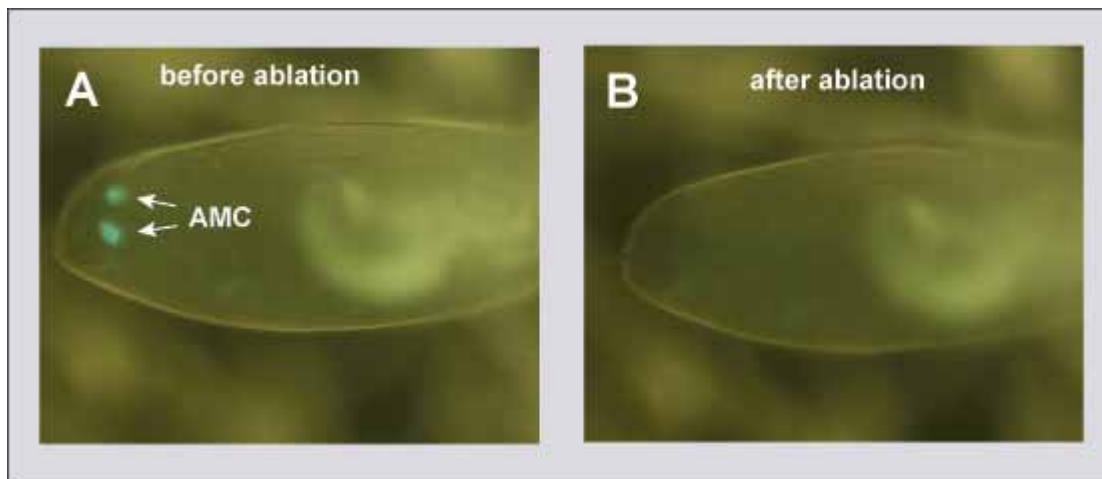


Figure 3.2: Laser ablation of AMCs. Both AMCs were ablated by laser microbeam

Table-3.2: Olfactory responses of control larvae.**Table-3.2a: Butanol:**

Time (min.)		1	2	3	4	5	6	7	8	9	10
Exp. No.	Ns	0	2	2	3	3	2	5	7	5	6
OT 1	No	0	2	2	2	1	1	1	0	1	0
	Nc	7	3	3	2	3	4	1	0	1	1
	ri	0	0	0	0,143	0,286	0,14	0,57	1	0,571	0,857
OT 2	Ns	1	9	12	12	10	10	8	4	8	9
	No	0	0	0	1	1	2	1	5	4	1
	Nc	14	6	3	2	4	3	6	6	3	5
	ri	0,0667	0,6	0,8	0,733	0,6	0,53	0,47	-0,1	0,267	0,533
OT 3	Ns	2	3	6	8	9	9	9	8	8	9
	No	3	2	0	1	1	0	1	1	1	0
	Nc	9	9	8	5	4	5	4	5	5	5
	ri	-0,071	0,07143	0,429	0,5	0,571	0,64	0,57	0,5	0,5	0,643
OT 4	Ns	3	10	11	13	14	15	11	13	9	12
	No	1	2	2	2	1	0	1	1	3	1
	Nc	16	8	7	5	5	5	8	6	8	7
	ri	0,1	0,4	0,45	0,55	0,65	0,75	0,5	0,6	0,3	0,55
OT 5	Ns	0	2	4	6	10	7	5	8	9	9
	No	4	4	5	3	1	1	1	4	2	2
	Nc	15	13	10	10	8	11	13	7	8	8
	ri	-0,211	-0,1053	-0,053	0,158	0,474	0,32	0,21	0,2	0,368	0,368
OT 6	Ns	4	6	11	11	8	11	11	11	10	12
	No	0	1	2	2	1	1	0	0	1	0
	Nc	14	11	5	5	9	6	7	7	7	6
	ri	0,2222	0,27778	0,5	0,5	0,389	0,56	0,61	0,6	0,5	0,667
OT 7	Ns	1	8	10	15	9	9	12	9	11	12
	No	7	1	0	2	4	0	4	2	3	1
	Nc	10	9	8	1	5	9	2	7	4	5
	ri	-0,333	0,38889	0,556	0,722	0,278	0,5	0,44	0,4	0,444	0,611
OT 8	Ns	4	3	3	3	3	4	4	7	6	5
	No	0	1	0	0	0	1	1	1	1	1
	Nc	7	7	8	8	8	6	6	3	4	5
	ri	0,3636	0,18182	0,273	0,273	0,273	0,27	0,27	0,5	0,455	0,364
OT 9	Ns	5	9	11	9	12	11	9	9	4	5
	No	1	1	1	1	1	1	1	2	4	5
	Nc	10	6	4	6	3	4	6	5	8	6
	ri	0,25	0,5	0,625	0,5	0,688	0,63	0,5	0,4	0	0
OT 10	Ns	0	9	8	10	11	12	13	10	13	7
	No	2	2	3	2	2	1	0	2	1	2
	Nc	17	8	8	7	6	6	6	7	5	10
	ri	-0,105	0,36842	0,263	0,421	0,474	0,58	0,68	0,4	0,632	0,263
OT 11	Ns	4	12	11	10	14	9	10	7	8	5
	No	1	0	1	0	0	1	1	1	3	3
	Nc	14	7	7	9	5	9	8	11	8	11
	ri	0,1579	0,63158	0,526	0,526	0,737	0,42	0,47	0,3	0,263	0,105
	RI mean	0,04	0,30133	0,397	0,457	0,493	0,49	0,48	0,5	0,391	0,451
	SD	0,2092	0,24155	0,258	0,197	0,17	0,18	0,14	0,3	0,177	0,258
	SEM	0,019	0,02196	0,023	0,018	0,015	0,02	0,01	0	0,016	0,023

Table-3.2b: Ethyl acetate:

Time (min.)		1	2	3	4	5	6	7	8	9	10
Exp.No.	Ns	1	4	6	8	7	6	7	8	9	8
OT 12	No	1	3	2	2	4	4	1	2	1	0
	Nc	14	9	8	6	5	6	8	6	6	8
	ri	0	0,0625	0,25	0,375	0,188	0,13	0,38	0,4	0,5	0,5
OT 13	Ns	3	2	3	3	4	7	7	12	9	11
	No	2	1	2	2	2	3	2	0	0	0
	Nc	9	11	9	9	8	4	5	2	5	3
	ri	0,0714	0,07143	0,071	0,071	0,143	0,29	0,36	0,9	0,643	0,786
OT 14	Ns	0	6	7	7	9	6	6	4	5	3
	No	0	0	0	0	0	1	0	0	0	0
	Nc	11	5	4	4	2	4	5	7	6	8
	ri	0	0,54545	0,636	0,636	0,818	0,45	0,55	0,4	0,455	0,273
OT 15	Ns	0	3	7	8	8	9	11	12	11	10
	No	1	2	2	1	1	0	0	1	0	0
	Nc	13	9	5	5	5	5	3	1	3	4
	ri	-0,071	0,07143	0,357	0,5	0,5	0,64	0,79	0,8	0,786	0,714
OT 16	Ns	2	2	4	8	9	4	8	6	6	7
	No	0	0	0	1	1	0	0	1	1	0
	Nc	12	12	10	5	4	10	6	7	7	7
	ri	0,1429	0,14286	0,286	0,5	0,571	0,29	0,57	0,4	0,357	0,5
OT 17	Ns	0	0	6	9	8	6	7	4	5	6
	No	0	1	1	0	1	0	0	3	0	0
	Nc	14	13	7	5	5	8	7	7	9	8
	ri	0	-0,0714	0,357	0,643	0,5	0,43	0,5	0,1	0,357	0,429
OT 18	Ns	1	2	4	6	7	7	7	4	4	6
	No	0	0	1	1	0	0	1	2	1	0
	Nc	15	14	11	9	9	9	8	10	11	10
	ri	0,0625	0,125	0,188	0,313	0,438	0,44	0,38	0,1	0,188	0,375
OT 19	Ns	0	4	3	8	9	8	10	12	9	8
	No	0	1	2	3	0	0	1	0	0	1
	Nc	16	11	11	5	7	8	5	4	7	7
	ri	0	0,1875	0,063	0,313	0,563	0,5	0,56	0,8	0,563	0,438
OT 20	Ns	1	1	5	1	4	6	7	9	12	9
	No	2	2	5	3	0	0	0	0	0	0
	Nc	13	13	6	12	12	10	9	7	4	7
	ri	-0,063	-0,0625	0	-0,125	0,25	0,38	0,44	0,6	0,75	0,563
OT 21	Ns	0	2	2	7		79	10	9	9	11
	No	0	0	0	0	0	0	0	0	0	0
	Nc	13	11	11	6	6	4	3	4	4	2
	ri	0	0,15385	0,154	0,538	0	0,95	0,77	0,7	0,692	0,846
OT 22	Ns	1	1	4	5	7	9	10	10	11	12
	No	0	2	0	0	1	1	1	0	0	0
	Nc	12	10	9	8	5	3	2	3	2	1
	ri	0,0769	-0,0769	0,308	0,385	0,462	0,62	0,69	0,8	0,846	0,923
OT 23	Ns	1	5	6	9	13	11	12	11	12	7
	No	0	0	0	0	0	0	1	0	0	1
	Nc	17	13	12	9	5	7	5	7	6	10
	ri	0,0556	0,27778	0,333	0,5	0,722	0,61	0,61	0,6	0,667	0,333

Time (min.)		1	2	3	4	5	6	7	8	9	10
OT 24	Ns	2	1	5	9	11	12	11	10	11	13
	No	0	0	0	0	0	1	1	0	0	2
	Nc	16	17	13	9	7	5	6	8	7	3
	ri	0,1111	0,05556	0,278	0,5	0,611	0,61	0,56	0,6	0,611	0,611
OT 25	Ns	5	4	2	6	4	11	4	12	14	13
	No	0	3	2	3	3	1	1	0	0	0
	Nc	13	11	14	9	11	6	13	6	4	5
	ri	0,2778	0,05556	0	0,167	0,056	0,56	0,17	0,7	0,778	0,722
OT 26	Ns	1	5	9	7	8	9	8	9	9	7
	No	0	0	0	0	0	0	0	0	0	0
	Nc	10	6	2	4	3	2	3	2	2	4
	ri	0,0909	0,45455	0,818	0,636	0,727	0,82	0,73	0,8	0,818	0,636
OT 27	Ns	8	14	14	15	15	16	15	14	13	16
	No	0	0	0	0	0	0	0	0	1	1
	Nc	12	6	6	5	5	4	5	6	6	3
	ri	0,4	0,7	0,7	0,75	0,75	0,8	0,75	0,7	0,6	0,75
	RI mean	0,0722	0,16829	0,3	0,419	0,456	0,53	0,55	0,6	0,601	0,587
	SD	0,1216	0,22334	0,242	0,231	0,258	0,22	0,18	0,2	0,188	0,192
	SEM	0,0076	0,01396	0,015	0,014	0,016	0,01	0,01	0	0,012	0,012

Table-3.2c: Propionic acid:

Time (min.)		1	2	3	4	5	6	7	8	9	10
OT 28	Exp.No.	Ns	6	6	6	5	7	5	5	6	6
	No	1	0	0	0	0	0	0	0	0	0
	Nc	1	2	2	3	1	3	3	2	2	2
	ri	0,625	0,75	0,75	0,625	0,875	0,63	0,63	0,8	0,75	0,75
OT 29	Ns	2	6	3	3	4	4	3	4	6	6
	No	0	0	1	0	1	0	1	0	0	0
	Nc	6	2	4	5	3	4	4	4	2	2
	ri	0,25	0,75	0,25	0,375	0,375	0,5	0,25	0,5	0,75	0,75
OT 30	Ns	0	3	4	4	5	7	6	7	8	9
	No	0	0	0	3	2	2	1	2	3	0
	Nc	16	13	12	9	9	7	9	7	5	7
	ri	0	0,1875	0,25	0,063	0,188	0,31	0,31	0,3	0,313	0,563
OT 31	Ns	0	1	3	8	9	11	11	10	9	8
	No	0	1	1	0	0	0	0	0	1	0
	Nc	16	14	12	8	7	5	5	6	6	8
	ri	0	0	0,125	0,5	0,563	0,69	0,69	0,6	0,5	0,5
OT 32	Ns	0	2	3	6	6	7	7	4	5	7
	No	0	2	1	0	0	0	1	1	0	4
	Nc	16	12	12	10	10	9	8	11	11	5
	ri	0	0	0,125	0,375	0,375	0,44	0,38	0,2	0,313	0,188
OT 33	Ns	0	4	8	9	9	7	3	4	10	8
	No	0	0	0	3	1	0	0	0	0	1
	Nc	20	12	8	4	6	9	13	12	6	7
	ri	0	0,25	0,5	0,375	0,5	0,44	0,19	0,3	0,625	0,438

Time (min.)		1	2	3	4	5	6	7	8	9	10
Exp.No.											
OT 34	Ns	0	2	3	4	7	6	8	8	7	7
	No	0	0	0	2	2	0	0	1	0	0
	Nc	14	12	11	8	5	8	6	5	7	7
	ri	0	0,14286	0,214	0,143	0,357	0,43	0,57	0,5	0,5	0,5
OT 35	Ns	1	4	10	12	12	11	11	11	11	12
	No	0	1	1	1	2	1	2	1	1	1
	Nc	17	13	7	5	4	6	5	6	6	5
	ri	0,0556	0,16667	0,5	0,611	0,556	0,56	0,5	0,6	0,556	0,611
OT 36	Ns	1	2	4	10	9	10	10	11	12	16
	No	0	0	1	1	3	1	1	2	1	0
	Nc	18	17	14	8	7	8	8	6	6	3
	ri	0,0526	0,10526	0,158	0,474	0,316	0,47	0,47	0,5	0,579	0,842
OT 37	Ns	0	7	12	12	13	13	12	10	10	11
	No	0	1	0	0	0	0	0	0	0	0
	Nc	18	10	6	6	5	5	6	8	8	7
	ri	0	0,33333	0,667	0,667	0,722	0,72	0,67	0,6	0,556	0,611
OT 38	Ns	5	9	11	11	11	9	12	11	10	12
	No	0	0	0	0	0	0	0	0	0	0
	Nc	13	9	7	7	7	9	6	7	8	6
	ri	0,2778	0,5	0,611	0,611	0,611	0,5	0,67	0,6	0,556	0,667
OT 39	Ns	0	5	10	10	13	13	14	12	15	14
	No	0	0	1	1	1	3	1	1	3	2
	Nc	20	15	9	9	6	4	5	7	2	4
	ri	0	0,25	0,45	0,45	0,6	0,5	0,65	0,6	0,6	0,6
OT 40	Ns	5	12	13	12	10	12	11	11	11	11
	No	1	0	0	0	0	0	1	1	1	1
	Nc	8	2	1	2	4	2	2	2	2	2
	ri	0,2857	0,85714	0,929	0,857	0,714	0,86	0,71	0,7	0,714	0,714
OT 41	Ns	3	10	17	19	18	17	17	16	13	10
	No	0	0	0	0	0	1	0	0	1	1
	Nc	17	10	3	1	2	2	3	4	6	4
	ri	0,15	0,5	0,85	0,95	0,9	0,8	0,85	0,8	0,6	0,6
OT 42	Ns	4	15	22	22	23	23	22	21	19	23
	No	2	2	1	1	1	1	2	1	2	1
	Nc	20	9	3	3	2	2	2	4	5	2
	ri	0,0769	0,5	0,808	0,808	0,846	0,85	0,77	0,8	0,654	0,846
	RI mean	0,1182	0,35285	0,479	0,526	0,566	0,58	0,55	0,5	0,571	0,612
	SD	0,1766	0,2768	0,281	0,247	0,217	0,17	0,2	0,2	0,131	0,169
	SEM	0,0118	0,01845	0,019	0,016	0,014	0,01	0,01	0	0,009	0,011

Ns : Number of animals inside the source area

No: Number of animals inside the opposite side

Nc: Number of animals at the central region

3.1.4 Measurement of Response Index (RI) of control flies:

The response indices were calculated, for every minute and for each experiment, based on the respective values of N_s , N_o and N_c and it was calculated by using the following formula:

$$\text{Response Index (RI)} = (N_s - N_o) / (N_s + N_o + N_c).$$

The means of the response indices of each minute for three chemicals used were plotted against the time (Figure 3.3). Here, actually, I was not going to compare the response indices for the chemical used; I was just looking for the times when the maximum number of animals reached the source region.

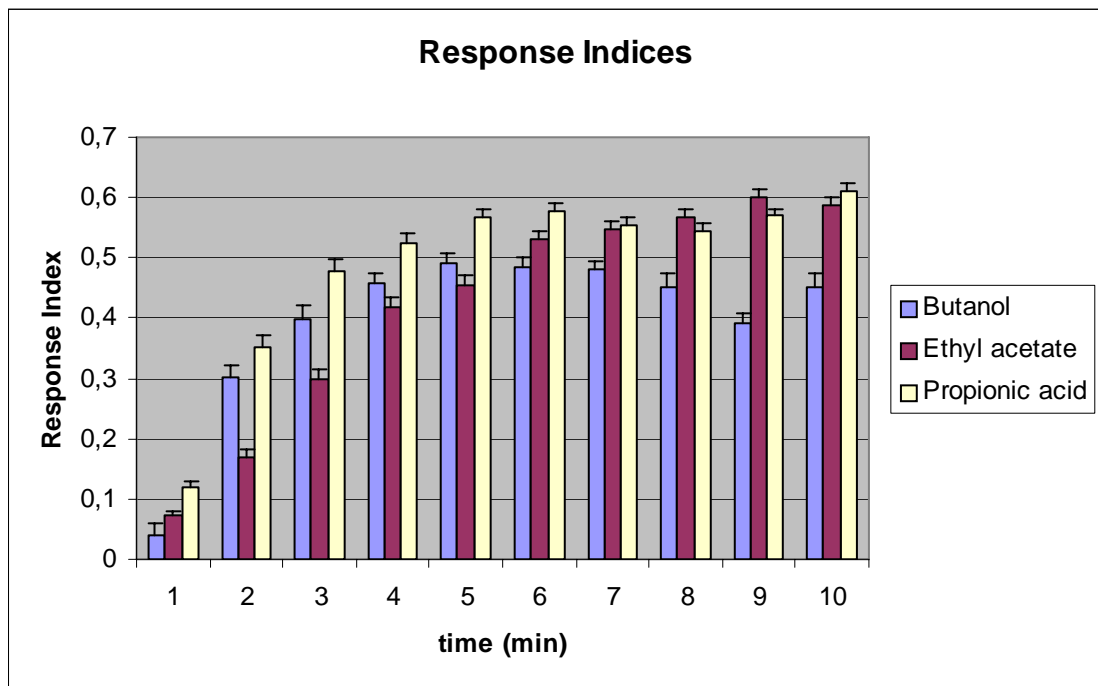


Figure 3.3: Response Index measurement for the chemical butanol (blue), ethyl acetate (red) and propionic acid (yellow). One microlitre of undiluted butanol, ethyl acetate and propionic acid were used. Each bar consists of 11- 15 tests. Error bars indicate SEM.

3.1.5 Olfactory test for ablated flies:

The olfactory tests of the ablated flies were performed in the same manner as for the wild type flies. We used 1 μ l of undiluted Butanol for our experiment. A total number of 9 experiments (7-15 animals each) were performed and the results of these experiments are summarized in Table 3.3.

Table 3.3: Olfactory responses of ablated larvae to butanol

Time (min.)		1	2	3	4	5	6	7	8	9	10
Exp.No.	Ns	0	1	1	2	6	4	6	5	5	5
	OT1ab										
	No	0	1	0	0	0	0	0	0	0	0
	Nc	15	13	14	13	9	11	9	10	10	10
	ri	0	0	0,0667	0,1333	0,4	0,2667	0,4	0,3333	0,3333	0,3333
OT2ab	Ns	1	1	1	1	1	1	1	1	2	4
	No	0	0	2	1	1	1	2	2	2	2
	Nc	7	7	4	6	6	6	5	5	4	2
	ri	0,125	0,125	-0,143	0	0	0	-0,125	-0,125	0	0,25
OT3ab	Ns	0	0	0	0	1	0	0	0	0	1
	No	0	0	0	0	0	0	0	0	0	0
	Nc	4	4	4	4	3	4	4	4	4	3
	ri	0	0	0	0	0,25	0	0	0	0	0,25
OT4ab	Ns	0	1	1	2	2	2	2	2	3	4
	No	0	1	0	0	0	0	0	0	0	0
	Nc	4	2	3	2	2	2	2	2	1	0
	ri	0	0	0,25	0,5	0,5	0,5	0,5	0,5	0,75	1
OT5ab	Ns	0	0	1	2	1	1	1	1	1	1
	No	0	0	0	0	0	1	1	0	1	1
	Nc	4	4	3	2	3	2	2	3	2	2
	ri	0	0	0,25	0,5	0,25	0	0	0,25	0	0
OT6ab	Ns	0	0	1	1	1	1	1	2	2	2
	No	0	0	0	0	0	0	0	0	0	0
	Nc	4	4	3	3	3	3	3	2	2	2
	ri	0	0	0,25	0,25	0,25	0,25	0,25	0,5	0,5	0,5
OT7ab	Ns	1	1	1	1	1	1	1	1	2	2
	No	0	0	0	0	1	0	0	0	0	0
	Nc	3	3	3	3	2	3	3	3	2	2
	ri	0,25	0,25	0,25	0,25	0	0,25	0,25	0,25	0,5	0,5
OT8ab	Ns	1	0	1	2	2	2	2	2	2	2
	No	0	0	0	0	0	0	0	0	0	0
	Nc	3	4	3	2	2	2	2	2	2	2
	ri	0,25	0	0,25	0,5	0,5	0,5	0,5	0,5	0,5	0,5
OT9ab	Ns	0	1	1	1	1	1	1	1	1	1
	No	0	0	0	0	0	0	0	0	0	0
	Nc	4	3	3	3	3	3	3	3	3	3
	ri	0	0,25	0,25	0,25	0,25	0,25	0,25	0,25	0,25	0,25
	RI mean	0,0694	0,0694	0,1582	0,2648	0,2667	0,2241	0,225	0,2731	0,3148	0,3981
	SD	0,1102	0,1102	0,1477	0,2013	0,1837	0,1958	0,2257	0,2216	0,2725	0,2788
	SEM	0,0122	0,0122	0,0164	0,0224	0,0204	0,0218	0,0251	0,0246	0,0303	0,031

3.1.6 Comparison of Response Indices between ablated and control flies in response to butanol:

The mean Response Indices of non ablated flies was compared with that of the ablated flies (Figure 3.4; Table 3.4) and it was found that the RI's of ablated flies are always smaller compared to nonablated flies except in the 1st minute. But it is interesting that the RIs of ablated flies increased with time. This result indicates that the response of ablated flies is initially reduced compared to that of non ablated flies, but the reaching of response index to the extent that of wild type animals also indicates that laser ablation might simply delayed the olfactory sensation process.

Table 3.4: Response index values of ablated and non ablated flies.

Ablated	RI mean	0,0694	0,0694	0,1582	0,2648	0,2667	0,2241	0,225	0,2731	0,3148	0,3981
	SD	0,1102	0,1102	0,1477	0,2013	0,1837	0,1958	0,2257	0,2216	0,2725	0,2788
	SEM	0,0122	0,0122	0,0164	0,0224	0,0204	0,0218	0,0251	0,0246	0,0303	0,031

Non-ablated	RI mean	0,0400	0,3013	0,397	0,457	0,493	0,490	0,480	0,500	0,391	0,451
	SD	0,2092	0,2415	0,258	0,197	0,1700	0,180	0,140	0,300	0,177	0,258
	SEM	0,0190	0,0219	0,023	0,018	0,0150	0,020	0,010	0,00	0,016	0,023

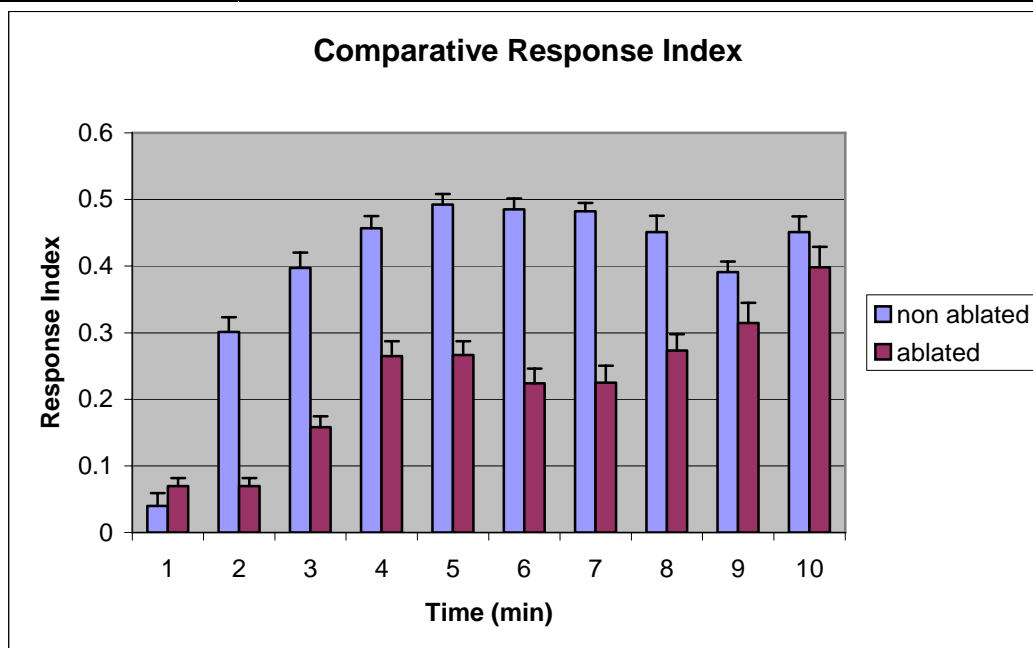


Figure 3.4: comparative response index measurement for ablated (red bar) and non-ablated (blue bar). 1 μ l of undiluted butanol was used. Each bar consists of 8-11 tests and error bars indicates SEM.

3.2 Bolwig's organ (BO) as a test system for the analysis of the specificity and efficiency of ablation:

3.2.1 Differential expression patterns of photoreceptor cells in BO confer a strategical approach for determination of the specificity and efficiency of laser ablation:

In laser ablation and laser heat shock experiments, specificity and the efficiency of the ablation events should be very much perfect and precise. To analyse the specificity and efficiency of ablation we chose Bolwig's organ as a model system. The reasons behind selecting Bolwig's organ as model systems are based

on the differential expression patterns of photoreceptor cells in Bolwig's organ (BO). Bolwig's organ (Bolwig 1946), the so called larval eye, is a bilateral cluster of 12 photoreceptor cells close to the larval mouth hook (Figure 3.5) derived from a

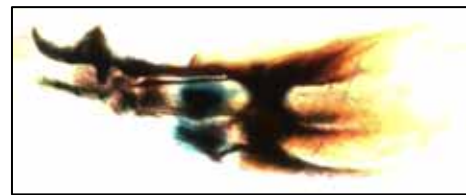


Figure 3.5: Bolwig's organs (blue) at mouth hook

coherent group of approximately 30 cells of the optic lobe placode (Grenningloh, Rehm et al. 1991; Schmucker, Jackle et al. 1997) described the progressive development of BO and the establishment of Bolwig's nerve (BN). The basic principle lying behind our objective is the differential expression of rhodopsin types within the 12 cells of the BO. BO was reported to express immunoreactivity to Rh1, Rh3 and Rh4 (Pollock and Benzer 1988) and recently it was found that Rh5 and Rh6 are also expressed in BO (Helfrich-Forster,

Edwards et al. 2002; Malpel, Klarsfeld et al. 2002). Malpel et al. (2002) reported that confocal reconstruction by double staining of the BN (Figure 3.6) in a *w; rh6-gfp/rh5-lacZ* larvae show that rh5 and rh6 are expressed in different cells.

Based on these observations we tried to use this system to evaluate the efficiency as well as the specificity of laser ablation technique. We could assess the efficiency of laser ablation by ablating one of the two BOs at the embryonic stage and looking for the unilateral damage at L3 stage. On the other hand, one could determine the specificity of the laser ablation technique by specifically ablating the group of

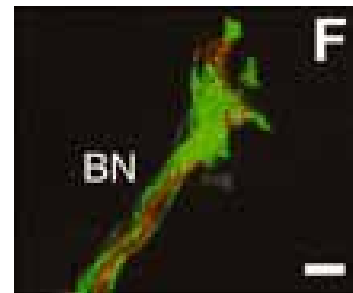


Figure 3.6: Confocal reconstruction by double staining of the BN in larvae (*w; rh6-gfp/rh5-lacZ*) shows that rh5 (red) and rh6 (green) are expressed in different cells (Malpel et al. 2002).

cells express a particular rhodopsin molecule in the BO without affecting the rest of the cells express other type of rhodopsin molecule.

3.2.2 Observations on the different marker gene expression patterns in BO:

A number of stocks were analyzed for the expression patterns of GFP and LacZ in the BO. The stocks used in the study are shown in Table 3.5. The stocks either show rh5 or rh6 promotor-controlled expression of marker genes or both markers are expressed in the same stocks by two different rhodopsin promoters. For instance, in lines *rh5-tau-lacZ* (III) [325] and *rh6-tau-lacZ* (III) [581], a *tau:lacZ* fusion marker is expressed under the control of the rh5 and rh6 promoters, respectively. In line *y w rh5-lacZ; rh6-GFP/CyO* [1016], lacZ expression is governed by the rh5 promoter and GFP expression is mediated by the rh6 promoter. We have noticed strong lacZ expression patterns in all lines (Figure 3.6). Expression starts in late stage embryos (st16-st17) and gets stronger in L1 and L3. We have also analyzed the GFP expression patterns in line *y w rh5-lacZ; rh6-GFP/CyO* [1016] and strong GFP expression was observed

in L1 larvae. But one problem was, in respect to the specificity dertermination of the laser ablation technique, to observe the discreet staining of GFP in the individual cells in the cell cluster of BO. So, we are not sure whether during the ablation of GFP expressing cells, LacZ expressing cells in BO were also damaged.

We have also analyzed the GFP

expression patterns in *rh5-Gal4 (II)* [569] line (figure 3.7) using four different UAS-GFP responder lines (see table 3.5). No embryonic expression was noticed, but 1st larval instar expression was apparent with all four *UAS:GFP* responders.

Sl.No.	Genotype	Stock
1	<i>rh5-tau-lacZ (X)</i>	600
2	<i>rh5-tau-lacZ (III)</i>	325
3	<i>rh6-tau-lacZ (III)</i>	581
4	<i>rh6-tau-lacZ (II)</i>	582
5	<i>w ; rh6-GFP/CyO</i>	277
6	<i>rh5-Gal4 (II)</i>	569
7	<i>w ; Cyo/Sp ; rh6-Gal4/TM2</i>	990
8	<i>y w rh5-lacZ; rh6-GFP/CyO</i>	1016
9	<i>UAS:GFPnls</i>	291
10	<i>UAS:GFPnls</i>	284
11	<i>UAS:GFP</i>	303
12	<i>w; UAS:GFP(nls) stinger</i>	1062

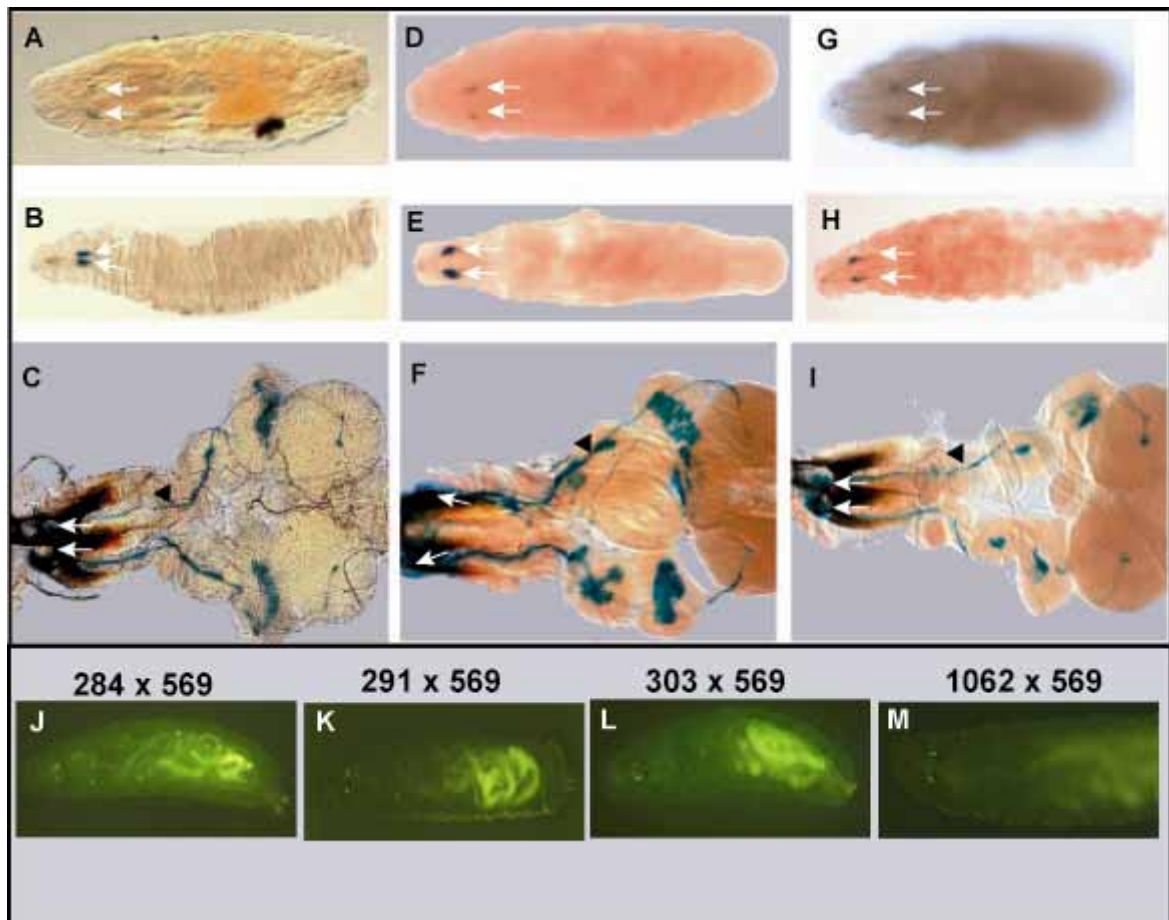


Figure 3.7: X-gal staining of different rhodopsin-lacZ constructs and GFP expression of rhodopsin-Gal4 construct. Expression starts at late stage embryos (st 17) [A, D and G] and becomes very prominent at 1st to 3rd Instar larvae (B-I). White arrows indicate BO and black arrow heads (in C, F, I) indicate Bolwig's Nerve (BN). A, B and C from line *rh5-tau-lacZ* (III); D, E and F from line *rh6-tau-lacZ* (III); G, H and I from line *y w rh5-lacZ; rh6-GFP/CyO*. J-M: GFP expression patterns at L1 from crosses with different *UAS:GFP* responder lines (mentioned in the picture).

3.2.3 Strategy for the determination of the specificity and efficiency of laser ablation:

Line *y w rh5-lacZ; rh6-GFP/CyO* (1016) and line *rh6-tau-lacZ* (III) (581) were selected for further studies regarding the efficiency determination of laser ablation.

The basic strategy behind our experiment was bringing together the expression of both GFP and lacZ under the control of one type of rhodopsin promoter. To achieve this goal,

females from *rh6-tau-lacZ (III)* (581) were crossed with males from *y w rh5-lacZ; rh6-GFP/CyO* (1016). Female larvae from this cross express lacZ under the control of both rh5 and rh6 and GFP is under the control of rh6. If laser ablation of GFP-expressing rh6-positive cells in BO were specific for rh6-positive cells, there should remain X-gal expression in the residual rh5-positive cells. The relevant genotypes of the larvae from the cross and the unilateral ablation of BO are shown in figure 3.8. Due to time limitations, the X-gal staining analysis of the ablated larvae was not performed.

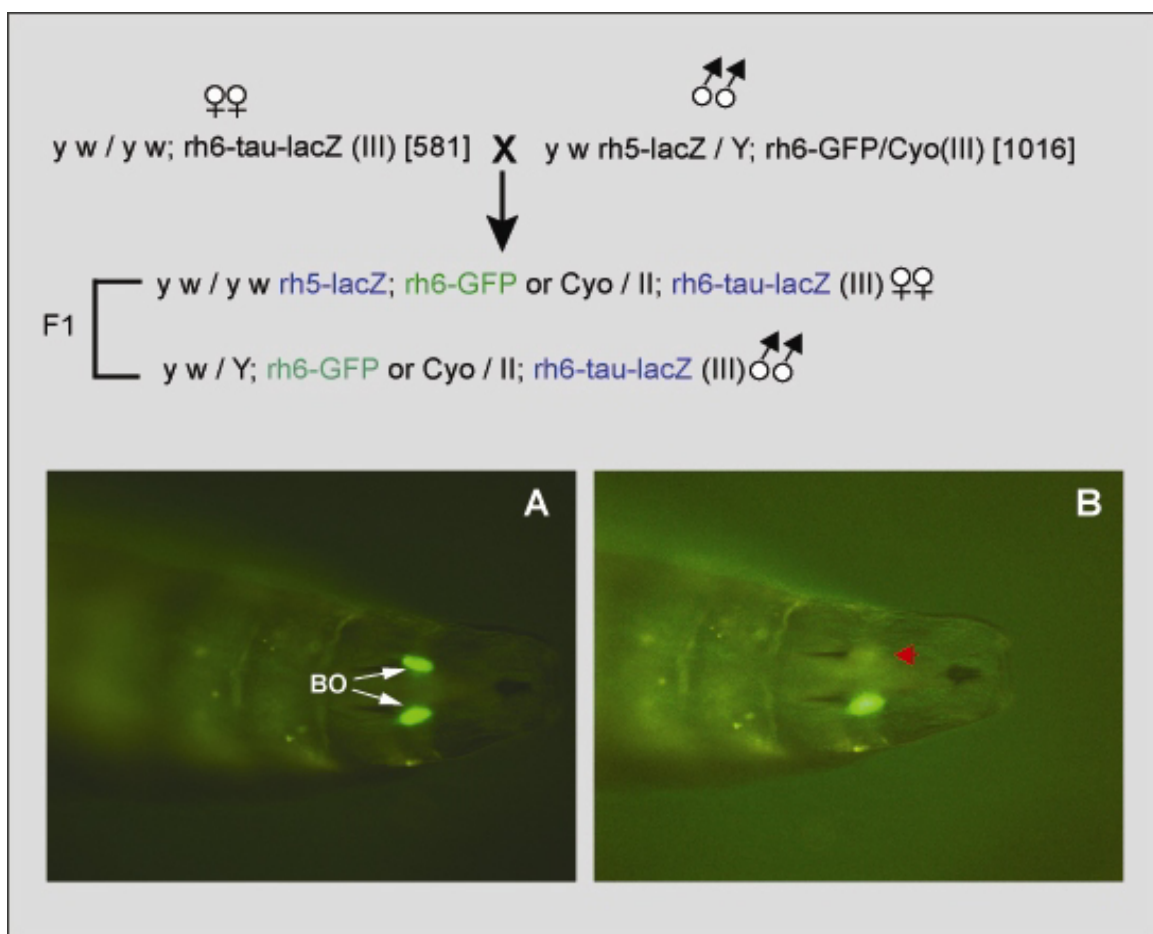


Figure 3.8: Determination the specificity and efficiency of laser ablation. Top panel shows the cross and relevant genotypes of the F1 larvae. Bolwig's organ is shown in larvae before (A) and after unilateral ablation (B). The ablated BO (in B) is pointed out by a red arrow head.

3.3 Ablations within the embryonic / larval optic lobe anlage:

The objective of my studies was to find out whether precursor cell(s), which give rise to the lobula plate giant neurons (LPGNs) in adult flies, can be identified in the structure of the early visual system in *Drosophila*. Details of the development and structure of the *Drosophila* embryonic and larval visual system have already been described (Green, Hartenstein et al. 1993; Schmucker, Jackle et al. 1997; Holmes, Raper et al. 1998). The relationship among the embryonic, larval and adult visual system has been explored with various fate mapping studies and cell ablation experiments and it has been shown that the larval eye-imaginal disc, which gives rise to the adult eyes, develops from the dorsal part of the embryonic head (Jurgens, Lehmann et al. 1986; Meinertzhagen and Hanson 1993). In my study, first, I wanted to identify *omb-Gal4* lines and/or *omb-GFP* direct fusion constructs which allow to visualize the embryonic OLA upon crossing with a UAS:GFP responder line. In a second step, A122, which gives nuclear lacZ expression in the HS/VS cells in the adult optic lobe, was recombined to the selected *omb-Gal4* to. A number of lines were characterized with regard to GFP expression pattern in the OLA of stage 16-17 embryos. Different lines used for the study are listed in table 3.6.

3.3.1 Characterisation of the relevant lines and crosses:

omb-J-Gal4:

Females from two different *UAS-GFP* responder lines (line 284 and line 291) were used for crossing with *omb-J-Gal4* males (line 438). These two crosses did not show selective expression in the optic lobe anlagen. Strong expression was observed in the salivary glands (Figure 3.9, panel A) apparently obscuring a potential OLA expression. Hofmeyer (2001, figure 50) using double staining and confocal fluorescence microscopy has shown that the posterior part of this expression pattern overlaps with the OLA. For my purpose (laser ablation under conventional fluorescence microscopy), the *ombJ-Gal4* line was not useful. It was shown that some P-element constructs carry a fortuitous salivary gland enhancer element and that removal of the leader enhancer sequence in the 5' UTR of the *Gal4* mRNA abolishes the expression of GFP in salivary gland (Gerlitz, Nellen et al. 2002).

omb-J-GFP (“OLA-GFP”):

In two direct enhancer reporter fusion constructs (*omb-J-GFP*), GFP expression is directly controlled by the *omb-J* regulatory element. No expression in the OLA was found in these constructs (data not shown). The weaker expression of *omb-J-lacZ* direct fusion constructs as compared to the expression from the indirect *omb-J-Gal4* construct using the UAS-*GAL4* mechanism was discussed by Hofmeyer (Hofmeyer, 2001).

A122; omb-J-Gal4:

The A122; *omb-J-Gal4* line (397) was crossed to two different UAS-GFP responder lines (284 and 291). No selective expression was observed in the optic lobe anlage, but strong expression was found in the salivary glands (Figure 3.9, panel B). This was expected from the parent chromosome (see above)

omb^{P3}-Gal4:

Females from *omb^{P3}-Gal4* line (line 55) were crossed to males from four different UAS-GFP responder lines. GFP expression in the OLA was found (Figure 3.9, panel C). These lines were subsequently used in the ablation studies. Expression in the parts of peripheral nervous system was also observed.

omb^{P4}-Gal4:

The *omb* enhancer trapline *omb^{P4}-Gal4* (line 47), where the *Gal4* element is inserted in an intron of *omb*, was crossed to four different UAS: GFP responder lines (lines 284, 291, 303, and 1062). In none of the crosses, expression was observed in the OLA. But in contrast, the same type of enhancer trap line, where the *Gal4* element is inserted in the upstream region (*omb^{P3}*), was able to give the desired expression (see above). Some expression in the peripheral nervous system was found in combination with line 1062 (Figure 3.9, panel C).

omb^{P6}-Gal4 and omb^{P7}-Gal4:

The *omb* enhancer trap line *omb^{P6}-Gal4* (line 504) and *omb^{P7}-Gal4* (line 742), where *Gal4* element is inserted directly upstream of the second exon of *omb*, were crossed to four different UAS: GFP responder lines. With one exception, no expression of GFP in the OLA was observed (Figure 3.9, panel C). Surprisingly, expression in OLA was observed in the combination of *omb^{P6}-Gal4* with *UAS:GFP* (line 303).

Table-3.6: Relevant genotypes of different omb-Gal4 lines and crosses

<u>Relevant genotype (GOP stock number)</u>
<i>UAS:GFPnls females</i> (284) x <i>omb-J-Gal4 males</i> (438)
<i>UAS:GFPnls females</i> (291) x <i>omb-J-Gal4 males</i> (438)
<i>omb-J-GFP</i> (“OLA-GFP”), line270
A122; <i>omb-J-Gal4</i> (397) x <i>UAS:GFPnls</i> (284)
A122; <i>omb-J-Gal4</i> (397) x <i>UAS:GFPnls</i> (291)
<i>omb^{P3}-Gal4 females</i> (55) x <i>UAS:GFPnls males</i> (284)
<i>omb^{P3}-Gal4 females</i> (55) x <i>UAS:GFPnls males</i> (291)
<i>omb^{P3}-Gal4 females</i> (55) x <i>UAS:GFP males</i> (303)
<i>omb^{P3}-Gal4 females</i> (55) x <i>UAS:GFPnls –stinger males</i> (1062)
<i>omb^{P4}-Gal4 females</i> (47) x <i>UAS:GFPnls males</i> (284)
<i>omb^{P4}-Gal4 females</i> (47) x <i>UAS:GFPnls males</i> (291)
<i>omb^{P4}-Gal4 females</i> (47) x <i>UAS:GFP males</i> (303)
<i>omb^{P4}-Gal4 females</i> (47) x <i>UAS:GFPnls–stinger males</i> (1062)
<i>omb^{P6}-Gal4 females</i> (504) x <i>UAS:GFPnls males</i> (284)
<i>omb^{P6}-Gal4 females</i> (504) x <i>UAS:GFPnls males</i> (291)
<i>omb^{P6}-Gal4 females</i> (504) x <i>UAS:GFP males</i> (303)
<i>omb^{P6}-Gal4 females</i> (504) x <i>UAS:GFPnls –stinger males</i> (1062)
<i>omb^{P7}-Gal4 females</i> (742) x <i>UAS:GFPnls males</i> (284)
<i>omb^{P7}-Gal4 females</i> (742) x <i>UAS:GFPnls males</i> (291)
<i>omb^{P7}-Gal4 females</i> (742) x <i>UAS:GFP males</i> (303)
<i>omb^{P7}-Gal4 females</i> (742) x <i>UAS:GFPnls –stinger males</i> (1062)

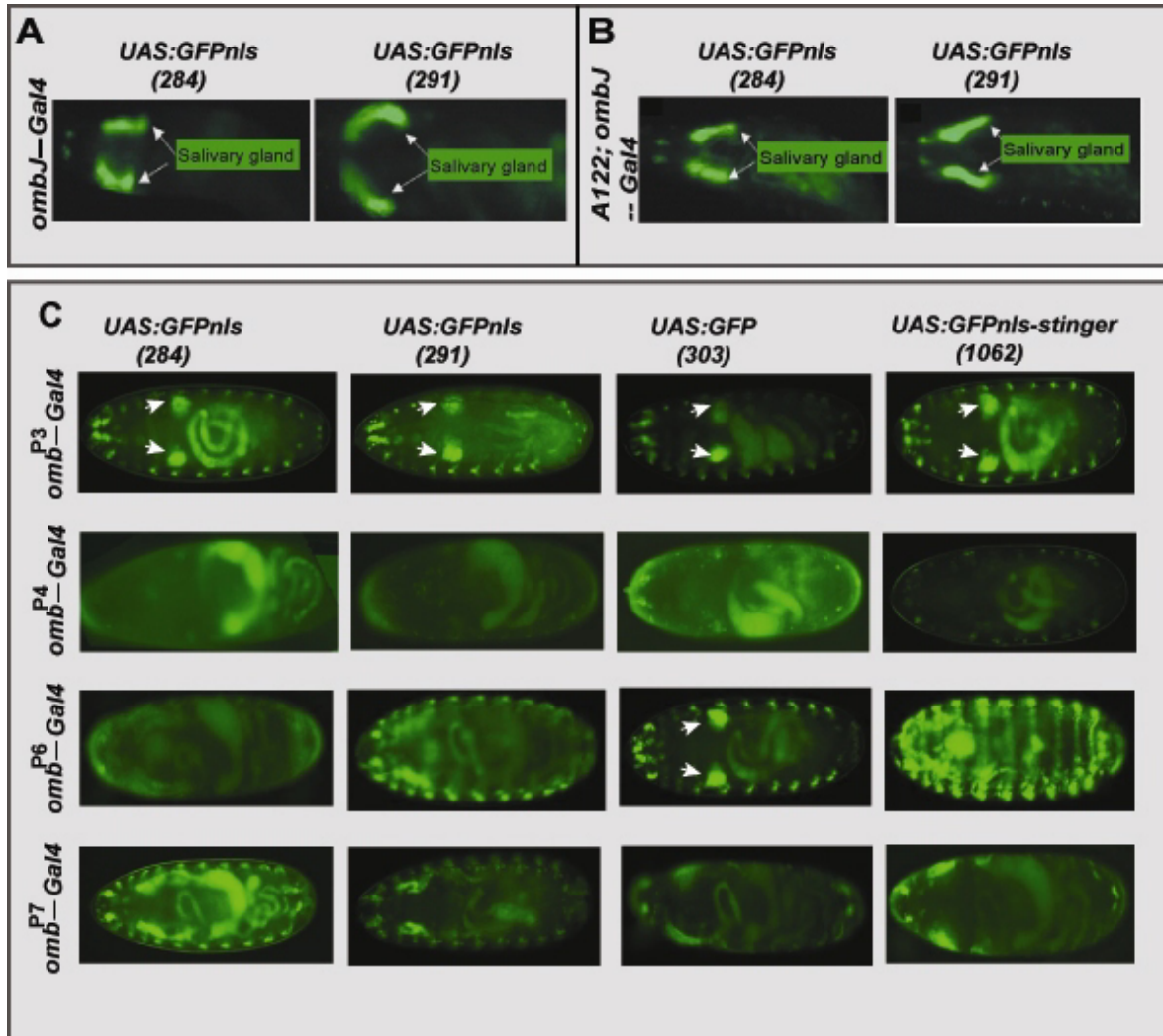


Figure 3.9: Characterization of different *omb-Gal4* lines. Relevant genotypes are given in each case. The direction of crosses is given in table 3.6. No GFP expression in OLA, but salivary glands was found in *ombJ-Gal4* (panel A) and *A122; ombJ-Gal4* (panel B) lines. Only *omb^{P3}-Gal4* line is able to give GFP expression in OLA with all UAS:GFP responders; expression in OLA is found in *omb^{P6}-Gal4* line with one UAS:GFP responder (line 303) [panel C]

3.3.2 Localization of HS/VS precursor cell(s) in the OLA of the *Drosophila* embryo

3.3.2.1 Characterisation of *omb^{P3}-A122*:

For identifying presumptive embryonic HS/VS precursor cell(s) we have chosen the enhancer-trap line *omb^{P3}-A122* (1023) where the P-element from enhancer-trap line A122 is recombined on to the *omb^{P3}-Gal4* chromosome. The enhancer-trap insertion A122 containing P[*lArB*] enhancer trap element gives a unique nuclear expression of the β -galactosidase in the adult lobula plate giant neurons. Although the highly specific expression of *lacZ* in HS/VS cells is found in adult brain staining, no or very little expression was reported during embryonic or larval development (Kerscher, Albert et al. 1995). In our case, line *omb^{P3}-A122* (1023) shows the GFP expression pattern in the embryonic OLA upon crossing with the *UAS:GFPnls* responder line (291) and *lacZ* expression in HS/VS neurons in the adult the optic lobe (Figure 3.10). Hence this line was useful to identify the potential precursor cells (if present among the GFP marked cells) by eliminating them at embryonic stage by unilateral ablation and see if HS/VS cells marked by *lacZ* expression are present or absent in the ablated side.

Assuming that one or more GFP labelled cells in the embryonic OLA might represent the precursor cell(s) for the adult HS/VS neurons, we tried

to divide the total cell population in the OLA into different arbitrary positions as seen from the dorsal side of the embryo (see figure 3.11). Those locations were designated as anterior half, posterior half, medial or lateral of anterior and posterior half etc. Ablation was done

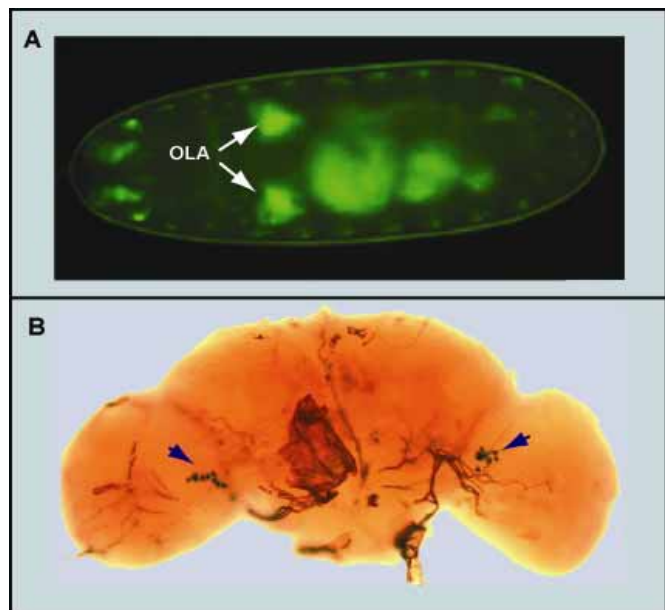


Figure 3.10: Expression patterns of line *omb^{P3}-A122* (1023). A: GFP expression in OLA using *UAS:GFPnls* responder line 291. B: *LacZ* expression in HS/VS neurons (arrow head) in the adult optic lobes.

in these different arbitrary positions and one of such locations is shown before and after ablation (see figure 311 C). For our experiments females from line *ombP³-A122* (1023) were crossed to males from line *UAS: GFP* (291) and embryos were collected for ablations at 18 hrs of egg deposition at 25°C.

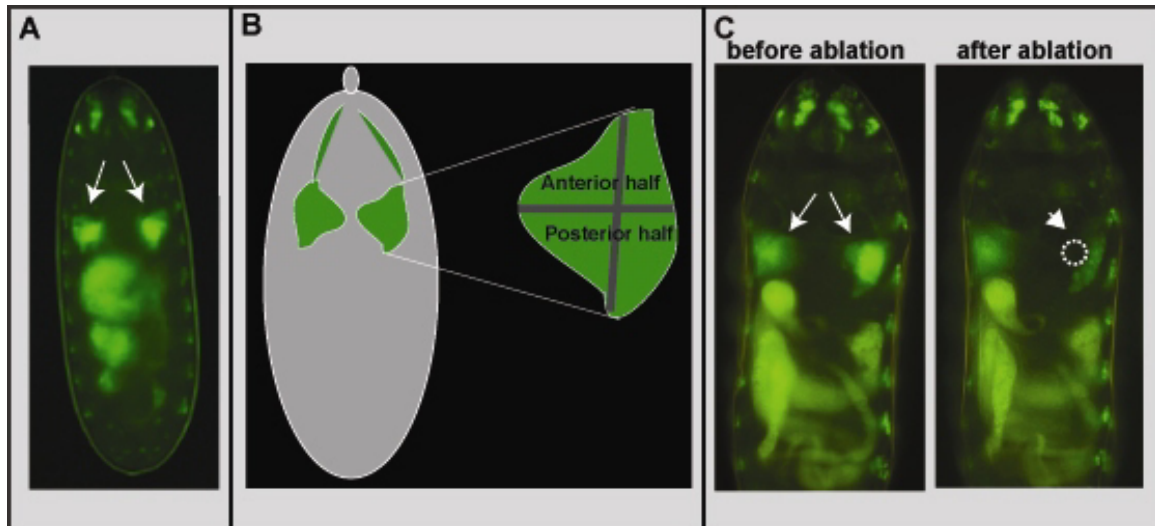

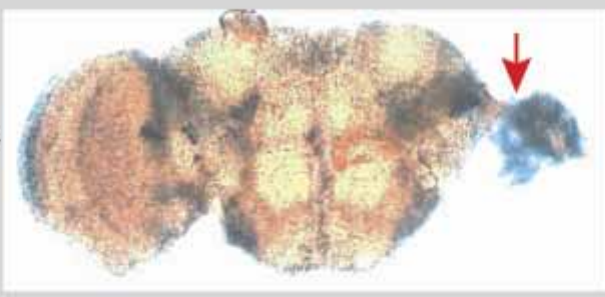



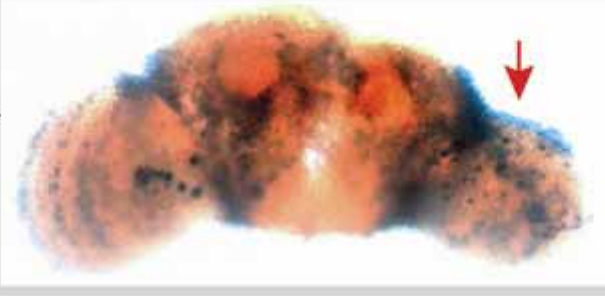






Figure 3.11: Strategy for ablations in the OLA (Anterior is up). A: OLA (white arrow) in embryos from *omb^{P3}-A122* (1023) x *UAS-GFPnls* (291) cross. B: Graphic showing arbitrary system of coordinates in OLA used during ablation experiments. C: Cells in a particular location (white open circle) of one OLA (arrow head) were ablated by laser microbeam.

3.3.2.2 Effects of ablations in different parts of the OLA:

Absence of HS and VS neurons and deformations of adult optic lobe structure:

As described in the previous section, we started ablations in different parts of the OLA and determined the presence of HS and VS cells in the adult optic lobe after X-gal staining. We observed a variety of results ranging from structural deformities of the optic lobes (partially or strongly damaged optic lobe), weak structural connectivity of optic lobe with the central brain due to the absence of HS and VS cells and probably other projection neurons in the optic lobe. These altered phenotypes of adult optic lobe structure were observed in combination in most of the cases where the ablation area was relatively broad. Some of the findings are shown in figure 3.12. At the end we were able to identify a group of cells at a particular location in the OLA where ablation had little effect on the overall structure of the optic lobe but eliminated the HS/VS cells from the adult optic lobe.

		HS/VS cells
		+
		+
		-
		-
		-




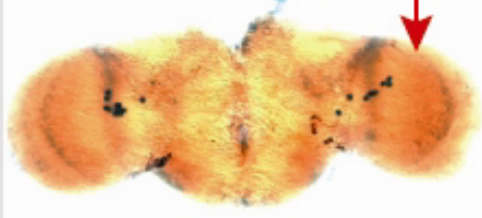

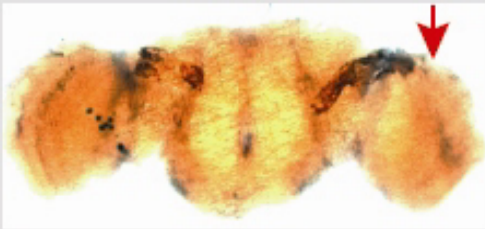
		HS/VS cells +
		+
		-

Figure 3.12: Effects of ablations in different locations in the OLA. Ablation regions are shown in red in the schematic diagram of whole embryo or in individual OLA and ablated sides of the brains (dorsal view) are indicated by red arrow. Presence (+) or absence (-) of HS/VS cells is indicated in the right panel.

Suspected migration or relocation of HS and VS cell bodies in the ablated side:

Damaged optic lobes and in a few cases, attenuated connections of the optic lobe to the central brain region were noticed in the ablated side of the OLA (figure 3.12). The extent of damage or malformation was related to the extent of ablation. But in some cases, where tissue in the optic lobes was damaged severely, HS and VS neurons were still present at the junction of optic lobe and the central brain and it seemed that HS/VS cell bodies were relocated toward the unaffected central brain region (see figure 3.13C). The location of the HS/VS cell bodies in the optic lobe varies from fly to fly in the wildtype too. In many cases, HS/VS cells were still present in their normal location when the damage of optic lobe was severe (figure 3.13A-B).

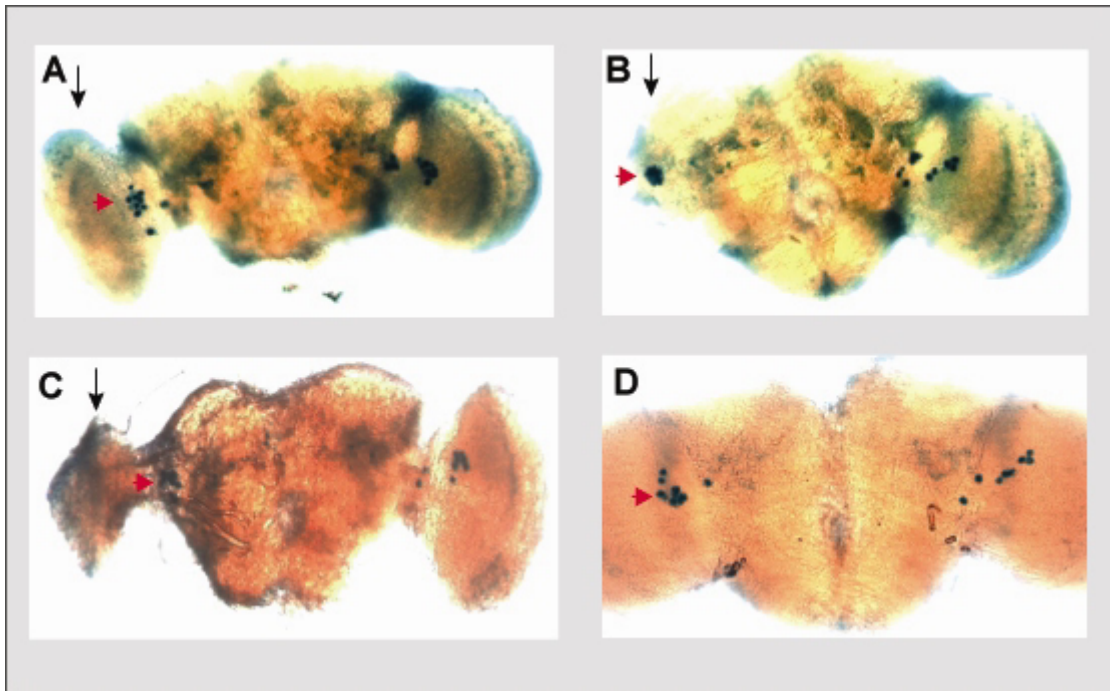


Figure 3.13: location of HS/VS cell bodies in the adult optic lobe. A and B: HS/VS cell bodies in severely damages optic lobe; C: suspected relocation of HS/VS cells towards the central brain; D: non ablated control brain. Arrow denotes ablated side. The HS/VS cells are shown in red arrow head.

3.4 Standardization of SELEX for the determination of OMB target selectivity:

"SELEX" (systematic evolution of ligands by exponential enrichment) is also known as "in vitro selection" or "in vitro evolution". One can simultaneous screen a highly diverse pool of different RNA or DNA molecules for binding affinity by using the SELEX technique. The two main components of this technique are the protein molecules for which the target is to be selected and the diverse pool of different RNA or DNA molecules from which the target has to be selected. The whole process has to be standardized before the actual selection experiment is done. The main steps involved in the process are as follows:

- i) making a degenerate pool of template DNA for SELEX, ii) preparing a DNA fragment which will serve as a positive control template during protein-DNA binding reaction, iii)

cloning of DNA fragments selected from the final cycle of the selection process. The first two steps mentioned above are presented in the materials and methods section.

Establishment of ligation conditions:

PCR products (pool) from selexHB random-92 using selexHBfor and selexHBrev were digested with *Bam*HI to generate a pool of 46 bp fragments. After digestion by *Bam*HI, 46 bp degenerate fragments and 23 bp tails from both ends were obtained. But a substantial amount of another fragments of about 70 bp (Figure 3.14) was also produced. This might come from the partial digestion of the 92 bp fragment producing 69 bp and 23 bp fragments. The 46 bp fragments were extracted and purified from the polyacrylamide gel.

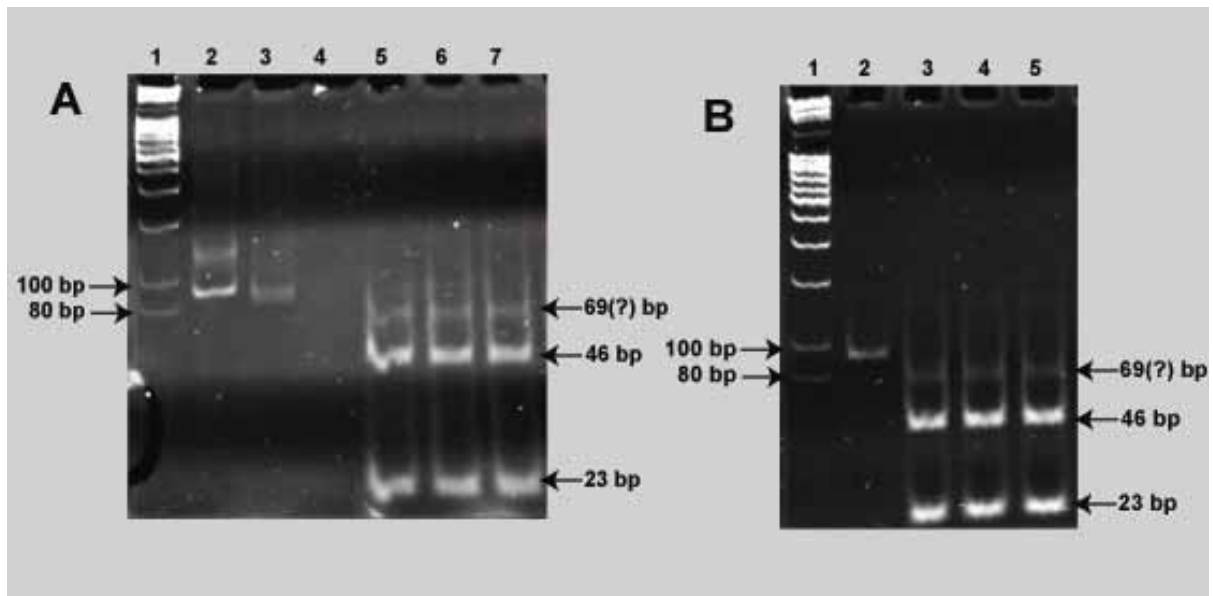


Figure 3.14: Standardization of PCR for efficient *Bam*HI digestion of amplified PCR pool. *Bam*HI digestion of PCR pool generated by 25 cycles of amplification (A) and 15 cycles of amplification (B). A: lane 1- Mass ruler (MBI); lane 2-PCR product from selexHB random-92; lane 3- *Hind*III digested PCR product (sample at lane 2); lane 5-7: *Bam*HI digested PCR product (sample at lane 2); B: lane 1- Mass ruler (MBI); lane 2-PCR product from selexHB random-92; lane 3-5: *Bam*HI digested PCR product from selexHB random-92

Self ligation was set up using the purified 46bp fragments with the purpose of generating 500 to 700 bp oligomers for sequencing. Ligation reaction was incubated at 22°C for 24h. Self-ligated products were checked on PAGE, but I did not see any multimeric ligated products ranging between 500 to 700 bp on the gel and it was assumed that the amount of

ligated products was too small to be seen on the gel. To overcome this problem, I purified the self ligated products through Qiagen PCR purification kit. It was assumed that, at least, monomers and the self ligated dimers will not be retained because only DNA fragments >100bp are retained by the column. The self-ligated material was then cloned into *Bam*HI digested pBluscript II KS (-) vector. Ten colonies each were pooled and PCR was set up using T7 and T3 primers. Products having different sizes were obtained from each amplification reaction (Figure 3.15). Colony PCR was set up using the T7 and T3 primers on individual colonies from pools which gave higher size products in PCR. For instance, individual colonies from pool 3 and pool 5 (lane 4 and 6, Figure 3.15A) were subjected to the colony PCR and it was found that some of the colonies (Figure 3.15B: lane 7 from pool 3 and lane 14 from pool 5) represent clones containing a product size of 500 bp to 1kb. Initially, a total number of 9 representative clones, named as pN40(1) to pN40(9), were selected and one of them was sequenced. It was found that the clone which was sequenced contained 19 different 46 bp fragments (see Box 3.1 and Table 3.7). These results indicate that improvements in ligation conditions might help to achieve a higher percentage of individual clones having a fragment size >500 bp.

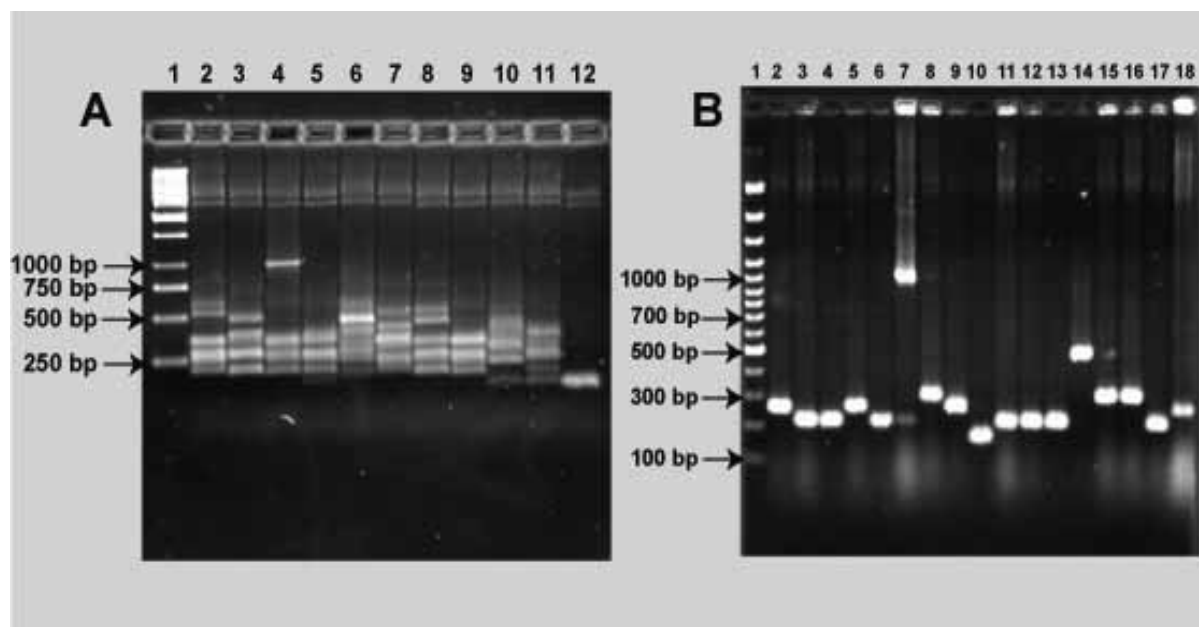


Figure 3.15: Screening strategy for potential clones of target molecules in SELEX. A: each lane shows the PCR products from a single pool of 10 colonies. 10 such pools were investigated. B: PCR from individual colonies of the selected pools from A [pool 3 (A: lane 4) and pool 5 (A: lane 6)] which show candidate clones having higher multimers of target molecules.

Box 3.1: Sequence of one candidate clone selected after screening by PCR (see figure 3.13):

Complete sequence of the clone pN40(1): **Vector sequence**

```

1   GNANCTCAC CGCGGTGGCG GCCGCTCTAG AACTAGTGGG TCC AAGTTTC
51  CATCCCATAG ACCAAAGAAA GACGAAAACA ATCGGATCCA GCCCTCAGTA
101 TTACTACTTT GGAACATTCG AACGCGCGGG GATCCGACCC CACAGACATT
151 GCGAAGTCGG CCCACCATCA CGCTCGGATC CTGGCACGGG GACTCCGGAG
201 GGGTAATACT TGGTCGTAGA TGGATCC TAA CAGGCGCATT TGTTATCTTC
251 GAATAAAGGC CATCCC GGA TCC CCGGACA ACCAATGAGA TGTTGTCTTT
301 CAGGCAAGAT TCG GATCCG TGCTCGTAAA GCGCAATTGA TACAGAATTC
351 CAGTTGGAA G GATCC AATGA CCATGAGCAG CCGCATATAT ACAATCCCTG
401 GGAATGGATC C AGTGGGGTTC GGGCGTGGCG TGTCGGGCGT GGAAGCATAT
451 AGGATCC TAG GGTCTGTATC ATAGATGGGT GCAGGGGACG GGCTGGTGG
501 ATCC AGTTCT GATCCCCTCT TACCCAAGTT CTGTGACAGA GAAAGGATCC
551 TCGGTACGTC TCCGTTGTGG GGAGAAATACA GTAAATGTCT GGATCC GCCC
601 AACGAGACGA AAGACAAGCC TAGCGGCGGC AGACCGGAT CC AAGTGGTA
651 ATAGCAGCAC ACCGGATGCA CACACTCAG CGGGATCCGG GGAACGCTGC
701 AGATGCTAAC TATTAGCACC CCAGGACTGG ATCC CTGATG GGGGCGAGAC
751 CGCTGGCCG ACCGGGTTC GATCGGATCC ATGCGCAGGG AGGGATCGGG
801 GCCCGGTATA ACGCACAAGT GGATCC CTGA TGGGCGCATC AACACTGGGG
851 AGTAATACGA TTTGCAAGAT CCTTTGACTC ACAAACAAA AGATCCAAAT
901 CTCTTCCAA CCGGATCCC CGGGCTGCAG GAATTCGATA TCAAGCTTAT
951 CGATACCGTC GACCTCGAGG GGGGGCCCG TACCAGTTTT

```

Table 3.7: sequences of 19 different fragments in clone pN40(1)

Fragment No.	Sequence (from 5')
1	AAGTTTCCATCCCATAGACCAAAGAAAGACGAAAACAATC
2	AGCCCTCAGTATTACTACTTTGGAACATTCGAACGCGCGG
3	GACCCACAGACATTGCGAAGTCGGCCCACCATCACGCTC
4	TGGCACGGGGACTCCGGAGGGGTAATACTTGGTCGTAGAT
5	TAACAGGCGCATTGTGTTATCTTCAATAAAGGCCATCCCC
6	CCGGACAACCAATGAGATGTTGTCTTTCAGGCAAGATTCG
7	GTGCTCGTAAAGCGCAATTGATACAGAATTCAGTTGGAA
8	AATGACCATGAGCAGCCGCATATATACAATCCCTGGGAAT
9	AGTGGGGTCGGGCGTGGCGTGTCCGGGCGTGGAAAGCATATA
10	TAGGGTCGTTATCATAGATGGGTGCAGGGACGGGCCTGGT
11	AGTTCTGATCCCCCTTTACCCAAGTTCTGTGACAGAGAAA
12	TCGGTACGTCTCCGTTGTGGGGAGAATACAGTAAATGTCT
13	GCCCAACGAGACGAAAGACAAGCCTAGCGGCGGCAGACGC
14	AAGTGGTAATAGCAGCACACCGGATGCACACACTTCAGCG
15	GGGGAACGCTGCAGATGCTAACTATTAGCACCCCAGGACT
16	CTGATGGGGGCGAGACCGCTGGCCGACCGGGTTCAGATC
17	ATGCGCAGGGAGGGATCGGGGCCGCTATAACGCACAAGT
18	CTGATGGGCGCATCAACACTGGGGAGTAATACGATTTGCA
19	TTTACTCACAAAACAAAAGATCCAAATCTCTTCCAACC

3.5 Genetic and molecular characterization of lethal *omb* mutant lines

3.5.1 Genetic characterization of lethal *omb* mutants

3.5.1.1 Purification of the stock *l(1)omb[12]/ FM7a,vw; II (171)*:

In one of the four lethal *omb* mutants, line *l(1)omb[12]/ FM7a,vw; II (171)*, a second site lethality appeared to be located on the X-chromosome that could not be rescued by the duplication *DpA1125*, which covers the *omb* locus. We tried to separate the second mutation from the locus by recombination. The genetic crosses involved in the purification steps are outlined in the Materials and Methods section. Out of 176 crosses set up initially, we were able to identify six potentially purified lines based on the F1 progeny (see Table 3.8) from cross E3. The selected lines were then tested by crossing females with males from line *w l(1)omb[D4]/Y; DpA1125/ln(2LR),Gla Bc (395)*. Males from the F1 progeny having the *l(1)omb[12]/Y; DpA1125/II* genotype should have red round eyes, if the second mutation is removed. We found that all six lines produced males with red round eyes in F1 (see Table 3.9). Three stocks were taken for stable stock maintenance and complementation tests for HS/V5 cell development.

Table 3.8: Phenotype (eye) analysis of F1 progenies from eight E3 crosses:

	Female		male	
	<i>B</i>, red	<i>B/B</i>, <i>w^a</i>	<i>B</i>, <i>w^a</i>	Red, round
E3 ⁶	61	15	15	33
E3 ¹⁰	35	22	20	0
E3 ¹³	45	22	13	0
E3 ³²	42	21	33	0
E3 ⁵⁹	41	16	20	0
E3 ⁶³	20	25	22	0
E3 ¹⁰³	16	9	26	0
E3 ¹¹⁰	25	5	14	7

Note: All stocks were tested for presence of a lethal factor on the X- chromosome In six stocks Bar, white-apricot males were found in considerable number.

Table 3.9: Phenotype (eye) analysis of F1 progenies from eight E4 crosses:

	female				male			
	<i>Bar(B), w^a</i>	<i>Gla, w^a, B/B</i>	<i>vermilion, round eye</i>	<i>Gla, red-round eye</i>	<i>Bar(B), w^a</i>	<i>Gla, w^a, B</i>	<i>red, round eye</i>	<i>Gla, red-round eye</i>
E4 ⁶	11	6	18	17	8	10	19	10
E4 ¹⁰	12	12	14	0	10	5	4	0
E4 ¹³	17	12	16	0	10	12	14	0
E4 ³²	13	10	16	0	11	10	11	0
E4 ⁵⁹	7	15	11	0	7	11	2	0
E4 ⁶³	10	5	5	0	9	6	10	0
E4 ¹⁰³	6	6	12	0	8	5	9	0
E4 ¹¹⁰	11	13	10	5	9	9	11	13

Note: E3¹³, E3³² and E3⁶³ stocks were maintained for further studies on HS-VS cell development.

3.5.1.2 Complementation phenomena associated with lethal *omb* alleles:

In an EMS screen for enhancers of the *omb* hypomorphic allele *bifid*, several lethal *omb* alleles have been isolated (Pflugfelder, unpublished). They were crossed to *In(1)ombH31* to monitor their effect on HS/VVS cell development. Surprisingly, paraffin section of adult heads of these transheterozygotes suggested that some of the lethal *omb* mutants complemented the HS/VVS phenotype of *In(1)ombH31* (Pflugfelder, unpublished). To verify this effect and to better characterize these lines, these crosses were repeated here in the genetic background of the enhancer trap insertion A122. Furthermore, it was attempted to identify the relevant DNA sequence changes.

Here, we have tested 4 lethal *omb* mutants over the deficiency chromosome *w Df(1)rb5 A122/FM6*. This chromosome in combination with other *omb* null alleles or with *In(1)omb^{H31}* does not develop HS and VS neurons in the central brain (Brunner, Wolf et al. 1992). But some of the newly isolated lethal

omb mutants were suspected not to be the null in this respect. To determine whether the mutant lines subjected to our studies have the ability to complement the *w Df(1)rb5 A122* chromosome, a series of crosses have been set up. In the first step, the DpA1125/*In(2LR)Gla, Bc* chromosomes had to be introduced to the lethal *omb* mutant lines to maintain them as stable stocks. The Glazed marker identifies the

Table 3.10: complementation phenomena associated with lethal *omb* alleles

Lines	Relevant genotype	HS/VS cell complementation
1039	<i>l(1) omb^{I1}/FM-GFP</i>	+ (partial)
171	<i>l(1) omb^{I2}/FM7a</i>	-
1041	<i>l(1) omb^{I3}/FM-GFP</i>	-
1042	<i>l(1) omb^{I5}/FM-GFP</i>	-

transheterozygous females [*w Df(1)rb5 A122/ l(1) omb*] without duplication. I have also tested if the presence of *Gla* has an effect on HS/VS cell development. This test is necessary because it was reported that *Gla* severely perturbs eye development (Brunner, Brunner et al. 1999) and hence may have an influence on optic lobe development. For this purpose *lacZ A122* (line 145) was crossed to line *l(1)omb^{D4}, w; Dp/In(2LR)Gla, Bc* (395). I did not notice any defects of the HS/VS cell bodies in the flies containing the *Gla* marker (figure 3.16A). On the other hand it was also shown that the *Gla* marker does not influence the HS/VS phenotype of *w Df(1)rb5 A122/ w l(1)omb^{D4}; II/ In(2LR)Gla, Bc* flies (Figure 3.16B). It was a positive tests for the assay system. In complementation experiments, transheterozygous females (*w Df(1)rb5 A122/ l(1)omb*) with Glazed eyes were tested for the development of the HS/VS cells in the optic lobes. Out of four alleles, one, *l(1) omb^{I1}*, showed partial complementation and developed fewer HS and VS cell bodies in the optic lobes (Figure 3.17; Table 3.10). These observations indicate that not all *omb* lethal mutants are null with respect to HS/VS cell development in the adult optic lobe.

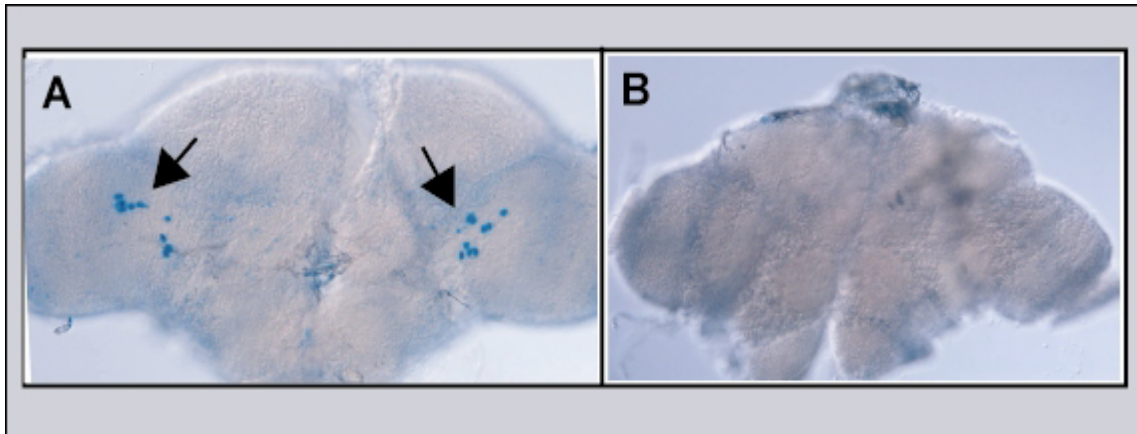


Figure 3.16: *Gla* has no influence in HS/Vs cell development. *Gla* did not affect HS/Vs development in line *lacZ A122* (145) [A] and also has no apparent influence on *w Df(1)rb5 A122/ w l(1)omb^{D4}* [B]

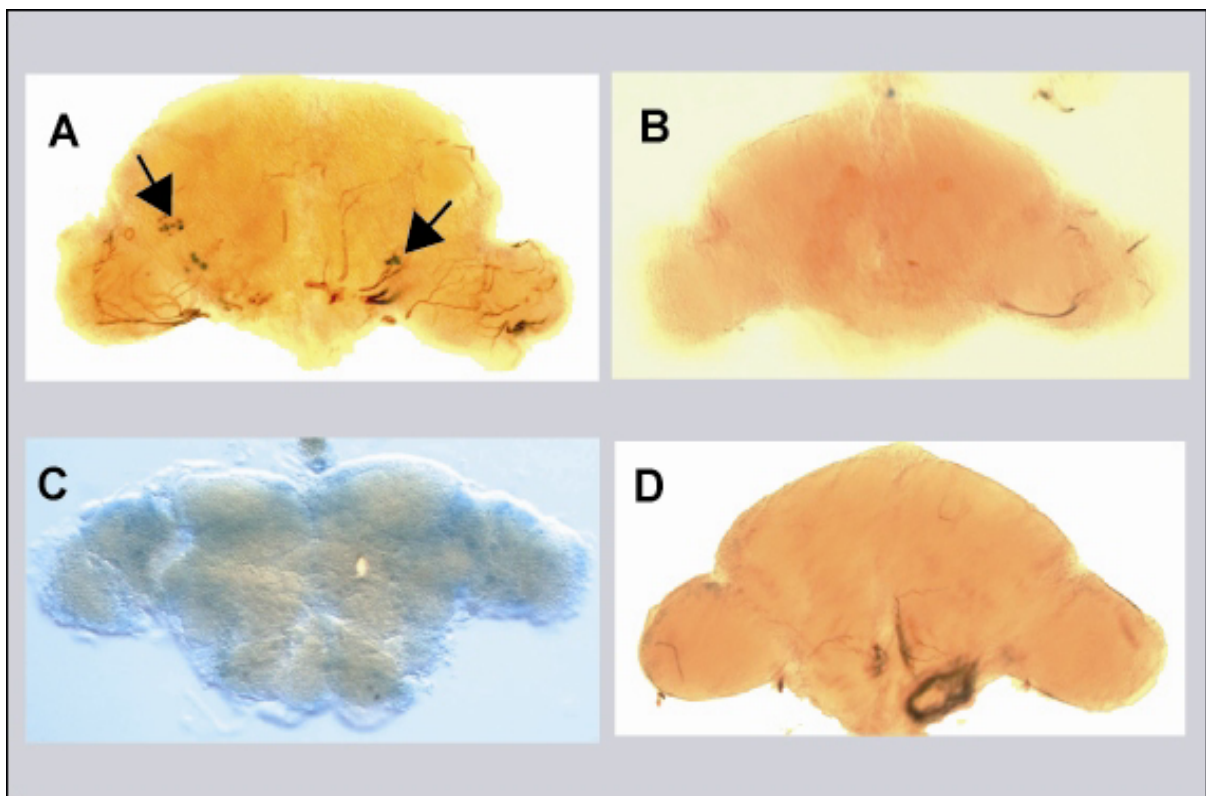


Figure 3.17: X-Gal staining of whole mount brains to test the complementation behaviour of *omb* lethal alleles. Allele *l(1)omb¹²* (B), *l(1)omb¹³* (C) and *l(1)omb¹⁵* (D) were not able to complement the HS/Vs cell development when combined with *w Df(1)rb5 A122* allele (143). *l(1)omb¹¹* (A) was able to partially complement (HS/Vs cells are indicated by arrows)

3.5.2 Molecular characterization of lethal omb mutant

3.5.2.1 Amplification of coding and relevant noncoding regions from omb transcript

In order to find out the molecular abnormalities in the *omb* locus in the lethal mutants subjected to study, I have done an investigation of the mutation associated with four EMS mutant lines. Mutations in all four lethal chromosomes are supposed to be the point mutations lying within the transcript or in the regulatory region of the *omb* gene. Mutation in the coding sequences may lead to missense, nonsense or frameshift mutations and mutation within an intron, especially in the intron-exon splicing junction, may lead to a non-functional transcript. To investigate the nature and location of mutations, all eight exons including intron-exon junctions were amplified from the genomic sequences of the respective mutants. Individual exon and intron-exon junctions were amplified using a single pair or multiple pairs of primers depending on the length of fragments to be amplified. For instance, part of the upstream sequence of exon I and exon I were amplified by a single pair of primers (omb 60/omb 59), 'intronI-exon II-intronII' was amplified by two pairs of primers (omb 27/omb 32, omb 33/omb 36), the smaller fragment comprising 'intronII-exon III-intronIII-exon IV-intronIV' was amplified by a single pair of primers (omb 62/omb 65) and so on. Details about the primers used for the amplification of all exons and intron-exon junctions are presented in Table 3.11 and depicted in Figure 3.18. PCR products for each of the primer pair were checked on the gel. Except for a few cases, amplifications of most of the fragments were specific. Non-specific products were obtained from the amplifications using omb 27/omb 32, omb 7/omb 10 and omb 33/omb 36 primer pairs with most genotypes (Figure 3.19). Problems also arose in the subsequent sequencing reactions of the amplified products from this region even after the gel purified samples were used for sequencing. The reason behind this problem might be the presence of extra binding site(s) of primers in the amplified products. New pairs of primers were designed to fix that problem.

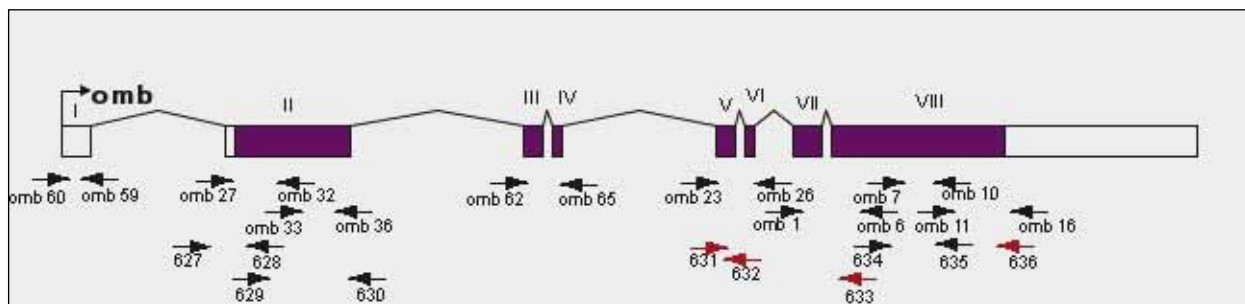


Figure 3.18: Optomotor blind transcript along with primer pairs used for PCR (black arrows) and sequencing (red arrows) purposes. The purple coloured section is the coding region.

Table 3.11 : Primers pairs used to amplify exons and relevant intron-exons junctions of *omb* are shown with their respective positions in genomic sequence (GI: 28381560)

	Primer pairs	Start	End	Product size (bp)
Exon I	Omb 60/Omb59	23090	23482	393
Intron I— Exon II	Omb 27/Omb32	38675	39629	955
Exon II—Intron II	Omb 33/Omb 36	39538	40076	539
Intron I—Exon II	627/628	38662	39416	755
Exon II—Intron II	629/630	39381	40112	732
Intron II—Exon III—Intron III — Exon IV—Intron IV	Omb 62/Omb 65	61130	61664	535
Intron IV—Exon V—Intron V — Exon VI—Intron VI	Omb 23/Omb 26	88625	89063	439
Intron VI—Exon VII—Intron VII — Exon VIII	Omb 1/Omb 6	92552	93223	672
Exon VIII	Omb 7/ Omb 10	93169	93730	562
Exon VIII	Omb 11/Omb 16	93663	94493	831
Exon VIII	634/635	93127	93733	607

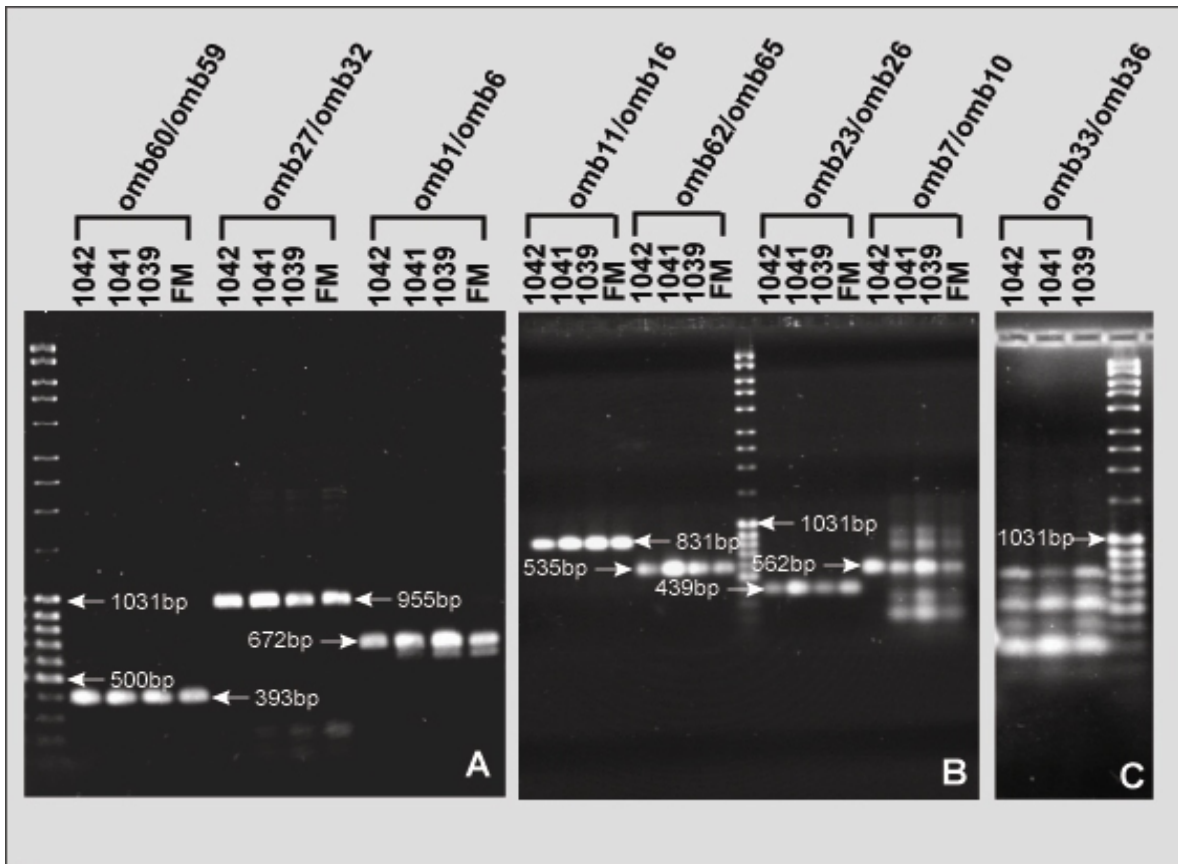


Figure 3.19: PCR amplification of different exons and intron-exons junctions of *omb*. Stock number for each of the mutant line is indicated corresponding to the respective lane. Primer pairs used for amplification of different exons and intron-exon junctions are shown on the top panel.

3.5.2.2 Molecular lesion in *omb* lethal alleles:

Mutations were found in two lethal *omb* alleles. They are *l(1) omb^{I3}* and *l(1) omb^{I5}*. No mutations have been detected in *l(1) omb^{I1}* and *l(1) omb^{I2}* alleles. Sequencing information along with several detected polymorphism is presented in Appendix 5. Molecular lesions associated with the *omb* lethal alleles are shown schematically (Figure 3.21) and are listed in Table 3.12

Molecular lesion in *l(1) omb^{I3}* allele:

I found a missense mutation in this allele in the T-box. Alanine (GCG) at position 508 in the wild type sequence was replaced by Valine (GTG) (see Figure 3.20). As this residue lies in the DNA binding domain and is involved in contacting DNA, it is expected to have consequences on the DNA binding property. This point is discussed in the discussion section.

Molecular lesion in *l(1) omb¹⁵* allele:

Mutation in this allele associated with a non-sense mutation giving rise to premature termination at amino acid position 599. Glutamine (CAG) in wild type is replaced by a stop codon (TAG) (see Figure 3.20). This truncated protein devoid of the C-terminal domain conceivably would not be active as a transcription factor and/or might affect the DNA binding property of the protein itself.

Allele	DNA lesion	Protein lesion
<i>l(1) omb¹⁵</i>	CAG To TAG	Gln To Stop
<i>l(1) omb¹³</i>	GCG To GTG	Ala To Val
<i>l(1) omb¹²</i>	Not found	---
<i>l(1) omb¹¹</i>	Not found	---

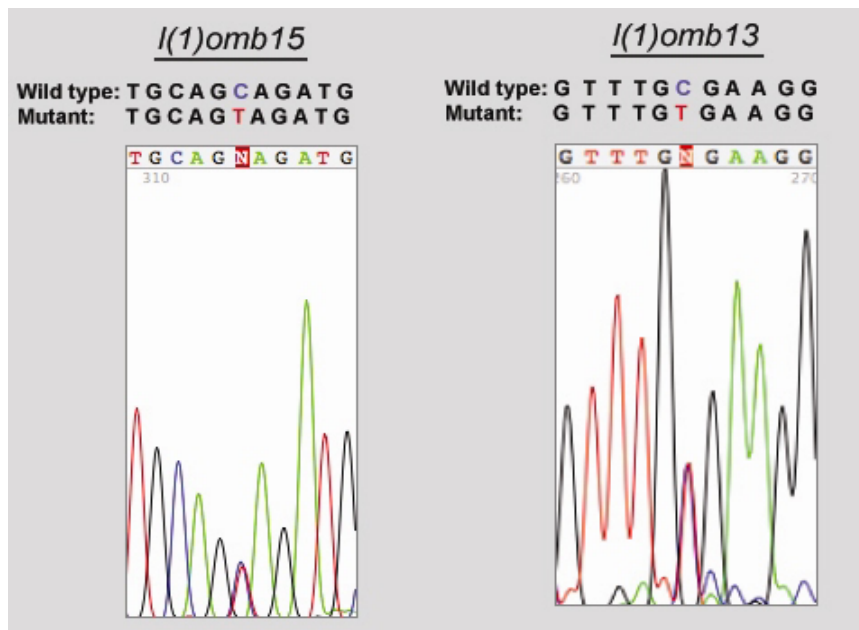


Figure 3.20: Chromatogram showing the mutations in the sequences from two lethal mutants.

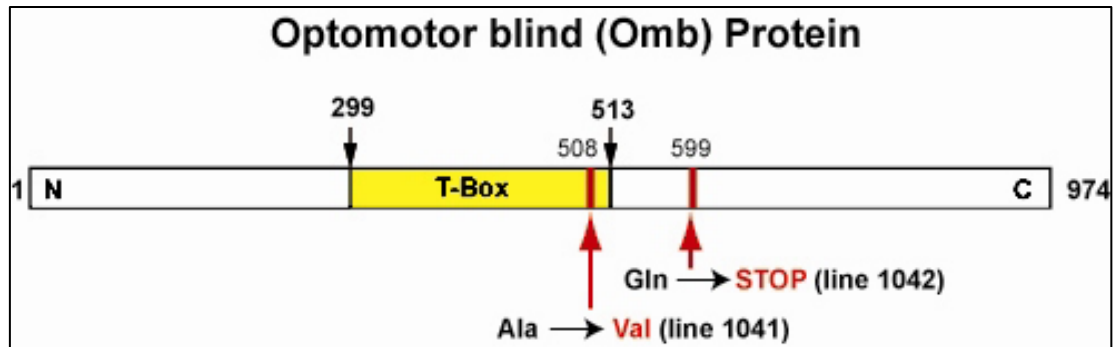


Figure 3.21: Molecular lesions in *omb* lethal alleles. Numbers at the ends and top of the bar denote the position of amino acids. Vertical black lines at both sides limit the T-Box (shown in yellow). Mutation positions are shown by bold red vertical lines.

3.5.2.3 DNA Binding properties of mutant OMB-T:

OMB which is a member of T-box gene family shares a conserved DNA binding domain, called T-domain, with the other members of the family. The first gene in the T-box family discovered was the mouse *Brachyury* (Bra) or T protein. It binds a highly specific 24 bp palindrome (AATTTTCACACCT AGGTGTGAAATT) [Bra Palindrome] as determined by the 'SELEX' approach (Kispert and Herrmann 1993). In our experimental approach, we have chosen the 24 bp Bra palindrome as the probe to determine the binding properties of OMB-T. Protein expression and probe preparations are discussed in Materials and Methods.

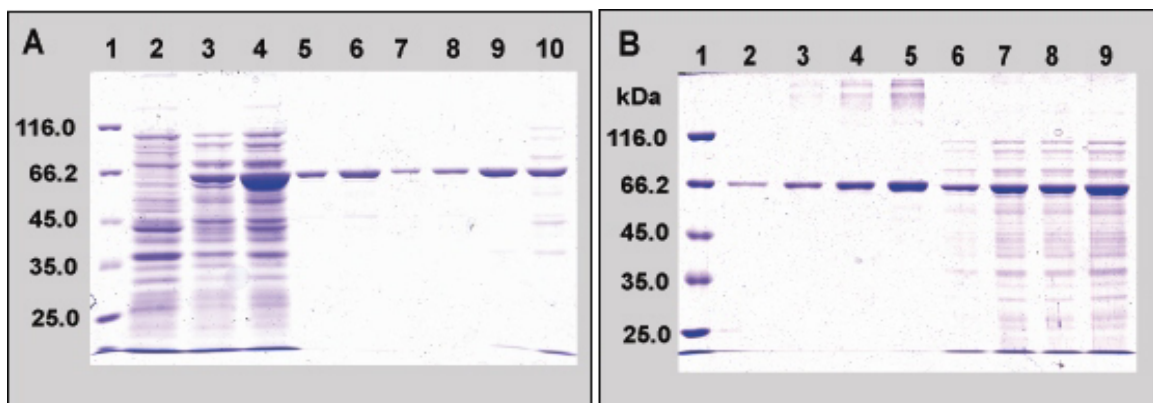


Figure 3.22: SDS-PAGE (10%) of wild type and mutant MBP-OMB-T fusion protein. A (wild type): lanes: 1-marker; 2-Uninduced; 3-induced; 4-crude extract; 5-6-purified (fraction 2+3); 7-8-purified (fraction 4+5); 9-insoluble matter; 10-flow through. B: concentration determination of wild type and mutant MBP-OMB-T fusion protein. Lanes: 1-marker; 2-5- different amount of BSA (200ng, 400ng, 800ng and 1.6µg respectively); 6&8 mutant protein ; 7&9: wild type protein.

Before starting with the DNA binding experiment, bacterially expressed wild type and mutant OMB-T were analysed on 10 % SDS-PAGE (Figure 3.22). First, wild type OMB-T was subjected to band shift assay and it was found that OMB-T can specifically bind the Bra palindrome, but could not bind a Scalloped probe, used as a negative control (Figure 3.23). A competition binding experiment using specific and non-specific cold competitors showed the specific binding of OMB-T to the Bra palindrome (Figure 3.24). The Xa digested products from MBP-OMB-T fusion proteins are similarly capable to bind to the Bra palindrome. On the other hand, no DNA binding capability of the mutant OMB-T with the A508V missense mutation was observed (Figure 3.25). This result proves that Ala at 508th position in OMB plays a vital role in DNA binding.

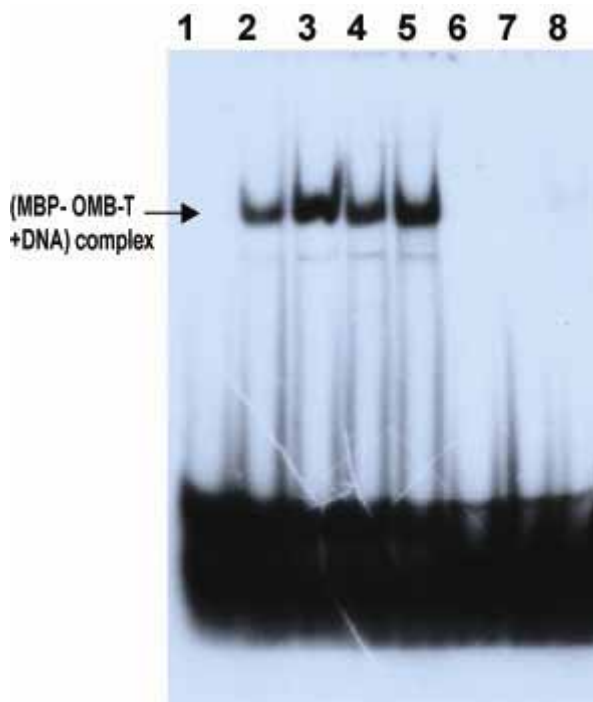


Figure 3.23: Binding of OMB-T to the Bra palindrome. OMB-T from crude extract (lane 4 &5) binds Bra palindrome as specifically as the purified fraction (lane 2 &3). OMB-T did not bind to the non-specific template for Scalloped protein (lane 7 &8). 1µg (lane 2) and 3µg (lane 3) of purified MBP-fusion proteins were used for binding reactions. Crude extract containing the corresponding amount of fusion protein, i.e. 1µg (lane 4) and 3µg (lane 5) were used for binding reaction. Free probes were also run on the gel (lane 1, bra palindrome; lane 6, scalloped template)

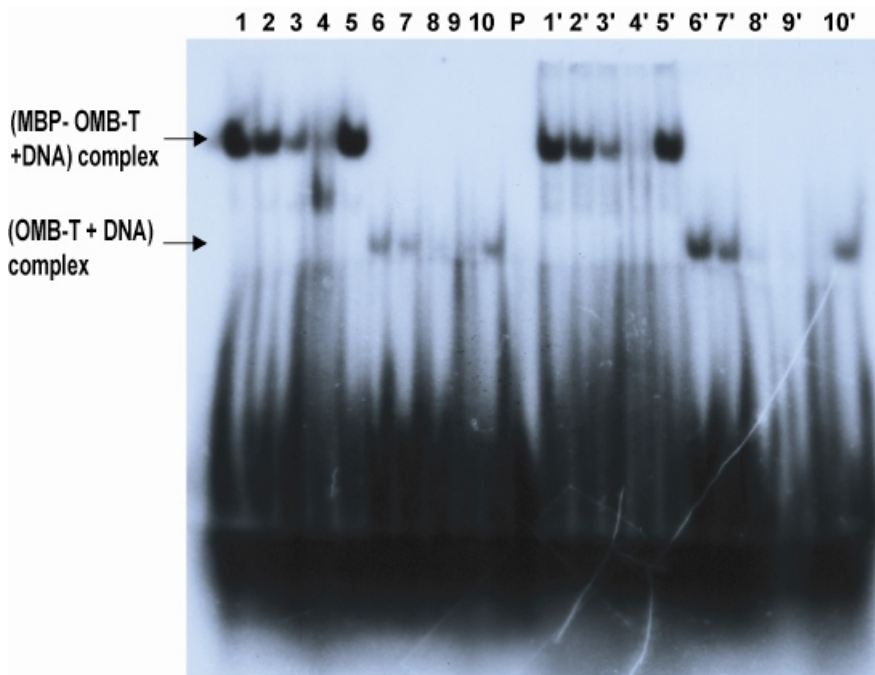


Figure 3.24: OMB-T selectively binds the Bra palindromic sequence. The selective binding of MBP-OMB-T fusion protein (lane 1) is gradually reduced with the increasing amount of specific cold competitor (3-, 30-, 300-fold in lane 2, 3 & 4 respectively), but the binding is not hampered by 300 fold excess amount of non specific competitor (lane 5). Xa digested fusion protein also shows specific binding to Bra palindrome (lane 6 without competitor and lane 7-9 with specific and lane 10 with non specific cold competitors). P: free probe. Samples in Lane 1'-10' are in the same sequence as in 1-10 but experiments were done with crude protein instead of purified protein (lane 1-10).

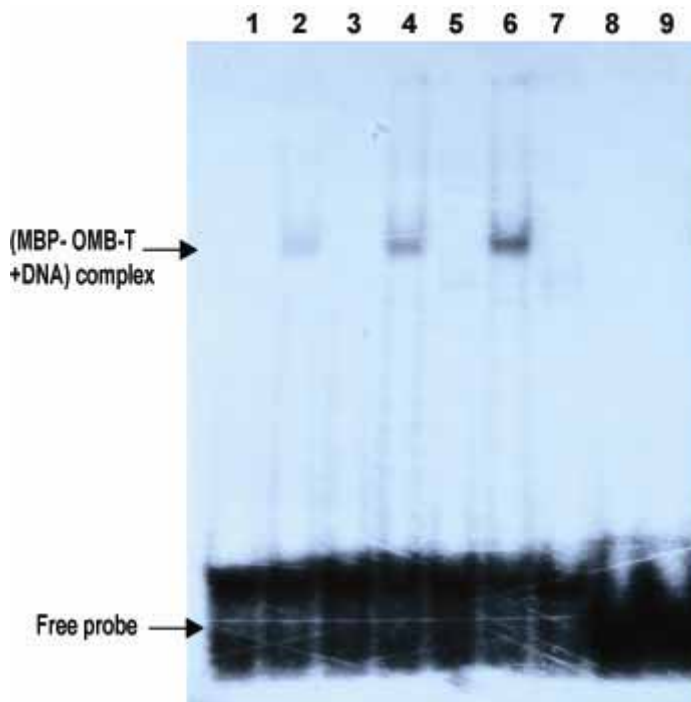


Figure 3.25: The A508V mutation abolishes the DNA binding capability of OMB-T. Wild type OMB-T can form an increasing amount of protein-DNA complex with increasing protein concentration (lane 2: 0.2 μl, lane 4: 0.6 μl and lane 6: 1.0 μl of crude extract). No DNA-protein complex was detected for mutant OMB-T (lane 3, 5 and 7 with increasing amount of crude extract). OMB-T did not bind to the non-specific template for scalloped protein (lane 8 & 9). Lane 1 is free Bra probe.

4. Discussion

4.1 AMCs in larval olfaction:

The delayed response of AMC-ablated flies to olfactory stimulus may be due to partial damage of the AMC. Possibly, some of the cells in the AMC are still alive. Alternatively the presence of some other chemosensory organs like the ventral organ (Singh and Singh 1984) and other external putative chemoreceptors, like ‘labial organ’ and ‘knob in pit’ sensillum (Kankel, Ferrus et al. 1980) may be involved. In case of partial ablation, we have to make sure that cells are dead after a laser hit. The effect of partial ablation was evident in some cases, where it was found that instead of damaging the cell, the laser beam was simply bleaching GFP in the cells as the targeted cells start to fluoresce again a few minutes after treatment and was mimicking the cell damage. There might be another reason for the slow approach of the response index to the wild type value: ablated flies might have some motor problem. To clarify the exact reasons behind the abnormality in the olfactory response of the ablated flies, one should carry out a control ablation that leaves the AMC intact. Cell death could be ascertained by incorporating a *GFP-LacZ* double marker and looking for the presence of AMC (by LacZ expression pattern) in the ablated larvae.

4.2 Presence of precursor cell(s) for HS/VS neurons in the embryonic optic lobe anlagen:

We have already discussed in the introductory part the evidence for a single cell origin of the HS/VS neurons in the larval optic lobe of the house fly visual system (Geiger and Nassel 1981). Electro-physiological studies and Golgi staining have been used to explore the nature of these neurons regarding their number, arborisation patterns and electro-physiological properties (Fischbach and Dittrich 1989; Haag, Theunissen et al. 1997). Recently, the dendritic arborisation patterns of these giant neurons in the *Drosophila* adult optic lobe have been visualised by labelling individual cells by the MARCM technique (Scott, Raabe et al. 2002). In our study, we have identified a small group of cells in a

specific location in the embryonic optic lobe anlagen presumed to contain the precursor cell(s) for adult HS/VN neurons in *Drosophila melanogaster*. Although this is a very preliminary finding with respect to the number of prospective precursor cell(s), the result at least might be helpful in exploring the embryonic origin of these giant neurons with the help of restricted expression of marker genes in this suspected region.

It would be very useful if one could combine the laser heat shock techniques with the MARCM system. The use of the heat shock promoter to drive the expression of FLP in the MARCM system has been established (Golic and Lindquist 1989) and in all cases the conventional heat shock method, where whole organisms are shifted to higher temperature for heat shock, has been used. Tissue-specific promoter or enhancer elements were used to facilitate the tissue specific expression of marker genes. One could introduce the laser beam, in place of conventional methods of heat shock, as a source of heat and *omb-Gal4* for tissue specificity.

4.3 Mutation in evolutionary conserved residues:

Missense mutations in evolutionary conserved residues are likely to strongly affect the structural and functional properties of a protein. The implications of different mutations in the T-box genes have been studied extensively from the clinical point of view. To date about dozens of mutations have been identified in different T-box proteins in Human, Mouse, Xenopus, Zebrafish and other animals. It was found that the mutations, especially in the highly conserved T-box region, are associated with several diseases in Human. These diseases include Holt-Oram-Syndrome (HOS) (Cross, Ching et al. 2000; Yang, Hu et al. 2000; Ghosh, Packham et al. 2001; Brassington, Sung et al. 2003; Fan, Duhagon et al. 2003), Ulnary-Mammary-syndrome (UMS) (Bamshad, Lin et al. 1997; Bamshad, Le et al. 1999), DeGeorge syndrome (DGS) (Gong, Gottlieb et al. 2001; Yagi, Furutani et al. 2003) Isolated ACTH deficiency (Pulichino, Vallette-Kasic et al. 2003) and Cleft palate with ankyloglossia (CPX) (Braybrook, Lisgo et al. 2002).

Heartstrings (*hst*) (Garrity, Childs et al. 2002) and *van gogh* (*vgo*) (Piotrowski, Ahn et al. 2003) are mutations in zebrafish *Tbx5* and *Tbx1*, respectively. A list of mutations in the various T-box genes is presented in Table 4.1 and the mutations are also pointed out in a multiple alignment of T-box proteins (Appendix 9). A number of mutations are missense

Table 4.1: Mutations in different T-box genes depicted in aligned sequences were tabulated below

T-Box genes	Accession number	Number of residues(aa)	Mutation(s)	Reference
TBX1_HUMAN	O43435	398	F148Y	(Stoller and Epstein 2005)
			G310S	(Stoller and Epstein 2005)
			G350D	(Gong, Gottlieb et al. 2001)
			P396L	(Gong, Gottlieb et al. 2001)
TBX2_HUMAN	Q13207	702		
TBX3_HUMAN	O15119	743	L143P	(Bamshad, Le et al. 1999)
			S343TER	(Bamshad, Le et al. 1999)
			E360TER	(Bamshad, Le et al. 1999)
			Y149S	(Bamshad, Le et al. 1999)
TBX5_HUMAN	Q99593	518	Q49K	(Yang, Hu et al. 2000)
			I54T	(Yang, Hu et al. 2000)
			E69TER	(Basson, Bachinsky et al. 1997)
			W121G	(Brassington, Sung et al. 2003)
			G195A	(Brassington, Sung et al. 2003)
			S196TER	(Brassington, Sung et al. 2003)
			T223M	(Brassington, Sung et al. 2003)
			R237Q	(Basson, Bachinsky et al. 1997)
			R237W	(Brassington, Sung et al. 2003)
			S261C	(Brassington, Sung et al. 2003)
			R279TER	(Brassington, Sung et al. 2003)
			G169R	(Cross, Ching et al. 2000)
			E316TER	(Cross, Ching et al. 2000)
			E190TER	(Cross, Ching et al. 2000)
			S252I	(Cross, Ching et al. 2000)
			R279TER	(Cross, Ching et al. 2000)
G80R	(Ghosh, Packham et al. 2001)			
W64TER	(Fan, Duhagon et al. 2003)			
TBX6_HUMAN	O95947	436		
TBX10_HUMAN				
TBX19_HUMAN	O60806	448	T58A	(Pulichino, Vallette-Kasic et al. 2003)
			S128F	(Pulichino, Vallette-Kasic et al. 2003)
			I171T	(Pulichino, Vallette-Kasic et al. 2003)
			R179TER	(Pulichino, Vallette-Kasic et al. 2003)
			R286TER	(Pulichino, Vallette-Kasic et al. 2003)
TBX22_HUMAN	Q9Y458	519	G118C	(Braybrook, Doudney et al. 2001)
			T260M	(Braybrook, Doudney et al. 2001)
			E56TER	(Braybrook, Doudney et al. 2001)
			L214P	(Braybrook, Doudney et al. 2001)
			S195-F196 ins S	(Braybrook, Doudney et al. 2001)
TBX1_Zebrafish	AY294284	460	R293TER	(Piotrowski, Ahn et al. 2003)
			N121TER	(Piotrowski, Ahn et al. 2003)
TBX5_Zebrafish	NP_570990	485	Q316TER	(Garrity, Childs et al. 2002)
XBRA_T	P24781	432		
Ce_TBX2		423	K164D	(Miyahara, Suzuki et al. 2004)
			K164R	(Miyahara, Suzuki et al. 2004)
OMBdm	A40213	974	A508V	
			Q599TER	
BRA_MOUSE	P20293	436		

mutations where a single amino acid substitution is enough to cause the diseases. Nonsense mutations which cause the premature truncation of proteins prior to or within the T-box region abolish the function in several T-Box gene mutations. In a few cases, mutations affecting the C-terminus end of proteins are responsible for the diseases (see section 4.5). These findings indicate the presence of functional domains in the C-terminal part also in other T-domain proteins

It is observed that residues at the end of the T-domain are more conserved than residues elsewhere within the T-domain, especially, the Ala at 508th position of OMB is highly conserved among other T-box proteins (Appendix 9). More importantly, this residue was found to be in contact with the DNA in a DNA-protein complex of human TBX3 protein (Coll, Seidman et al. 2002) as well as in Xbra (Muller and Herrmann 1997). So it is likely that this mutated OMB protein would lack DNA binding capacity to some extent and we showed that the A508V mutation indeed abolishes the DNA binding capacity of OMB.

4.4 Consequences for OMB DNA Binding affinity of the *l(1) omb¹³* mutation:

Mutation in the evolutionary conserved residues of a protein molecule responsible for DNA binding activity presumably would affect its DNA binding affinity. Molecular consequences of different point mutations in T-box genes have been also explored (see table 4.2). But it is always a matter of study to know the extent to which binding is affected. Previous studies on DNA-protein complexes of the T-domain of human TBX3 and that of from *Xenopus laevis* have revealed that the stretch of amino acids, NPFAKAF, interacts with the DNA (marked pink in the alignment at Appendix 9) and the molecular interactions between T-domains of human TBX3 and Xbra and their respective target DNA were analysed in detail (Coll, Seidman et al. 2002). A pair-wise alignment of human TBX3 and mutant OMB (A508V) is shown (see Figure 4.1) to facilitate a comparison between these two proteins. The positions of Phe279, Ala280 and Phe283 in the DNA-protein complex of TBX3 are shown in Figure 4.2. The side chains of Phe 279 and Phe 283 point deeply into the minor groove assisted by Pro278, Ala280, Lys281 and Gly282 and

interestingly, the area of minor groove where Phe280 is sandwiched between two sugar moieties of opposite DNA backbones becomes narrow [O4'-O4' distance is 7Å between T (bp1) and G (bp3)]. Thus, the replacement of the relatively small amino acid Ala with Val might have an impact on the positioning of the side chain of the adjacent Phe in the narrow minor groove. This might adversely affect the DNA binding property of the protein.

Table 4.2 : Biochemical consequences of different point mutations in T-Box genes

T-Box Genes	Mutations	Associated diseases	Molecular consequences	References
TBX5_Human	R237Q	Holt-Oram-Syndrome	No DNA binding; minor effect on transcriptional activation	(Ghosh, Packham et al. 2001; Hiroi, Kudoh et al. 2001; Fan, Duhagon et al. 2003)
	R279 TER	Holt-Oram-Syndrome		(Plageman and Yutzey 2004)
	G80R	Holt-Oram-Syndrome	No DNA binding	(Ghosh, Packham et al. 2001)
TBX19_Human	T58A	Isolated ACTH deficiency	Reduced DNA binding; 10% transcriptional activation	(Pulichino, Vallette-Kasic et al. 2003)
	S128F	Isolated ACTH deficiency	No DNA binding; no transcriptional activation	(Pulichino, Vallette-Kasic et al. 2003)
	I117T	Isolated ACTH deficiency	No DNA binding; no transcriptional activation	(Pulichino, Vallette-Kasic et al. 2003)
TBX2_Human	R122A		No DNA binding	

OMB_A508V_	PPPPYFPAAALAALAGS--PAGPHPGLYPGGGLRFPPHHPGAHPHAHHLGSAYTTAEDVV	298
TBX3_HUMAN	FLPHRAPDFAMSAVLGHQPFFFPALTLPPNGAAALSPLGALAKPIMDQLVGA---AETGI	76
Cons	* * *:::* * * * * * . : . . *:* :* . *	** :
OMB_A508V_	LASAVAHQLHPAMRPLRALQPEDDGVVDDPKVTLEGKDLWEKFKLGTENVITKSGRQMF	358
TBX3_HUMAN	PFSSLGPOAH--LRPLKTMEPEEE--VEDDPKVHLEAKELWDQFHKRGTEMVITKSGRRMF	133
Cons	*:: * * :***:::***: * ***** **,*:*:* ** *****:***	
OMB_A508V_	PQMKFRVSGLDAKAKYILLLDIVAADDYRYKFHNSRWMVAGKADPEMPKRMVYIHPDSPTT	418
TBX3_HUMAN	PPFKVRCSGLDKKAKYILLMDIIAADDCRYKFHNSRWMVAGKADPEMPKRMVYIHPDSPAT	193
Cons	* :* . * ***** *****:***:*** *****:*****:***	
OMB_A508V_	GEQWMQKVVVTFHKLKLTNNISDKHGFVSTTILNSMHKYQPRFHLVRANDILKLPYSTFRT	478
TBX3_HUMAN	GEQWMSKVVTFHKLKLTNNISDKHGFVSTTILNSMHKYQPRFHIVRANDILKLPYSTFRT	250
Cons	***** . ***:***** ***** *****:*****:*****	
OMB_A508V_	YVFKETEFIAVTAYQNEKITQLKIDNNPEVKGLRDTGAGKREKN----CYRQALMSNRGS	534
TBX3_HUMAN	YLFPETEFIAVTAYQNDKITQLKIDNNPFAKGFRTGNGRREKRKQLTLQSMRVFDERHK	310
Cons	*:* *****:*****:***** . **:* ** *:* ** . :::* .	

Figure 4.1: Pair-wise alignment of T-Box regions from Mutant OMB and Human TBX3. Most of the residues are identical in the two proteins. The amino acid stretch NPEAKGF (sky blue) is responsible for contact with the DNA in the TBX3-DNA complex. Ala at 508 position of OMB is replaced by Val in *l(1) omb¹³*.

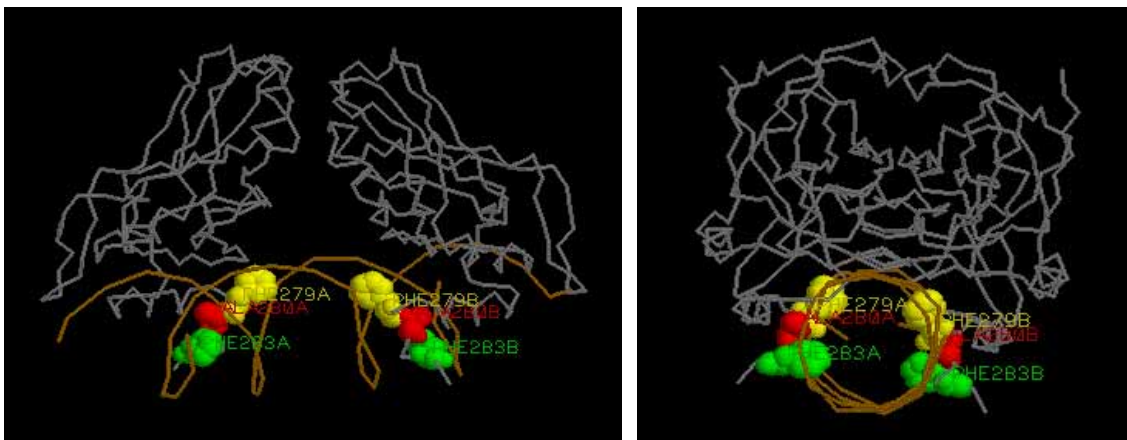


Figure 4.2: T-domain-DNA complex of Human TBX3 (PDB code: 1H6F). Phe279 (yellow), Ala280 (red) and Phe283 (green) are marked in the complex shown in two different angles using the *Rasmol* programme (Coll, Seidman et al. 2002).

4.5 Mutation in the lethal *l(1) omb^{I5}* allele:

The mutation associated with the *l(1) omb^{I5}* allele causes premature termination of translation leading to a truncated OMB protein devoid of most of the C-terminal domain. Mutations, which lead to truncation of the C-terminal domain of some T-box proteins are reported to cause disease in human and other organisms (see Table 4.3 and Figure 4.3). These observations indicate the presence of transcriptional activation or repression or other interaction domains within the C-terminal part of the T-box proteins. With this viewpoint, it is likely that the *l(1) omb^{I5}* allele would produce a protein which is functionally inactive. The presence of nonsense codons within a transcript might affect the RNA abundance (Nagy and Maquat 1998). Therefore, the mutant transcript might be less stable due to nonsense-mediated decay.

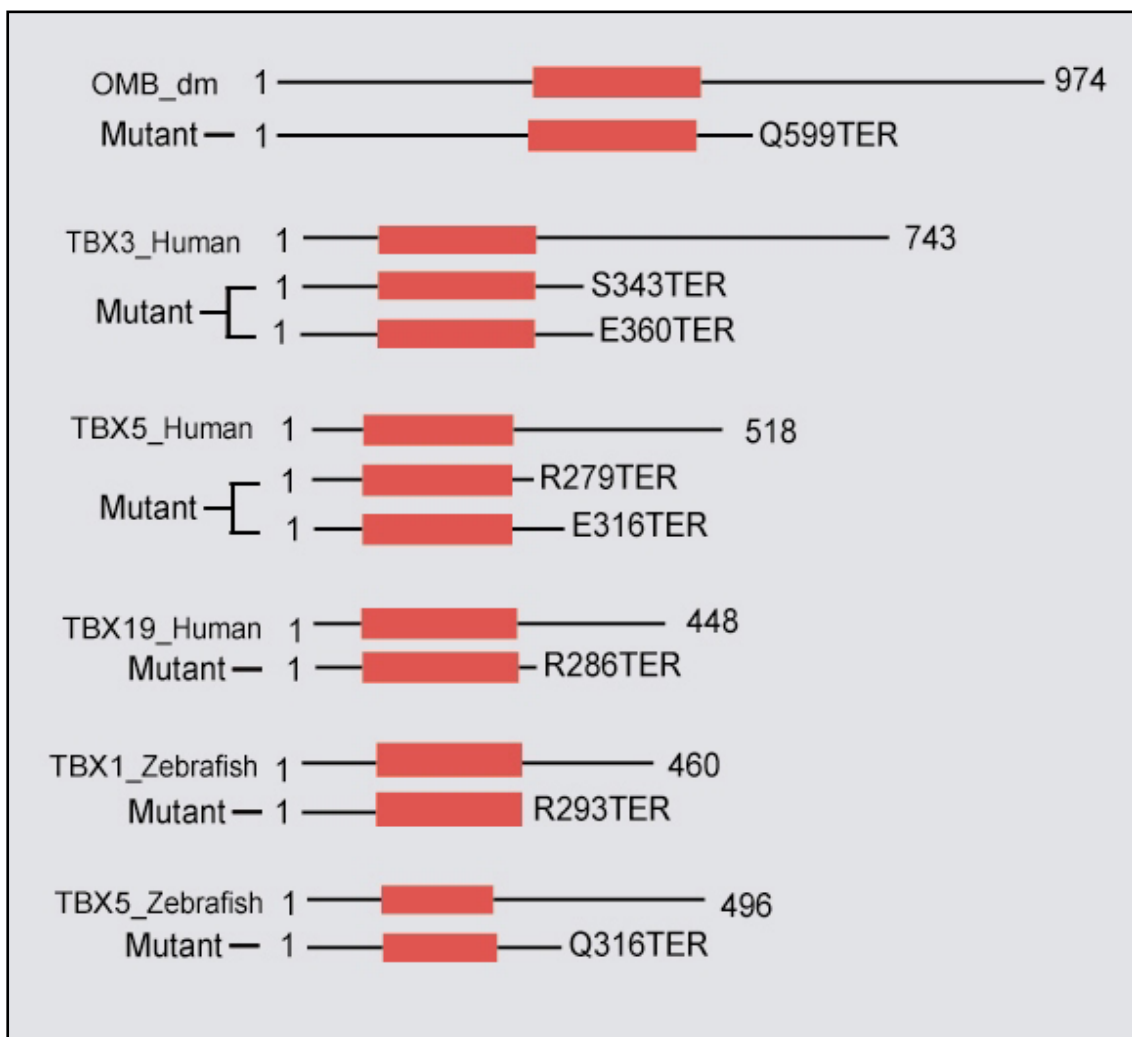


Figure 4.3: Nonsense mutations leading to truncated T-box proteins, which are devoid of most of the C-terminal domains, are responsible for developmental defects in human and in zebrafish.

Table 4.3: T-Box gene mutations and human diseases

T-Box gene	Human Diseases	Nonsense mutations
<i>TBX3_Human</i>	Ulnar-Mammary-Syndrome (UMS)	S343TER; E360TER;
<i>TBX5_Human</i>	Holt-Oram-syndrome (HOS)	R279TER; E316TER;
<i>TBX19_Human</i>	Isolated ACTH deficiency	R286TER;
<i>TBX1_Zebrafish</i>	Zebrafish <i>van gogh</i> (<i>vgo</i>)	R293TER;
<i>TBX5_Zebrafish</i>	Heartstrings (<i>hst</i>)	Q316TER;

4.6 Cause of lethality in *l(1) omb¹¹* and *l(1) omb¹²* lethal *omb* mutants:

I was not able to identify the mutations in two of the four lethal *omb* mutants. The failure to identify mutations in the coding or splice-relevant regions of *omb* in the *l(1) omb¹¹* and *l(1) omb¹²* alleles suggest that they are regulatory in nature. Most human T-box genes are haplo-insufficient (Packham and Brook 2003). While *omb* appears haplo-normal, many aspects of *Drosophila* development are quite sensitive to the level of *omb* expression (Pflugfelder, unpublished). In lethal mutants (hemi- or homozygotes), the *omb* expression level cannot be reliably determined because loss or reduction of *omb* function can cause delayed development and changes in proliferation/maintenance of tissue (Pflugfelder 1995). Cowles et al. (Cowles, Hirschhorn et al. 2002) proposed an elegant way by which an influence of allelic variation on gene expression can be assessed. The activity of individual alleles is tested in transheterozygous individuals. The only requirement for the assay is the presence of discriminating single nucleotide polymorphisms (SNP) between the two alleles. These can be detected by single-base extension analysis (SBE).

My sequencing analysis of *l(1)omb* mutants identified several SNPs which could be used for such analysis. Tissue of FM-balanced flies (assuming normal *omb* expression from the FM allele) from several developmental stages should be analysed in case changes in gene expression are temporally restricted.

Identification of the causative mutation in the extensive cis-regulatory region of *omb* will remain a daunting task and probably will require large-scale intragenic recombination experiments.

5. Summary – Zusammenfassung

Summary:

The horizontal and vertical system neurons (HS and VS cells) are part of a conserved set of lobula plate giant neurons (LPGNs) in the optic lobes of the adult brain. Structure and physiology of these cells are well known, predominantly from studies in larger Dipteran flies. Our knowledge about the ontogeny of these cells is limited and stems predominantly from laser ablation studies in larvae of the house fly *Musca domestica*. These studies suggested that the HS and VS cells stem from a single precursor, which, at least in *Musca*, has not yet divided in the second larval instar. A regulatory mutation (*In(1)omb[H31]*) in the *Drosophila* gene *optomotor-blind* (*omb*) leads to the selective loss of the adult HS and VS cells. This mutation causes a transient reduction in *omb* expression in what appears to be the entire optic lobe anlage (OLA) late in embryogenesis.

Here, I have reinitiated the laser approach with the goal of identifying the presumptive embryonic HS/VS precursor cell in *Drosophila*. The usefulness of the laser ablation approach which has not been applied, so far, to cells lying deep within the *Drosophila* embryo, was first tested on two well defined embryonic sensory structures, the olfactory antenno-maxillary complex (AMC) and the light-sensitive Bolwing's organ (BO). In the case of the AMC, the efficiency of the ablation procedure was demonstrated with a behavioral assay. When both AMCs were ablated, the response to an attractive odour (n-butanol) was clearly reduced. Interestingly, the larvae were not completely unresponsive but had a delayed response kinetics, indicating the existence of a second odour system. BO will be a useful test system for the selectivity of laser ablation when used at higher spatial resolution.

An *omb-Gal4* enhancer trap line was used to visualize the embryonic OLA by GFP fluorescence. This fluorescence allowed to guide the laser beam to the relevant structure within the embryo. The success of the ablations was monitored in the adult brain via the enhancer trap insertion *A122* which selectively visualizes the HS and VS cell bodies. Due to their tight clustering, individual cells could not be identified in the embryonic OLA by conventional fluorescence microscopy. Nonetheless, systematic ablation of subdomains of the OLA allowed to localize the presumptive HS/VS precursor to a small area within the OLA, encompassing around 10 cells. Future studies at higher resolution should be able to identify the precursor as (an) individual cell(s).

Most known lethal *omb* alleles do not complement the HS/VS phenotype of the *In(1)omb[H31]* allele. This is the expected behaviour of null alleles. Two lethal *omb* alleles that had been isolated previously by non-complementation of the *omb* hypomorphic allele *bifid*, have been reported, however, to complement *In(1)omb[H31]*. This report was based on low resolution paraffin histology of adult heads. Four mutations from this mutagenesis were characterized here in more detail (*l(1)omb[11]*, *l(1)omb[12]*, *l(1)omb[13]*, and *l(1)omb[15]*). Using *A122* as marker for the adult HS and VS cells, I could show, that only *l(1)omb[11]* can partly complement the HS/VS cell phenotype of *In(1)omb[H31]*. In order to identify the molecular lesions in these mutants, the exons and exon/intron junctions were sequenced in PCR-amplified material from heterozygous flies. Only in two mutants could the molecular cause for loss of *omb* function be identified: in *l(1)omb[13]*, a missense mutation causes the exchange of a highly conserved residue within the DNA-binding T-domain; in *l(1)omb[15]*, a nonsense mutation causes a C-terminal truncation. In the other two mutants apparently regulatory regions or not yet identified alternative exons are affected.

To see whether mutant OMB protein in the missense mutant *l(1)omb[13]* is affected in DNA binding, electrophoretic shift assays on wildtype and mutant T-domains were performed. They revealed that the mutant no longer is able to bind the consensus palindromic T-box element.

Zusammenfassung

Die HS und VS Neuronen ("Horizontal- und Vertikal-System") sind Teil eines konservierten Satzes von Riesenneuronen der Lobulaplatte (LPGNs) in den optischen Loben des adulten Fliegengehirns. Die Struktur und Physiologie dieser Zellen ist wohl untersucht, vornehmlich durch Studien an grossen dipteren Fliegen. Unser Wissen über die Ontogenese dieser Zellen ist beschränkt und stammt vor allem aus Laserablationsexperimenten, die an Larven der Hausfliege *Musca* durchgeführt worden sind. Diese Untersuchungen legten nahe, dass die HS- und VS-Zellen von einer einzigen Vorläuferzelle abstammen, die, zumindest in *Musca*, sich im zweiten larvalen Instar noch nicht geteilt hat. Eine regulatorische Mutation im *optomotor-blind* (*omb*) Gen von *Drosophila* (*In(1)omb[H31]*) bewirkt selektiv den Verlust der adulten HS- und VS-Zellen. Diese Mutation führt zu einer transienten Reduktion der *omb* Expression wahrscheinlich in der ganzen Anlage der optischen Loben (OLA) am Ende der Embryogenese.

Die Lasertechnik wurde hier erneut aufgegriffen mit dem Ziel, die HS/Vs-Vorläuferzelle(n) zu identifizieren. Die Anwendbarkeit der Laserablation, die bislang in *Drosophila* noch nicht an Zellen eingesetzt wurde, die innerhalb des Embryos liegen, wurde zunächst an zwei gut-definierten embryonalen sensorischen Strukturen getestet, dem olfaktorischen Antennomaxillarkomplex (AMC) und dem Licht-sensitiven Bolwig'schen Organ (BO). Im Fall des AMC wurde der Erfolg der Behandlung mit einem Verhaltenstest nachgewiesen. Bei Ablation beider AMCs, war die Reaktion auf einen attraktiven Geruch (n-Butanol) deutlich reduziert. Interessanterweise, waren die Larven nicht völlig unresponsiv sondern wiesen eine verzögerte Reaktionskinetik auf, was auf die Existenz eines weiteren olfaktorischen Systems deutet. Das Bolwig'sche Organ ist ein nützliches Testsystem, um die Selektivität der Laserablation zu charakterisieren, wenn diese bei höherer räumlicher Auflösung durchgeführt werden sollte.

Eine *omb-Gal4* enhancer trap Linie wurde verwendet, um die embryonale OLA durch GFP Fluoreszenz zu visualisieren. Diese Fluoreszenz erlaubt es, den Laserstrahl auf die relevante Struktur innerhalb des Embryos zu richten. Der Erfolg der Ablationen wurde im adulten Gehirn mittels der enhancer trap Insertion A122 nachgewiesen, mit der die Zellkörper der HS/Vs-Zellen selektiv darstellbar sind. Wegen ihrer engen Nachbarschaft, konnten die OLA Zellen mit konventioneller Fluoreszenzmikroskopie nicht einzeln erfasst werden. Dennoch erlaubte es die systematische Ablation von Teilbereichen der OLA, die

präsumptive HS/VS-Vorläuferzelle in einem kleinen Bereich zu lokalisieren, der noch etwa 10 Zellen umfasst. In weiteren Experimenten bei höherer räumlicher Auflösung sollte es möglich sein, die Vorläuferzelle direkt zu identifizieren.

Die meisten bekannten lethalen *omb* Allele komplementieren den HS/VS-Phänotyp von *In(1)omb[H31]* nicht. Bei zwei *omb* Lethallallelen, die in einer früheren Arbeit dadurch isoliert worden waren, dass sie das *omb* Hypomorph *bifid* nicht komplementierten, gab es jedoch Hinweise, dass sie *In(1)omb[H31]* komplementieren können. Diese Hinweise basierten auf Paraffinhistologie adulter Fliegenköpfe mit geringer räumlicher Auflösung. Vier Mutanten aus dieser Mutagenese wurden hier in größerem Detail analysiert (*l(1)omb[11]*, *l(1)omb[12]*, *l(1)omb[13]*, and *l(1)omb[15]*). Mit A122 als Marker für die adulten HS- und VS-Zellen konnte ich nachweisen, dass nur *l(1)omb[11]* den HS/VS-Phänotyp von *In(1)omb[H31]* partiell komplementieren kann. Um die Mutationen in diesen Mutanten molekular zu identifizieren, wurden Exons und Exon-Intron Bereiche mittels PCR aus heterozygoten Fliegen amplifiziert und anschliessend sequenziert. Nur in zwei der vier Mutanten konnte die molekulare Ursache für den Funktionsverlust in *omb* identifiziert werden: in *l(1)omb[13]* führt eine Missensmutation zum Austausch einer hochkonservierten Aminosäure innerhalb der DNA-bindenden T-Domäne. In *l(1)omb[15]* verursacht eine Nonsense-Mutation eine C-terminale Trunkation. Wahrscheinlich sind in den beiden anderen Mutanten regulatorische Bereiche des Gens betroffen oder bislang noch nicht identifizierte alternative Exons.

Um zu sehen, ob in der Missense-Mutante *l(1)omb[13]* die DNA-Bindungsfähigkeit beeinträchtigt ist, wurden elektrophoretische Mobilitätstest mit Komplexen aus wildtypischer bzw. mutanter T-Domäne mit einer Zielsequenz durchgeführt. Diese zeigten, dass die mutante T-Domäne nicht mehr in der Lage ist, an das palindromische Konsensus-T-Box-Element zu binden.

6. References

- Ananthan, J., A. L. Goldberg, et al. (1986). "Abnormal proteins serve as eukaryotic stress signals and trigger the activation of heat shock genes." Science **232**(4749): 522-4.
- Avery, L. (1993). "Motor neuron M3 controls pharyngeal muscle relaxation timing in *Caenorhabditis elegans*." J Exp Biol **175**: 283-97.
- Avery, L. and H. R. Horvitz (1989). "Pharyngeal pumping continues after laser killing of the pharyngeal nervous system of *C. elegans*." Neuron **3**(4): 473-85.
- Bamshad, M., T. Le, et al. (1999). "The spectrum of mutations in TBX3: Genotype/Phenotype relationship in ulnar-mammary syndrome." Am J Hum Genet **64**(6): 1550-62.
- Bamshad, M., R. C. Lin, et al. (1997). "Mutations in human TBX3 alter limb, apocrine and genital development in ulnar-mammary syndrome." Nat Genet **16**(3): 311-5.
- Banga, S. S., B. T. Bloomquist, et al. (1986). "Cytogenetic characterization of the 4BC region on the X chromosome of *Drosophila melanogaster*: localization of the mei-9, norpA and omb genes." Chromosoma **93**(4): 341-6.
- Bargmann, C. I. (1993). "Genetic and cellular analysis of behavior in *C. elegans*." Annu Rev Neurosci **16**: 47-71.
- Bargmann, C. I. and L. Avery (1995). "Laser killing of cells in *Caenorhabditis elegans*." Methods Cell Biol **48**: 225-50.
- Bargmann, C. I. and H. R. Horvitz (1991). "Chemosensory neurons with overlapping functions direct chemotaxis to multiple chemicals in *C. elegans*." Neuron **7**(5): 729-42.
- Basson, C. T., D. R. Bachinsky, et al. (1997). "Mutations in human TBX5 [corrected] cause limb and cardiac malformation in Holt-Oram syndrome." Nat Genet **15**(1): 30-5.
- Blackwell, T. K. and H. Weintraub (1990). "Differences and similarities in DNA-binding preferences of MyoD and E2A protein complexes revealed by binding site selection." Science **250**(4984): 1104-10.
- Bolwig, N. (1946). Sense and sense organs of the anterior end of the house fly larvae. Vidensk Medd Dansk Naturh Forenh Kbh. **109**: 81-217.
- Brand, A. H., A. S. Manoukian, et al. (1994). "Ectopic expression in *Drosophila*." Methods Cell Biol **44**: 635-54.
- Brassington, A. M., S. S. Sung, et al. (2003). "Expressivity of Holt-Oram syndrome is not predicted by TBX5 genotype." Am J Hum Genet **73**(1): 74-85.
- Braybrook, C., K. Doudney, et al. (2001). "The T-box transcription factor gene TBX22 is mutated in X-linked cleft palate and ankyloglossia." Nat Genet **29**(2): 179-83.

- Braybrook, C., S. Lisgo, et al. (2002). "Craniofacial expression of human and murine TBX22 correlates with the cleft palate and ankyloglossia phenotype observed in CPX patients." Hum Mol Genet **11**(22): 2793-804.
- Brisson, J. A., A. R. Templeton, et al. (2004). "Population Genetics of the Developmental Gene optomotor-blind (omb) in *Drosophila* polymorpha: Evidence for a Role in Abdominal Pigmentation Variation." Genetics **168**(4): 1999-2010.
- Brunner, A., R. Wolf, et al. (1992). "Mutations in the proximal region of the optomotor-blind locus of *Drosophila melanogaster* reveal a gradient of neuroanatomical and behavioral phenotypes." J Neurogenet **8**(1): 43-55.
- Brunner, E., D. Brunner, et al. (1999). "The dominant mutation Glazed is a gain-of-function allele of wingless that, similar to loss of APC, interferes with normal eye development." Dev Biol **206**(2): 178-88.
- Chalfie, M., J. E. Sulston, et al. (1985). "The neural circuit for touch sensitivity in *Caenorhabditis elegans*." J Neurosci **5**(4): 956-64.
- Chin-Sang, I. D. and A. D. Chisholm (2000). "Form of the worm: genetics of epidermal morphogenesis in *C. elegans*." Trends Genet **16**(12): 544-51.
- Coll, M., J. G. Seidman, et al. (2002). "Structure of the DNA-bound T-box domain of human TBX3, a transcription factor responsible for ulnar-mammary syndrome." Structure (Camb) **10**(3): 343-56.
- Cowles, C. R., J. N. Hirschhorn, et al. (2002). "Detection of regulatory variation in mouse genes." Nat Genet **32**(3): 432-7.
- Cross, S. J., Y. H. Ching, et al. (2000). "The mutation spectrum in Holt-Oram syndrome." J Med Genet **37**(10): 785-7.
- Fan, C., M. A. Duhagon, et al. (2003). "Novel TBX5 mutations and molecular mechanism for Holt-Oram syndrome." J Med Genet **40**(3): e29.
- Ferguson, E. L. and H. R. Horvitz (1985). "Identification and characterization of 22 genes that affect the vulval cell lineages of the nematode *Caenorhabditis elegans*." Genetics **110**(1): 17-72.
- Fischbach, K. F. and A. Dittrich (1989). "The optic lobe of *Drosophila melanogaster*. I. A Golgi analysis of wild-type structures." Cell Tissue Res **258**: 441-475.
- Garcia-Bellido, A. and J. R. Merriam (1969). "Cell lineage of the imaginal discs in *Drosophila* gynandromorphs." J Exp Zool **170**(1): 61-75.
- Garrity, D. M., S. Childs, et al. (2002). "The heartstrings mutation in zebrafish causes heart/fin Tbx5 deficiency syndrome." Development **129**(19): 4635-45.
- Geiger, G. and D. R. Nassel (1981). "Visual orientation behaviour of flies after selective laser beam ablation of interneurons." Nature **293**(5831): 398-9.

- Gerlitz, O., D. Nellen, et al. (2002). "A screen for genes expressed in Drosophila imaginal discs." Int J Dev Biol **46**(1): 173-6.
- Ghosh, T. K., E. A. Packham, et al. (2001). "Characterization of the TBX5 binding site and analysis of mutations that cause Holt-Oram syndrome." Hum Mol Genet **10**(18): 1983-94.
- Gibson, C., E. Golub, et al. (1991). "Structure and expression of the bovine amelogenin gene." Biochemistry **30**(4): 1075-9.
- Goldschmidt, R. (1935). "Gen und Ausseneigenschaft. I-II ." Zeit. ind. Abst. Vererb. **69**: 38-131.
- Golic, K. G. and S. Lindquist (1989). "The FLP recombinase of yeast catalyzes site-specific recombination in the Drosophila genome." Cell **59**(3): 499-509.
- Gong, W., S. Gottlieb, et al. (2001). "Mutation analysis of TBX1 in non-deleted patients with features of DGS/VCFS or isolated cardiovascular defects." J Med Genet **38**(12): E45.
- Green, P., A. Y. Hartenstein, et al. (1993). "The embryonic development of the Drosophila visual system." Cell Tissue Res **273**(3): 583-98.
- Grenningloh, G., E. J. Rehm, et al. (1991). "Genetic analysis of growth cone guidance in Drosophila: fasciclin II functions as a neuronal recognition molecule." Cell **67**(1): 45-57.
- Grimm, S. (1997). Das T-Box Protein Optomotor-blind von Drosophila melanogaster: DNA-Bindungseigenschaften und die Rolle in der Imaginalentwicklung, Universität Würzburg.
- Haag, J., F. Theunissen, et al. (1997). "The intrinsic electrophysiological characteristics of fly lobula plate tangential cells: II. Active membrane properties." J Comput Neurosci **4**(4): 349-69.
- Haag, J., A. Vermeulen, et al. (1999). "The intrinsic electrophysiological characteristics of fly lobula plate tangential cells: III. Visual response properties." J Comput Neurosci **7**(3): 213-34.
- Halder, G. and S. B. Carroll (2001). "Binding of the Vestigial co-factor switches the DNA-target selectivity of the Scalloped selector protein." Development **128**(17): 3295-305.
- Halfon, M. S., H. Kose, et al. (1997). "Targeted gene expression without a tissue-specific promoter: creating mosaic embryos using laser-induced single-cell heat shock." Proc Natl Acad Sci U S A **94**(12): 6255-60.
- Hartenstein, V. (1988). "Development of Drosophila larval sensory organs: Spatiotemporal pattern of sensory neurons, peripheral axonal pathways and sensilla differentiation." Development **102**: 869-886.

- Haworth, K., W. Putt, et al. (2001). "Canine homolog of the T-box transcription factor T; failure of the protein to bind to its DNA target leads to a short-tail phenotype." Mamm Genome **12**(3): 212-8.
- Heimbeck, G., V. Bugnon, et al. (1999). "Smell and taste perception in *Drosophila melanogaster* larva: toxin expression studies in chemosensory neurons." J Neurosci **19**(15): 6599-609.
- Heisenberg, M. (1972). Behavioral diagnostics; a way to analyze visual mutants of *Drosophila*. Information Processing in the Visual Systems of Arthropods. Berlin, Springer Verlag: 265-268.
- Heisenberg, M., and K. Götz (1975). "The use of mutations for the partial degradation of vision in *Drosophila melanogaster*." J. Comp. Physiol. **98**: 217-241.
- Heisenberg, M., Wonneberger, R. and Wolf, R. (1978). "Optomotor-blind H31-- a *Drosophila* mutant of the lobula plate giant neurons." J.comp. Physiol **124**: 287--296.
- Helfrich-Forster, C., T. Edwards, et al. (2002). "The extraretinal eyelet of *Drosophila*: development, ultrastructure, and putative circadian function." J Neurosci **22**(21): 9255-66.
- Herrmann, B. G. and A. Kispert (1994). "The T genes in embryogenesis." Trends Genet **10**(8): 280-6.
- Hiroi, Y., S. Kudoh, et al. (2001). "Tbx5 associates with Nkx2-5 and synergistically promotes cardiomyocyte differentiation." Nat Genet **28**(3): 276-80.
- Hofmeyer, K. (2001). The optic lobe regulatory region of *Drosophila melanogaster* gene *optomotor-blind*, *PhD Thesis*, Universität Würzburg.
- Holmes, A. L., R. N. Raper, et al. (1998). "Genetic analysis of *Drosophila* larval optic nerve development." Genetics **148**(3): 1189-201.
- Jurgens, G., R. Lehmann, et al. (1986). "Segmental organization of the head in the embryo of *Drosophila melanogaster*." Roux's Arch. Dev. Biol **195**: 359-377.
- Kankel, D., A. Ferrus, et al. (1980). The structure and development of the nervous system. The genetics and biology of *Drosophila*: 295-368.
- Kerscher, S., S. Albert, et al. (1995). "Molecular and genetic analysis of the *Drosophila* mas-1 (mannosidase-1) gene which encodes a glycoprotein processing alpha 1,2-mannosidase." Dev Biol **168**(2): 613-26.
- Kimble, J. E. and J. G. White (1981). "On the control of germ cell development in *Caenorhabditis elegans*." Dev Biol **81**(2): 208-19.
- Kispert, A. and B. G. Herrmann (1993). "The Brachyury gene encodes a novel DNA binding protein." EMBO J. **12**: 3211-3220.

- Krapp, H. G. and R. Hengstenberg (1996). "Estimation of self-motion by optic flow processing in single visual interneurons." Nature **384**(6608): 463-6.
- Li, Q. Y., R. A. Newbury-Ecob, et al. (1997). "Holt-Oram syndrome is caused by mutations in TBX5, a member of the Brachyury (T) gene family." Nat Genet **15**(1): 21-9.
- Maienschein, J. (1972). "Cell lineage, ancestral reminiscence, and the biogenetic law." J. Hist. Biol. **11**: 129-158.
- Malpel, S., A. Klarsfeld, et al. (2002). "Larval optic nerve and adult extra-retinal photoreceptors sequentially associate with clock neurons during *Drosophila* brain development." Development **129**(6): 1443-53.
- McCarter, J., B. Bartlett, et al. (1997). "Soma-germ cell interactions in *Caenorhabditis elegans*: multiple events of hermaphrodite germline development require the somatic sheath and spermathecal lineages." Dev Biol **181**(2): 121-43.
- McIntire, S. L., E. Jorgensen, et al. (1993). "The GABAergic nervous system of *Caenorhabditis elegans*." Nature **364**(6435): 337-41.
- Meinertzhagen, I. A. and T. E. Hanson (1993). The development of the optic lobe. The Development of *Drosophila melanogaster*. I. M. B. a. A. M. Arias. New York, Cold Spring Harbor Laboratory Press: 1363-1492.
- Mitchell, H. K. and L. S. Lipps (1978). "Heat shock and phenocopy induction in *Drosophila*." Cell **15**(3): 907-18.
- Miyahara, K., N. Suzuki, et al. (2004). "TBX2/TBX3 transcriptional factor homologue controls olfactory adaptation in *Caenorhabditis elegans*." J Neurobiol **58**(3): 392-402.
- Muller, C. W. and B. G. Herrmann (1997). "Crystallographic structure of the T domain-DNA complex of the Brachyury transcription factor." Nature **389**(6653): 884-8.
- Nagy, E. and L. E. Maquat (1998). "A rule for termination-codon position within intron-containing genes: when nonsense affects RNA abundance." Trends Biochem Sci **23**(6): 198-9.
- Oliver, B., N. Perrimon, et al. (1987). "The ovo locus is required for sex-specific germ line maintenance in *Drosophila*." Genes Dev **1**(9): 913-23.
- Packham, E. A. and J. D. Brook (2003). "T-box genes in human disorders." Hum Mol Genet **12 Spec No 1**: R37-44.
- Papayioannou, V. E. (2001). "T-box genes in development: from hydra to humans." Int Rev Cytol **207**: 1-70.
- Papayioannou, V. E. and L. M. Silver (1998). "The T-box gene family." Bioessays **20**(1): 9-19.

- Pflugfelder, G. O. and M. Heisenberg (1995). "Optomotor-blind of *Drosophila melanogaster*: a neurogenetic approach to optic lobe development and optomotor behaviour." Comp Biochem Physiol A Physiol **110**(3): 185-202.
- Pflugfelder, G. O., H. Roth, et al. (1992). "The lethal(1)optomotor-blind gene of *Drosophila melanogaster* is a major organizer of optic lobe development: isolation and characterization of the gene." Proc Natl Acad Sci U S A **89**(4): 1199-203.
- Pflugfelder, G. O., H. Schwarz, et al. (1990). "Genetic and molecular characterization of the optomotor-blind gene locus in *Drosophila melanogaster*." Genetics **126**(1): 91-104.
- Pierantoni, R. (1976). "A look into the cock-pit of the fly. The architecture of the lobular plate." Cell Tissue Res **171**(1): 101-22.
- Piotrowski, T., D. G. Ahn, et al. (2003). "The zebrafish van gogh mutation disrupts *tbx1*, which is involved in the DiGeorge deletion syndrome in humans." Development **130**(20): 5043-52.
- Plageman, T. F., Jr. and K. E. Yutzey (2004). "Differential expression and function of *Tbx5* and *Tbx20* in cardiac development." J Biol Chem **279**(18): 19026-34.
- Pollock, J. A. and S. Benzer (1988). "Transcript localization of four opsin genes in the three visual organs of *Drosophila*; RH2 is ocellus specific." Nature **333**(6175): 779-82.
- Pollock, R. and R. Treisman (1990). "A sensitive method for the determination of protein-DNA binding specificities." Nucleic Acids Res. **18**(21): 6197-204.
- Pulichino, A. M., S. Vallette-Kasic, et al. (2003). "Human and mouse TPIT gene mutations cause early onset pituitary ACTH deficiency." Genes Dev **17**(6): 711-6.
- Roulet, E., S. Busso, et al. (2002). "High-throughput SELEX SAGE method for quantitative modeling of transcription-factor binding sites." Nat Biotechnol **20**(8): 831-5.
- Sambrook, J., Fritsch, E.F., Maniatis, T (1989). Molecular cloning: A laboratory manual. Cold Spring Harbor, NY, Cold Spring Harbor Laboratory Press.
- Schmucker, D., H. Jackle, et al. (1997). "Genetic analysis of the larval optic nerve projection in *Drosophila*." Development **124**(5): 937-48.
- Schmucker, D., H. Taubert, et al. (1992). "Formation of the *Drosophila* larval photoreceptor organ and its neuronal differentiation require continuous Kruppel gene activity." Neuron **9**(6): 1025-39.
- Scott, E. K., T. Raabe, et al. (2002). "Structure of the vertical and horizontal system neurons of the lobula plate in *Drosophila*." J Comp Neurol **454**(4): 470-81.

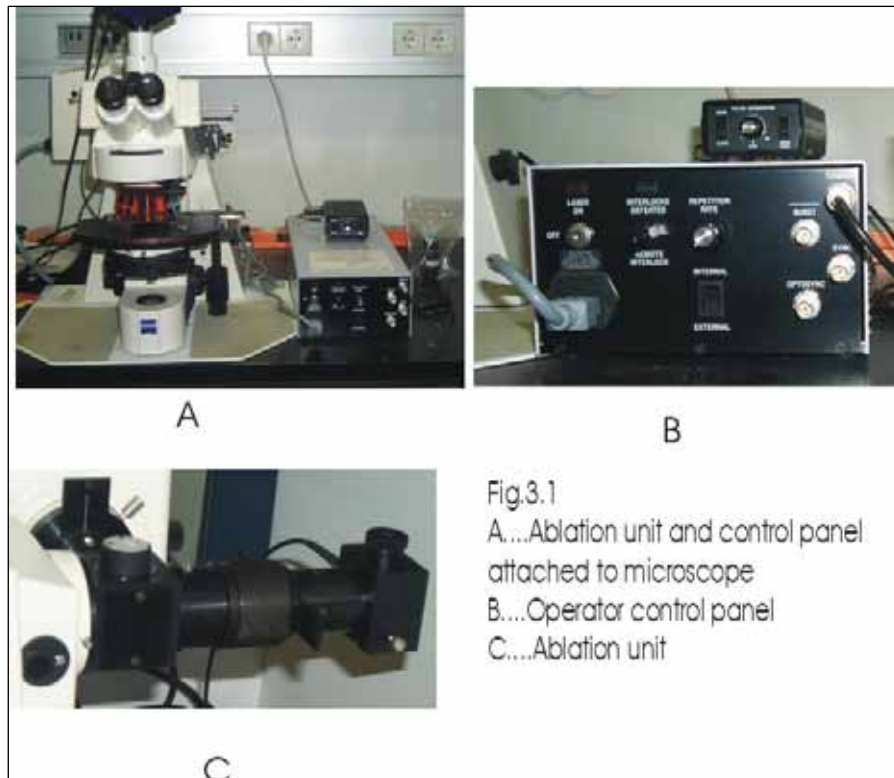
- Singh, R. and K. Singh (1984). "Fine structure of the sensory organs of *Drosophila melanogaster* Meigen larva (Diptera: drosophilidae)." Int J Insect Morphol Embryol **13**: 255-273.
- Smith, J. (1999). "T-box genes: what they do and how they do it." Trends Genet **15**(4): 154-8.
- Steller, H., K. F. Fischbach, et al. (1987). "Disconnected: a locus required for neuronal pathway formation in the visual system of *Drosophila*." Cell **50**(7): 1139-53.
- Stent, G. S. (1987). "Cell lineage in development." FEBS Lett **215**(1): 1-8.
- Stent, G. S. (1998). "Developmental cell lineage." Int J Dev Biol **42**(3): 237-41.
- Stocker, R. F. (1994). "The organization of the chemosensory system in *Drosophila melanogaster*: a review." Cell Tissue Res **275**(1): 3-26.
- Stoller, J. Z. and J. A. Epstein (2005). "Identification of a novel nuclear localization signal in *Tbx1* that is deleted in DiGeorge syndrome patients harboring the 1223delC mutation." Hum Mol Genet.
- Stringham, E. G. and E. P. Candido (1993). "Targeted single-cell induction of gene products in *Caenorhabditis elegans*: a new tool for developmental studies." J Exp Zool **266**(3): 227-33.
- Sulston, J. E., D. G. Albertson, et al. (1980). "The *Caenorhabditis elegans* male: postembryonic development of nongonadal structures." Dev Biol **78**(2): 542-76.
- Sulston, J. E., E. Schierenberg, et al. (1983). "The embryonic cell lineage of the nematode *Caenorhabditis elegans*." Dev Biol **100**(1): 64-119.
- Taverner, N. V., J. C. Smith, et al. (2004). "Identifying transcriptional targets." Genome Biol **5**(3): 27.
- Thiesen, H.-J. and C. Bach (1990). "Target Detection Assay: a versatile procedure to determine DNA binding sites as demonstrated on SP1 protein." Nucleic Acids Res. **18**: 3203-3209.
- Weisblat, D. A., G. Harper, et al. (1980). "Embryonic cell lineages in the nervous system of the glossiphoniid leech *Helobdella triserialis*." Dev Biol **76**(1): 58-78.
- Weisblat, D. A., R. T. Sawyer, et al. (1978). "Cell lineage analysis by intracellular injection of a tracer enzyme." Science **202**(4374): 1295-8.
- White, J. G., W. B. Amos, et al. (1987). "An evaluation of confocal versus conventional imaging of biological structures by fluorescence light microscopy." J Cell Biol **105**(1): 41-8.
- White, P. H. and D. L. Chapman (2005). "Dll1 is a downstream target of *Tbx6* in the paraxial mesoderm." Genesis **42**(3): 193-202.

Yagi, H., Y. Furutani, et al. (2003). "Role of TBX1 in human del22q11.2 syndrome." Lancet **362**(9393): 1366-73.

Yang, J., D. Hu, et al. (2000). "Three novel TBX5 mutations in Chinese patients with Holt-Oram syndrome." Am J Med Genet **92**(4): 237-40.

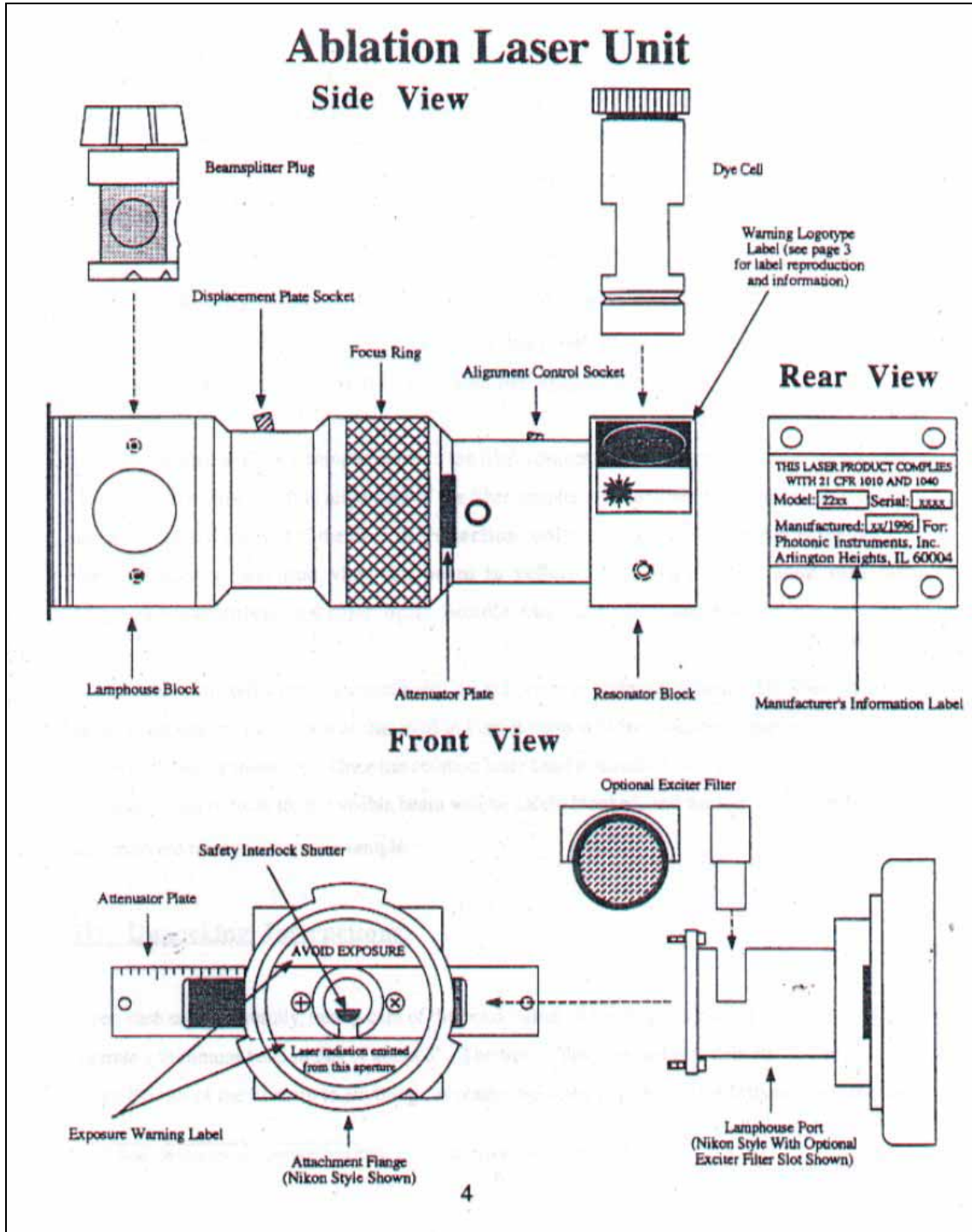
7. Appendix

Appendix 1: Set up and specifications of laser unit



Specifications: (Source: Laser Science, Inc.)

Wavelength	337.1 nm
Spectral Bandwidth	0.1 nm
Repetition Rate	1 to 30 Hz, up to 60 Hz in burst mode
Pulse Width, FWHM	4 nsec
Pulse Energy	300 μ J
Pulse to Pulse Energy Stability	<4% std. dev.
Peak Power	75 kW
Average Power	6 mW at 20 Hz
Beam Area	35 mm ²
Beam Divergence, Full Angle	0.3 mrad
Optosync Output	TTL, rising edge trigger; 50 ohm drive capability
Optical Pulse to Optosync Delay	50 nsec; <500 psec std. dev. jitter
Sync Output	TTL, rising edge trigger
Burst Input	TTL, HIGH=disable
External Trigger Input	TTL, rising edge trigger
Trigger In to Optical Pulse Out	700 nsec nominal; <40 nsec std. dev. jitter
Power Consumption	1.5 A 110 VAC; 1 A 220 VAC
Dimensions, l x w x h	18.2 x 7.6 x 4.6 in; 46.3 x 19.3 x 11.7 cm



Appendix 2: Locations of primers in genomic DNA fragment covering omb region

23041 tggacacccat acacacacac atttaacggt taagcogttg tccttttttc **OMB60**
 23101 **aaaggatg**g attcgaatgt gcgtgagtta tccggcgtgt tgttatctcg gctcggacca
 23161 aataggatac aaaaaaac tagcataaac cggttctgag taagtgtca attactcaca
 23221 cacacacaca cacacatgca aagaagtgt cactcaaac gaagcgaac gaggcgaatt
 23281 cgtgcctctg cctctgccga cgtcgactgt gctgccgtgg tgggttttgt gaagcaaagc
 23341 gtgcgagcaga gtggcgaata gcgtcattca aaattggaat t**ctttagta aacgtcgaca**
 23401 **cttcatatga aacgaagagc qgagatcaca qcggaaaatc caggggt**gta cgtgggttta
 23461 aa**acgcacag agggatttca ct**caaagaa gaaagaatac gtttatactt atatagggtt
 23521 agaccaggag ggtaggctac gtataaagac aagaagaagg aaagcaaaga aagaatggcc
 38581 actaacttta ataatcaaac gggaaatttt tttctctaa actttttttt ttaataaat
 38641 ctatctaat aaccgtcata a**tgacggttc tcgaaaaatct caagcggcga cct**aactaa
 38701 aaatcatatt tacgtttttt atag**caatga aacatqaatt tttttgaaac aacaagaaga**
 38761 **gaaataaaqt qtacaagtca qtgagtgctc caaacaacaaa qttttaaaaa aaaagaaaca**
 38821 **aaaacaagta cctgtagaac aaaacaacaaa taaagcatct aaaaatttca aaagtcaaac**
 38881 **tagagagatc ctttttttgg aqagatcgc** qtgqgaaacc ctttctqcat gacgcacttg
 38941 **gttqtttgaa acggttatgt gatga**^{START}**gac** gacgtccagg agctgctatt tcatcagtct
 39001 **gctgaggatc cattcgccag qttcgccaat qggatggcat atcatccatt tctgcagcta**
 39061 **acgcaacgac ccaactgactt cagcgtttcc tcgctgttga cggcgggtag caacaataac**
 39121 **aacagcggca acaccaacag cggaaacaac aactccaatt ccaacaacaa caccaattca**
 39181 **aacaccaata acaccaacaa tctcgtggcc gtttcaccaa cgggtggtgq tqcgcagta**
 39241 **tcqccgcaaa qcaaccacag cagcagcaac accaccacca ccagcaacac caacaactcc**
 39301 **agttccaata acaacaataa taacagtacc cataataata acaacaacca cacgaataac**
 39361 **acaacaata ataataataa cacaagtcaa aagcaaggac acacttgag caccac**cgag
 39421 **gaaccgcat cqcccgtgq cacaccaccg ccacaaatg ttggtctacc qccaatacca**
 39481 **cgccccaaca acaacagcag tagcagcagc agcaacaact cagcttcagc cggcc**cat
 39541 **ccgtcgacc acccaac**cg cgcacatcac tcaccagta cgggtgccgc cgcaccgccc
 39601 **cgccgccc**a **caggcttgc gccacc**ca cgcgccacc acctgcaaca acaacagcag
 39661 **caacaacagc acccgcccc accaccacca ccgtacttcc cagctcggc actgcccgt**
 39721 **ctagctgqaa gtccggccgq accgcatccg ggtctgtatc ccggcgtgq attgccttc**
 39781 **ccgccgacc acccaggtgc ccatccgac gcccatcacc tgggcagcgc ctatactacc**
 39841 **gccgagcagc tcgtccttgc ctcggccgtc gcccatcagc tqcatccgc gatgcaccg**
 39901 **ctcggggcgc ttcagcccga ggcagatgc gtcgtcagtg atcccaaggt cacgctggag**
 39961 **gqcaaaagacc tqtgggagaa qttccacaaa ctgggcacgq aatggtcat caccaagac**
 40021 **ggcag**gtgag ttctatactc attttacagg gtatt**aaqg tctccaaca tttac**gtg
 40081 taaaatcgaa **tctcgattag aattcgaacg aa**tgtagctt tatacaaaag aattgtttt
 40141 ggatatgctt tgccgcata ttggcaata attgtgacct ttgccgagct tttggcaatc
 40201 gagggcacag atctggggcc gaaggtcagc tcacagcccg ggcaagcagc cttggccact
 61021 gagaaccaga acgtggtctt gagtcttagg ctttataagc cgcactgatt **aagct**ttat
 61081 ttgattagcc cgagaaaatg accatagccc ccctgatatt ctcgaccat **c ctgaccgtag**
 61141 **cacacacc**a tctctaattc ctcatttggc tcaactcctg attttctttt ttttttccat

Exon I

Exon II

61201 cttactcgtt gcagacaaat gtttccqcaa atgaaatttc gtgtttcggg actggatgcc
61261 aaggctaaat acatcttgc t actggacatt gtggcggcgg acgattatcg ttataaattt
61321 cataataggt gagtttgaag cgctggcgtt ttgcaaaacg cattcaatcc catataatcg
61381 ttataatcgt aatataatta cagtcgctg atgggtggctg qcaaagcggg tcccagatg
61441 ccaaaacgca tqtatatcca tccagattcg cccacaacgg gtgagcaatg gatgcagaaa
61501 gttgtttcat ttcacaaatt aaaattgacc aacaatatta gtgataaaca tggatttcta
61561 agtactgtac gtcttctttg tttaccgcat tagttatcta agatacaaca caaccacaca
61621 atccataact aaagaaaaaa aaaacagcat ccaaaactca acgataccaa ggaatacaac
61681 tggatttaca attatttagc gtcgcctagt agcggtatta gtccaaaatt aagcgttatt
61741 atctcatgat aattgcgagt gtgtgtgtgt gagatcataa ggactgactt ttaattctc
61801 ctaacagtaa gtgcgcactt tagctccagc tcatccattg atgttctgt cttaaaaagt
88561 ttggtctccc gtttttggtt tccctcgggt ggtcgaaacg aactagccat ggccgtctga
88621 caat ttcact aatccccgt ccatcttgcat ctatttttat ttgcccgcc gcagacgatc
88681 ctgaactcga tgcacaagta ccagcccggt tccacctgg tgcgagccaa tgacatcctg
88741 aagctgccc actccacgt tccgacgtac gtcttcaagg agaccgatt catcgcctc
88801 acagcatatc aaaatgagaa ggtgagtagt actcagcttg tagtcgatga atcgaccatt
88861 aatcgttttc tttcccacag ataactcaat tgaaaatcga taacaatccg tttgcgaagg
88921 gctttcgtga tactggtgcc gqcaagcggg aaaagaaagt agtatcacta gtgaatagtt
88981 atgaatacgg gactcatcaa gtgctctttt cctttgataa tgcacttga tgggtggttc
89041 aaactgaggt caaaaatgct gctagcttat acgaaatgtc ttaatcatta cgtggtacaa
89101 gtaatccata gtcaaattac agtttaaaaa tgcttgcttc ctaaacttgc tctcctca
92401 gatattttag caaccaacaa tattttcaa gctacaatcc tgatcccaac gcaaatccg
92461 ctggataatc aaccgcgaaa ttcagcagag aggtagaagg ctaagggcag acgacatagg
92521 ctaagctagt tggatagatg atggatagat taaggggttcc cattctcggc gctgtgatcc
92581 acgccaaagt gctaattatc actattcgat ctgactattg gatgttctaa tttgtggccc
92641 cgtctctcgt acaactgtt ttacagccag qcactgatgt cqaaccgagg qtccgattcg
92701 gacaagttga atccgacgca tqtgagcagc tcgcgggcac cgtccacct gggccacgcc
92761 ggccgctccg ctcatctgca tcccctgccc qcctgcttg ataatcagca qgacgacgac
92821 gacaagctcc tggacgtggt gggctccgca cagagctccg tactcccgt cagccactcg
92881 ctgcagcaga tgcacqcca ccagcactcc ggtaagtaat gatccaaca atactcgtag
92941 agctattcaa caaaaagaag cagaagaat ctaacaattc ctgcacattt ctaatcctca
93001 ctaataataa tottgacatt ctatttttgt ttatttcttc aagcagctct gqctgcttgg
93061 tttaatcact tggctgccc tggagccgga qcctccgaac atgcagctgc ggcggcggcc
93121 aatgcccagt cggagatgc actgctcgt cgtttcagg cggaccccga tqtggagcgg
93181 gatggcagc attcgaattg ctccgaaagc ctccgcccga gtaaccggcg tgcctttaag
93241 cccacctcga cgggcagtc caaggagcg qtgggcggcg ctgcagctgc cgcagcggct
93301 gqcttgaatc ccggtgccc tagctatccg tcaccgaata tctcgttggg tccgccatt
93361 caccctcgc cgcatttgtt qccttacctg tatccacatg qcctgtatcc accgcccat
93421 ctgggcctgc tgcacaatcc cgtgcagcg qcggccatga qtccgctg cctgaatccg
93481 ggtctgctct tcaatgccc actggcctg qcgcgccagc atccgcttt gtttgccac
93541 gcctacccgg cggcgggtca cacaccgta tcaccattac aagccctaaa gqccatcgc
93601 ttttcccgat agattttgc cggcagttg gqctccgct tcgatcagc gactcgggga
93661 tccaacgcaa atcctcggg agatcctca qcggcggcg qcggcggct ggtctcctt
93721 gtggtgga atggtcccag gactctgagt tccagccctc qtccccgacc tgcctcccac
93781 tcgcqccca ctcgaccgat ttcgatgta cccacaacgc qcctatcct gatgaagcaa
93841 ccacgtggcg gtggtgctg qcgcggtgt qcccaatcgc agcactcgc ttcggaactt
93901 aagagcatg agaagatgt caacggactg gaggttcaac acaatggcag tgcggcggca
93961 gcagcggcg ctcttcagct gcccagagaa gctgccagc atcatcatca caccagcgc
94021 caccaccagc agcagcagca tcagtcgcac caccagcaac agcaccacca gcaaccgca

Exon III

Exon IV

Exon V

Exon VI

Exon VII

Exon VIII

OMB25

OMB65

631

632

OMB26

OMB1

634

OMB7

OMB6

OMB11

OMB9

635

94081 caaccacatc cgcaccacca gacccatcta cactcgcacc atggggcgac aacgggcggt
94141 acggatcagc ~~ga~~caattact ggacggccgc tccgattgtg aggatgccgg tctcgaattg
94201 gaactagagt ~~tgaggaggga~~ ~~tgtcggag~~at ctggatcagg atccggatga gcaggacgag
94261 gatcgcagct cggtcacga tcttgatctg gacgtcgacg tctgaccgcg aacggatcag
94321 cgacattgcc tctagcctct gaactacacg gccaccgtct ttgtggttta gcgtagtgt
94381 tatgtacata tatatatcgg acgatttqga ccctagacta taggcatttg tagcatatat
94441 agtgtgtatt cctctctcgt tgcgaactca ~~ctc~~~~gcccgt~~ ~~ttatcggcag~~ ~~tgt~~taagtaa
94501 catctttttt tttttttgct tcgtttctaa gcaaagccta gccctagaa atcgctggcg
94561 attcgctggc aaagtgatgg agaggtctaa ttgaagacag aaggtagcaa aaacagaaga
94621 aaaaaaaaa ataacacaaa aaggaaacaa aaaacaggaa aaagttaagg cgacgtggca
94681 agagaatcgt cgtaactttt agcgccttga aggttccaga cttcaagatc aaacagacgg
94741 aataaaatga gaagtaaggg caaggggcta tcctcagaca aatttatgta tcaccatat
94801 atgtatattg attggattga aatagcaac atcaaagatg qcgctcttt atatacatct
94861 agaacacgca tatatatata tataaatata tatatatagt atatataqaa gctggtatat
94921 atacagaatg taaccttagt aaaacatata aqaaaaaaca aagaaaaaca aaaaccaca
94981 aaaaaaaaa

Appendix 3: Detail about the primers used for amplification and/or sequencing of the *omb* locus

primer number	name	sequence	Genomic (GI:28381560) location	Tm (°C)	Annealing (°C)
	Omb 60	CCC AAG AAG TCA AAG GAT GC	23090	57.3	48
	Omb 59	AGT GAA ATC CCT CTG TGC GT	23482	57.3	
	Omb 27	AAA TCT CAA GCG GCG ACC CC	38675	61.4	55
	Omb 32	GTG GGT GGC GGC AAG CCT GT	39629	65.5	
	Omb 33	CAT CCG TCG CAC CAC CCA AC	39538	63.5	52
	Omb 36	CAT AAA TGT TGG GAG ACC TT	40074	53.2	
	Omb 62	CCT GAC CGT AGC ACA CAC AC	61139	58.8	
	Omb 65	TCG TTG AGC TTT GGA TCG CG	61664	59.3	
	Omb 23	TTC ACT AAT CCC CCG TCC AT	88625	57.3	52
	Omb 26	AGC AGC TTT TTG ACC TCA GG	89063	57.6	
	Omb 1	AGG GGT TCC CAT TCT CGG CG	92552	63.5	55
	Omb 6	TAC TGC CGC CGA CGC TTT CC	93223	63.5	
	Omb 7	GAT GTG GAG CGG GAT GGC AG	93169	63.5	
	Omb 10	CTC CAC CAC ACC ACC ACC CA	93729	63.5	
	Omb 11	GAA CGC AAA TCG CTC GGG AG	93663	61.4	55
	Omb 16	ACA CTG GCG ATA AAC GGG CA	94493	59.4	
627		TGA CGG TTC TCG AAA ATC TCA A	38672	56.5	53
628		GTG GTG CTC AAG TGG TGT CCT T	39416	62.1	
629		CAC AAG TCA AAA GCA AGG ACA C	39381	58.4	50
630		TTC GTT CGA ATT CTA ATC GAG A	40112	54.7	
631		AAG CTG CCG TAC TCC ACG TTT C	88741	62.1	Sequencing primers
632		ACG TGC GAA ACG TGG AGT A	88768	56.7	
633		CTA CTC CCG CTC AGC CAC	92860	60.5	
634		AGT GCG GAG GAT GCA CTG	93127	58.2	52
635		CAT TCT CCA CCA CAC CAC CA	93733	56.7	
636		CCT CGA CAT CCT CCT CCA	94228	58.2	Sequencing primer

Appendix 4: Detail about the primers used for different experiments

Primer number	Name	Sequence	Length (bases)	Tm (°C)	purpose
673	selexHB random-92	TCC AAGCTT TCTGTATGTCG GGATCC N40GGATCCCCTAA CCGACTAAGCT TATT	92		Selex
674	selexHBfor	TCC AAGCTT TCTGTATGTCG	20		Selex
675	selexHBrev	AAT AAGCTT AGTCGGTTAGG	20		Selex
676	selexB/B-BraPal-upper	TCG GGATCC AACTCAGT AATTCACACCT AGGTGTGAA AT T TGACTCAA GGATCC CCT	58		Selex
677	selexB/B-BraPal-lower	AGG GGATCC TTGAGTCA AATTT CACACCT AGGTGTGAA ATTACTG AGTT GGATCC CGA	58		Selex
710	1xGTtop	GGCGATACACTTGTGGAATGTGTTTGAT TTGTTAGCC	37		Selex/EMS A
711	1xGTbottom	GGGGCTAACAAATCAAACACATTCCACA AGTGTATCG	37		Selex/EMS A
802	SG-70-SalI	ACA CAG TCG ACG ACG TCG TCC TTG CC	26		Cloning of T- domain of OMB
803	SG-71-SalI	TGT GTG TCG ACT TAG CCG GCA CCA GTA TC	29		Cloning of T- domain of OMB

Appendix 5: Suspected mutations in four lethal omb mutant lines:

Suspected mutation (line)	Seq. No.	seq.of suspected mutation site	Position in genomic seq (intron) [GI:28381560]	Position in cDNA seq (exon)	Nature of abnormalities	comments	Mutation or Polymorphism
Mutation 1 (1042)	2	TGCAGNA GATG	92887	2097 (VII)	C=T	In other three lines it is C; CAG(Gln) to TAG(stop) In others: Not present	Mutation
	19	TGCAGCA GATG			C>T		
	32	TGCAGNA GATG			C=T		
Mutation 2 (1042)	21	GGCAANGACCT	39966	1307 (II)	A=G	Genomic: GGCAANGACCT cDNA: GGCAAGGACCT but both code for lys (AAA/AAG) In others: present in 1039	Polymorphism
	45	GGCAANGACCT			A=G		
Mutation 3 (1042)	1	TGCTATTTTCAT	38989	331 (II)	T>C	Genomic: TGCTATTTTCAT cDNA: TGCTACTTCAT In others: present in 1039,171	Polymorphism
	172	TGCTACTTCAT			C>T		
Mutation 4 (1041)	76	GCTTG CAGTCG	88841 (V)		C>T	Genomic: GCTTGTAGTCG In others: present in 1039,171	Polymorphism
	93	GCTTG CAGTCG			C>T		
	144	GCTTG NAGTCG			C>T		
Mutation 5 (1041)	76	GTTTG NGAAGG	88915	1825 (VI)	C=T	Genomic: GTTTGCGAAGG cDNA: GTTTGCGAAGG mutant: GTTTGTGAAGG Ala(gcg) to Val (gtg) In others: Not present	Mutation
	93	GTTTG -GAAGG			Gap (but C=T)		
	144	GTTTG CGAAGG			C>T		
Mutation 6 (1041)	76	TAGTT N TGAAT	88981 (VI)		C>A (331 st)	Genomic: TAGTTATGAAT In others: present in 1039,171	Polymorphism
	93	TAGTT A TGAAT			A>C (18 th)		
	144	TAGTT N TGAAT			C=A (216 th)		

Suspected mutation (line)	Seq. No.	seq.of suspected mutation site	Position in genomic seq(intron) [GI:28381560]	Position in cDNA seq(exon)	Nature of abnormalities	comments	Mutation or Polymorphism
Mutation 7 (1039)	173	GGCAA A GACCT	39966	1307 (II)	Sequence not clear at the end	Genomic: GGCAA A GACCT cDNA: GGCAA G GACCT but both code for lys (AAA/AAG) In others: present in 1042	Polymorphism
	173	CCCGGNGGTGG	39765		Not clear, has peak of C, but T background is there.	Genomic: CCCGGCGGTGG	NO change in aa sequence
Mutation 8 (1039)	15	TGCTA N TTTCAT	38989	331 (II)	T≥C	Genomic: TGCTA T TTTCAT cDNA: TGCTA C TTTCAT In others: present in 1042,171	Polymorphism
	161	TGCTA N TTTCAT			C=T		
	169	TGCTA N TTTCAT			C=T		
Mutation 9 (1039)	77	GCTTG N AGTCG	88841 (V)		C=T (194 th)	Genomic: GCTTG T AGTCG In others: present in 1041,171	Polymorphism
	96	GCTTG C AGTCG		C>T (159 th)			
	145	GCTTG N AGTCG		C=T (79 th)			
Mutation 10 (1039)	77	TAGTT N TGAAT	88981 (VI)		C=A (335 th)	Genomic: TAGTT A TGAAT In others: present in 1041,171	Polymorphism
	96	TAGTT T TGAA		Not sure (20 th)			
	145	TAGTT N TGAAT		C=A (219 th)			
Mutation 12 (171)	213	TGCTA N TTTCAT	38989		C=T (303 rd)	In others: present in 1039,1042	Polymorphism
Mutation 16 (171)	111	GCTTG N AGTCG	88841 (V)		C=T (193 rd)	In others: present in 1039,1041	Polymorphism
	148	GCTTG N AGTCG		C=T (76 th)			
Mutation 17 (171)	111	TAGTT N TGAAT	88981 (VI)		C=A (303 rd)	In others: present in 1039,1041	Polymorphism
	148	TAGTT N TGAAT		C=A (216 th)			

Appendix 6: Fly stocks used in the experiments

Nr.	relevant feature	P	phenotype	stock description	purpose	obtained
47	omb ^{P4} /FM7	P	Streifen auf orange background	y w omb- <i>Gal4</i> ^{MD735} /FM7		
55	y w omb ^{P3} /FM7	P	Streifenaugen	dto (tatsächl. FM7!), omb- <i>Gal4</i>	original stock	M. Calleja 9/96
143	w Df(1)rb5 A122/FM6		B red	w Df(1)rb5 A122/FM6		Kerschermade
171	l(1)omb ¹² /FM7a		nur vermilion B Weibchen, keine w[a]BB W. umsetzen	l(1)omb ¹² v/FM7a		aus 92/93 bi enhanc. Muta
269	OLA-GFP	P	orange	X.9-2.5B/B in vector CPP-GFP; KHIII, p152D. prep 2A; Linie 6 auf II		gen. KH 11/98; 8/2000
270	OLA-GFP	P	braunrot - rot	X.9-2.5B/B in vector CPP-GFP; KHIII, p152D. prep 2A; Linie 7 auf III		gen. KH 11/98; 8/2000
284	<i>UAS:GFPnls</i>	P	orange	w[1118]; P14 (on III) (Donor Bruce Edgar)	Expression von Kern-lokalisiertem GFP	8/2000 Bloomington
291	<i>UAS:GFPnls</i>	P	W: orange-braun; M: rot	w[1118]; P{w[+mC]=UAS-GFP.nls}18(on III) (Donor Bruce Edgar)	Expression von Kern-lokalisiertem GFP	8/2000 Bloomington
294	Df(1)/FM7c, Kr- <i>Gal4</i> , UAS:GFP	P	red B females und FM7c Tiere	Df(1)JA27/FM7c, P{w[+mC]= <i>Gal4</i> -Kr.C}DC1, P{w[+mC]=UAS_GFP.S65T}DC5 (offensichtl alles auf FM7c chrs.	should express in Bolwig	8/2000 Bloomington
303	UAS:GFP	P	braun bis rot	UAS:GFP (S65T) = KH43 (on II)		J.-F. Ferveur /J.-R. Martin ex KH 8/2000
325	w; rh5-tau-lacZ (III)		y+	offensichtlich y+ transfo Vektor	laser ablation project	10/02 A. Hofbauer

334	FM7a/FM7a		y, w ^a , B	FM7a, y w ^a B v		
361	y w omb ^{P3} /FM6	P	rot Bar umsetzen	y w omb ^{P3} /FM6		IV-28, 12/97
395	l(1)ombD4, w; Dp/In(2LR)Gla, Bc		eyes: Glazed and white body: Black cells	w l(1)ombD4; DpA1125/In(2LR)Gla, Bc	Bc larval marker in l(1)omb	II-19, 8/95 IV-7 reconstructed
397	A122; ombJ-Gal4	P	wt	A122-lacZ; ombJgal4-1; III (#2)	HS/VS rescue	1/01 KH stock 7
438	omb-Gal4 438	P		X.9-2.5B/B, p221-4, II	omb-J	Dr. KH 97
504	omb ^{P6} /FM0	P	Streifenaugen. Homo males only small white wedge. homo females intensely red, expanded eyes. K bifid wings. Balancierte umsetzen	w Gal4 ^{omb1} /FMO, omb-Gal4	sei jump des Gal4 P-elements aus E132; homo-Linie geht nicht gut an	
569	rh5-gal4	P	very light orange (virgins nearly white), Cy		laser ablation project	10/02 A. Hofbauer
581	y w; rh6-tau-lacZ (III)	P		dito		10/02 von A. Hofbauer; originaly S. Britt
582	y w; rh6-tau-lacZ (II)	P		dito		10/02 von A. Hofbauer; originaly S. Britt
600	rh5-tau-lacZ (X)	P	fem: y, w, f (or sn?) male: y+ w f+		laser ablation project	10/02 A. Hofbauer
741	ombP7a/FM7c	P	Streifenaugen B females, FM7c males	w omb[P7a]/FM7c omb-Gal4	homo males tauchen nicht auf	VI-15B, 8/99
836	Gal4 GH 86	P	appear wt	w Gals4 GH86 (at 7C8/9)	for laser ablation with chemosensorybehavioral assay	6/02 Reini Stocker

					ref: Heimbeck et al. J. Ns. 19, 6599, 1999	
990	w; CyO/Sp; rh6-Gal4/TM2	P	bright orange, Cy, Sp	dito	laser ablation project	10/02 A. Hofbauer
1016	y w rh5-lacZ; rh6-GFP/CyO	P	orange Cy		for laser ablation	12/02 VII-29A
1017	w; rh5-Gal4/In(2LR)Gla Bc; UAS:GFP/TM3Sb	P	all are glazed; light eye colour, Sb Ordark eye colour Sb+		for laser ablation	12/02 VII-29B
1023	w omb[P3] A122/FM7c	P	Streifen augen Bar		Linie 10 for laser ablation	VII/31
1039	l(1)omb[11]/FM-GFP		red Bar; rel. viel y FM/FM BB females		to facilitate selection of hemizygous males for seq	VIII-3 2/03
1041	l(1)omb[13]/FM-GFP		red Bar; rel. viel y FM/FM BB females		to facilitate selection of hemizygous males for seq	VIII-3 2/03
1042	l(1)omb[15]/FM-GFP		red Bar; rel. viel y FM/FM BB females		to facilitate selection of hemizygous males for seq	VIII-3 2/03
1062	w; UAS:GFP(nls) stinger	P	females brown, male red eyes	homo on II	for strong localized GFP signals	4/01 from Olaf

Appendix 7: Established fly stocks of lethal *omb* mutant containing duplication over the *In(2LR)Gla,Bc*- chromosome

Nr.	relevant feature	phenotype	purpose	remarks
B4 ¹¹	I(1) <i>omb</i> [11] ; Dp/ <i>In(2LR)Gla, Bc</i>	Red eyes: Glazed and round, in both males and females	Males from these stocks to be used for complementation test for HS/VS cells development.	Stable stock
B4 ¹² (E3 ¹³)	I(1) <i>omb</i> [12] ; Dp/ <i>In(2LR)Gla, Bc</i>	Red eyes: Glazed and round, in both males and females	Males from these stocks to be used for complementation test for HS/VS cells development.	Stable stock From purified stock E3 ¹³
B4 ¹⁵	I(1) <i>omb</i> [15] ; Dp/ <i>In(2LR)Gla, Bc</i>	Red eyes: Glazed and round, in both males and females	Males from these stocks to be used for complementation test for HS/VS cells development.	Stable stock
E3 ¹³	I(1) <i>omb</i> ¹² /FM7a	red Bar females	To be used as stable lethal mutant stock with no 2nd mutation lethality.	Purified stock of line 171
E3 ³²	I(1) <i>omb</i> ¹² /FM7a	red Bar females	To be used as stable lethal mutant stock with no 2nd mutation lethality.	Purified stock of line 171
E3 ⁶³	I(1) <i>omb</i> ¹² /FM7a	red Bar females	To be used as stable lethal mutant stock with no 2nd mutation lethality.	Purified stock of line 171

Appendix 8: Genetic characterization of lethal omb mutants**A. Introduction of duplication/Gla marker in lethal mutants****A. Retest for non complementation:**

$l(1)omb[x]/FM-GFP; II \times w\ l(1)omb[D4]/Y; DpA1125/ln(2LR),GlaBc$ (395)



F1..... $l(1)omb[x]/Y; DpA1125/II$males (with vermilion eyes) were used in cross B1

B1 cross:

$l(1)omb[x]/FM-GFP; II \times l(1)omb[x]/Y; DpA1125/II$ (vermillion eye) males from A1



F1 $l(1)omb[x]/l(1)omb[x]; Dp/II$ these females were crossed in B2a

B2a cross:

$l(1)omb[x]/l(1)omb[x]; Dp/II \times w\ l(1)omb[D4]/Y; Dp/ln(2LR),GlaBc$ (B+ males from 395)



F1..... $l(1)omb[x]/Y; Dp/ln(2LR),GlaBc$ (these males were used in C1 and B3)

B2b cross: (repetition of cross B1)

$l(1)omb[x]/FM-GFP; II \times l(1)omb[x]/Y; DpA1125/II$ (vermillion eye) males from A1



F1... $l(1)omb[x]/l(1)omb[x]; Dp/II$ these females were crossed in B3

B3 cross:

$l(1)omb[x]/l(1)omb[x]; Dp/II$ (from B2b) $\times l(1)omb[x]/Y; Dp/ln(2LR),GlaBc$ (from B2a)



F1..... $l(1)omb[x]/l(1)omb[x]; Dp/ln(2LR),GlaBc$ (females) and $l(1)omb[x]/Y; Dp/ln(2LR),GlaBc$ (males)

[Use males and females for stable stock]

B. Lethal mutants tested for the effect on HS/VS cell development**C1 cross :**

w Df(1)rb[5] A122/FM6 (143) x l(1)omb[x]/ Y; Dp/ln(2LR),GlaBc



F1... w Df(1)rb[5] A122/ l(1)omb[x]; II/ ln(2LR),GlaBc

These glazed eyed females were tested for presence of HS/VS cells in the adult brain

C2 cross : cross to test the influence, if any, of Gla marker on HS/VS cell development

A122 (145) x w l(1)omb[D4]/Y; Dp/ln(2LR),GlaBc (395)



F1..... A122/ w l(1)omb[D4]; ln(2LR),GlaBc/II

Appendix 9: Alignment of OMB with other T-box proteins. Mutations in different T-box proteins are marked by arrow and details are given in table . Alignment was performed using the T-COFFEE program. Accession numbers of the respective proteins were mentioned in the table.

```

OMB_                MRYDVQELLHLHQAEDPFARFANGMAYHPFLQLTQRPTDFSVSSLLTAGS
NNNN
TBX1_HUMAN          -----
TBX2_HUMAN          -----MAYHPFHAPRPADFPMSAFLAA-----
TBX3_HUMAN          -----MSLSMRD-----
TBX4_HUMAN          -----
TBX5_HUMAN          -----
TBX6_HUMAN          -----MYHPRELYPSLGAGYRLGPAQPG-----
TBX19_HUMAN         -----MAMS-----
TBX22_HUMAN         -----MALSSRARAFSVEALVGR-----
BRA_MOUSE          -----MSSPG-----
T_XBRA             -----MSA-----
TBX1_Zebrafish     -----MISAISSPWLTLQSHFC-----
TBX5_zebrafish     -----
Ce_TBX2            -----

```

Cons

```

OMB_                SGNNTNSGNNNSNSNNNTNSNTNNTNNLVAVSPTGGGAQLSPQSNHSSSNTTTTTS
TBX1_HUMAN          -----
TBX2_HUMAN          -----
TBX3_HUMAN          -----
TBX4_HUMAN          -----
TBX5_HUMAN          -----
TBX6_HUMAN          -----
TBX19_HUMAN         -----
TBX22_HUMAN         -----
BRA_MOUSE          -----
T_XBRA             -----
TBX1_Zebrafish     -----
TBX5_zebrafish     -----
Ce_TBX2            -----

```

Cons

```

OMB_                NTNNSSSNNNNNSSTHNNNNNHNTNNNNNNNNNTSOKQGHHLSTTEEPSPAGTP
TBX1_HUMAN          -----MH-----
TBX2_HUMAN          -----AQPSFFP-----
TBX3_HUMAN          -----
TBX4_HUMAN          -----MLQ-----
TBX5_HUMAN          -----
TBX6_HUMAN          -----ADSSFFP-----
TBX19_HUMAN         -----ELGTRKP-----
TBX22_HUMAN         -----PSKRKLQ-----
BRA_MOUSE          -----TESAGKS-----
T_XBRA             -----TESCAKN-----
TBX1_Zebrafish     -----
TBX5_zebrafish     -----
Ce_TBX2            -----

```

Cons

```

OMB_ PPTIVGLPPIPPNNSSSSSSNSASAAAHPSSHPTAAHSPSTGAAAPPAGP
TBX1_HUMAN FSTVTRDMEAF TAS-----SL-----SSLGAAGGFPGAASPGADP
TBX2_HUMAN ALALPPGALAKPLP-----DPGLAGAAA
TBX3_HUMAN -----PVIPG TSM-----AYHP-----FLPHRAPDFAMSAVLG
TBX4_HUMAN DKGLSESEEA FRAP-----GPALGEASA
TBX5_HUMAN -----MADADEGFGLAHT
TBX6_HUMAN ALA-----
TBX19_HUMAN S-----
TBX22_HUMAN DPIQAEQPELREKKGGEEEEERRSSAAG-----
BRA_MOUSE L-----
T_XBRA V-----
TBX1_Zebrafish -----DVA AFTTS-----SL-----SSLNTPGSYHLSPPSPG
TBX5_zebrafish -----MADSEDTFRLQNS
Ce_TBX2 -----MAFNPFALGRPDLLL PFMGAGVGGPGA
    
```

Cons



E56TER(TBX22)

```

OMB_ TGLPPPTPPHHLQOQQQQOQHPAPPPPYFPAAALAALAGSPAGHPGLYPGGG
TBX1_HUMAN YG-----PREPPPPPPRYD-----PCAA
TBX2_HUMAN AA-----A-----AAAAAAE-----
TBX3_HUMAN -----HQPFFPAL TLP-----PNGA
TBX4_HUMAN AN-----A-----PEPALAA-----
TBX5_HUMAN -----PLEPDAKDLPCD-----SKPE
TBX6_HUMAN EG-----YRYPEL DTP-----KLD
TBX19_HUMAN -----DG-----TVS
TBX22_HUMAN -----KSEPLEKQPKTEPSTSASSGCGSDSGYG
BRA_MOUSE -----QY-----RVD
T_XBRA -----QY-----RVD
TBX1_Zebrafish -----DPYSHHESQF EPC-----PAAQ
TBX5_zebrafish -----PSDSEPKDLQNE-----GKSD
Ce_TBX2 GG-----PPPNLFFSMLQAGFP GPV GSP
    
```

Cons



```

OMB_ LRFPPHHPGAHPHAHHLGSA YTTAEDVVLASAVA-HQLHPAMRPLR-----ALQP
TBX1_HUMAN AAPGAPGPPPP- PHAY-----PFAPAAGAATSAAAEPEGP--GASCAAAAKAP-V
TBX2_HUMAN -----AGLHVSALGPHPPAAHLRSLKSL-----E
TBX3_HUMAN AALS L P GALAKPIMDQL-----VGAAETGIPFSSLGPO-----AHLRPLK-----TM-E
TBX4_HUMAN -----PGLSGAALGSPPGP-----GADVVA A-----A
TBX5_HUMAN SALGA-----PSK-SPSS-----PQA-----A
TBX6_HUMAN CFLSG-----MEA-APRTL-----AAHPPLPLLPPAMGTEPAP-----SA-----P
TBX19_HUMAN HLLNV-----VES-ELQA-----GR-----E
TBX22_HUMAN -----NS
BRA_MOUSE HLLSA-----VES-ELQA-----GS-----E
T_XBRA HLLSA-----VEN-ELQA-----GS-----E
TBX1_Zebrafish HAYNYSGSNSAQ-----APAQD SGTSNCSSSS-----SSSTPNK-----TL-V
TBX5_zebrafish KQNAA-----VSK-SPSS-----QT-----T
Ce_TBX2 -----P
    
```

Cons



E69TER(TBX5)

G80R(TBX5)



Q49K(TBX5) I54T(TBX5) N121T(TBX1_ZEB) T58A(TBX19) G118C(TBX22) L143P(TBX3) F148Y(TBX1)

OMB_ EDDGVVDDPKVTTLEGKDLWEKFHKLGT^{N121T}EMVITKSGRQMF^{L143P}PQMKFRVSGLDAAKAK

TBX1_HUMAN KKNAKVAGVSVQLEMKALWDEFNQLGT^{T58A}EMIVTKAGRRMFP^{G118C}TFQVKLFGMDPMAD

TBX2_HUMAN PEDEVEDDPKVTLEAKELWDQFHKLGT^{N121T}EMVITKSGRRMFP^{L143P}PFKVRVSGLDKAK

TBX3_HUMAN PEEVEEDDPKVHLEAKELWDQFHKRG^{T58A}TEMVITKSGRRMFP^{G118C}PFKVRVSGLDKAK

TBX4_HUMAN AAEQTIENIKVGLHEKELWKKFHEAG^{N121T}TEMIITKAGRRMFP^{L143P}SYKVKVTGMNP^{F148Y}PTK

TBX5_HUMAN FTQQGMEGIKVF^{N121T}LHERELW^{T58A}LK^{G118C}FHEVGT^{L143P}EMII^{F148Y}TKAGRRMFP^{G118C}SYKVKVTGLNPKTK

TBX6_HUMAN EALHSLPGVSLLENRELWKEFSSVGT^{N121T}EMII^{T58A}TKAGRRMFP^{G118C}ACRVSVTGLDPEAR

TBX19_HUMAN KGDPT^{N121T}EQQLQIILEDAPLWQRFKEVTNEMIVTKNGRRMFP^{L143P}VL^{F148Y}KISVTGLDPNAM

TBX22_HUMAN SESLEEKDIQ^{N121T}MELOQSELW^{T58A}KRFHDIGTE^{G118C}MIITKAGRRMFP^{L143P}SVRVK^{F148Y}VGLD^{F148Y}PGKQ

BRA_MOUSE KGDPTERELRVGLEESE^{N121T}SELW^{T58A}LRFKELTNEMIVTKNGRRMFP^{L143P}VL^{F148Y}KVNVSGLDPNAM

T_XBRA KGDPT^{N121T}EKELK^{T58A}VSLEERDLW^{G118C}TRFKELTNEMIVTKNGRRMFP^{L143P}VL^{F148Y}KVSMSGLDPNAM

TBX1_Zebrafish KKNPKVANINVQLEMKALWDEFNQLGT^{N121T}EMIVTKAGRRMFP^{L143P}TFQVKIFGMDPMAD

TBX5_zebrafish YIQQGMEGIK^{N121T}VY^{T58A}LHERELW^{G118C}TKFHEVGT^{L143P}EMII^{F148Y}TKAGRRMFP^{G118C}SYKVKVTGLNPKTK

Ce_TB^{N121T}X2 EDDGV^{T58A}TDDPKVELDERELW^{G118C}QQFSQCGTE^{L143P}MVITKSGRRIF^{F148Y}PAYRVKISGLDKK^{F148Y}SQ

Cons : * . ** . * . . ** : : * * ** : : * * : . * : :

Y149S(TBX3) W121G(TBX5) S128F(TBX19)

OMB_ YILLLDIVAADDYRYKF--HNSRWMVAGKADPE--MPKRM^{Y149S}YIHPDSPTTGEQWMO

TBX1_HUMAN YMLLMDFVPVDDKRYRYAFHSSSWLVAGKADPA--TPGRVHYHPDSPAKGAQWMK

TBX2_HUMAN YILLMDIVAADDCRYKFH--NSRWMVAGKADPE--MPKRM^{Y149S}YIHPDSPATGEQWMA

TBX3_HUMAN YILLMDI^{Y149S}AAADDCRYKF--HNSRWMVAGKADPE--MPKRM^{Y149S}YIHPDSPATGEQWMS

TBX4_HUMAN YILLIDIVPADDHRYKFC--DNKWMVAGKAEP--MPGRLYVHPDSPATGAHWMR

TBX5_HUMAN YILLMDIVPADDHRYKFA--DNKWSVTGKAEP--MPGRLYVHPDSPATGAHWMR

TBX6_HUMAN YLFLLDVIPVDGARYRWQ--GRRWEPSGKAEP--LPDRVYIHPDSPATGAHWMR

TBX19_HUMAN YSLLLD^{Y149S}FVPTD^{Y149S}SHRWKYV--NGEWVPAGKPEVS--SHSCVYIHPDSPNFGAHWMK

TBX22_HUMAN YHVAIDVVPVDSKRYRYVYHSSQW^{Y149S}VMVAGNTDHL^{Y149S}CIIPRFYVHPDSPCSGETWMR

BRA_MOUSE YSFLLD^{Y149S}FVTADNHRWKYV--NGEWVPGGKPEPQ--APSCVYIHPDSPNFGAHWMK

T_XBRA YTVLLD^{Y149S}FVAADNHRWKYV--NGEWVPGGKPEPQ--APSCVYIHPDSPNFGAHWMK

TBX1_Zebrafish YMLLMDFLPVDDKRYRYAFHSSSWLVAGKADPA--TPGRVHYHPDSPAKGAQWMK

TBX5_zebrafish YILLMDVVPADDHRYKFA--DNKWSVTGKAEP--MPGRLYVHPDSPATGAHWMR

Ce_TB^{Y149S}X2 YFVMMDLVPADEHRYKF--NNSR^{Y149S}WMIAGKADPE--MPKTLYIHPDSPSTGEHWMS

Cons * . : * : : * * : : . * * * : : . : * * * * * * * *

ins S(TBX22) K164D/R(Ce-TBX2) G169R(TBX5) L214P(TBX22) R179TER(TBX19) S196TER(TBX5) E190TER(TBX5) G195A(TBX5)

OMB_ KVVSE^{ins S}FHKLKLTNNISDKHG^{K164D/R}FVSTTTILNSMHKYQPRFHLVRA--NDILKLP

TBX1_HUMAN QIVSE^{ins S}FDK^{K164D/R}LKLTNNLLDDNGHI--ILNSMHRYQPRFHVVYDPR--KDSEKYA

TBX2_HUMAN KPVA^{ins S}FHKLKLTNNISDKHGF^{K164D/R}T--ILNSMHKYQPRFHIVRA--NDILKLP

TBX3_HUMAN KVVTFHKLKLTNNISDKHGQT--ILNSMHKYQPRFHIVRA--DILKLP

TBX4_HUMAN QLVSE^{ins S}FQKLKLTNNHLD^{K164D/R}PFGHI--ILNSMHKYQPRLHIVKAD--E--NNAFGSK

TBX5_HUMAN QLVSE^{ins S}FQKLKLTNNHLD^{K164D/R}PFGHI--ILNSMHKYQPRLHIVKAD--E--NNGFGSK

TBX6_HUMAN QPVSFHRV^{ins S}KL^{K164D/R}TNSTLD^{K164D/R}PHGHL--ILHSMHKYQPRIHLVRAAQ--LCSQH

TBX19_HUMAN APISF^{ins S}SKV^{K164D/R}KL^{K164D/R}TNK--LNGGGQI--MLNSLHKYEPQVHIVRVGS--AHR--

TBX22_HUMAN QII^{ins S}SFDRM^{K164D/R}KL^{K164D/R}TNNEMDDK^{K164D/R}GHI--ILQSMHKYKPRVHVIEQGS^{G169R}SV^{L214P}DL^{L214P}SQIQSLP

BRA_MOUSE APVSE^{ins S}FSK^{K164D/R}V^{K164D/R}KL^{K164D/R}TNK--MNGGGQI--MLNSLHKYEPRIHIVRVGG--PQR--

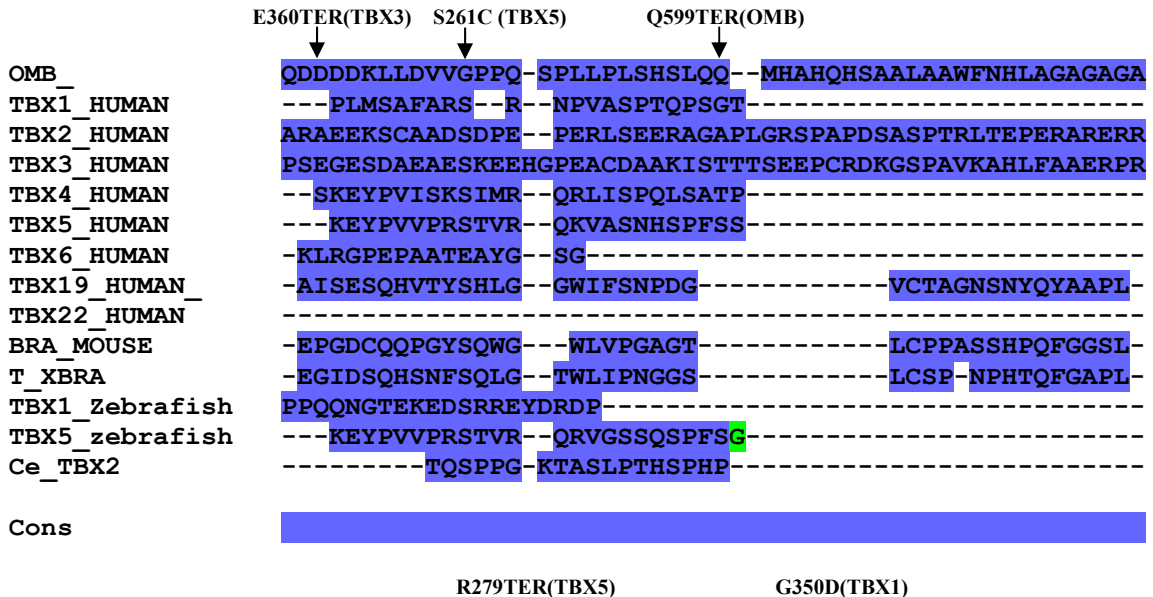
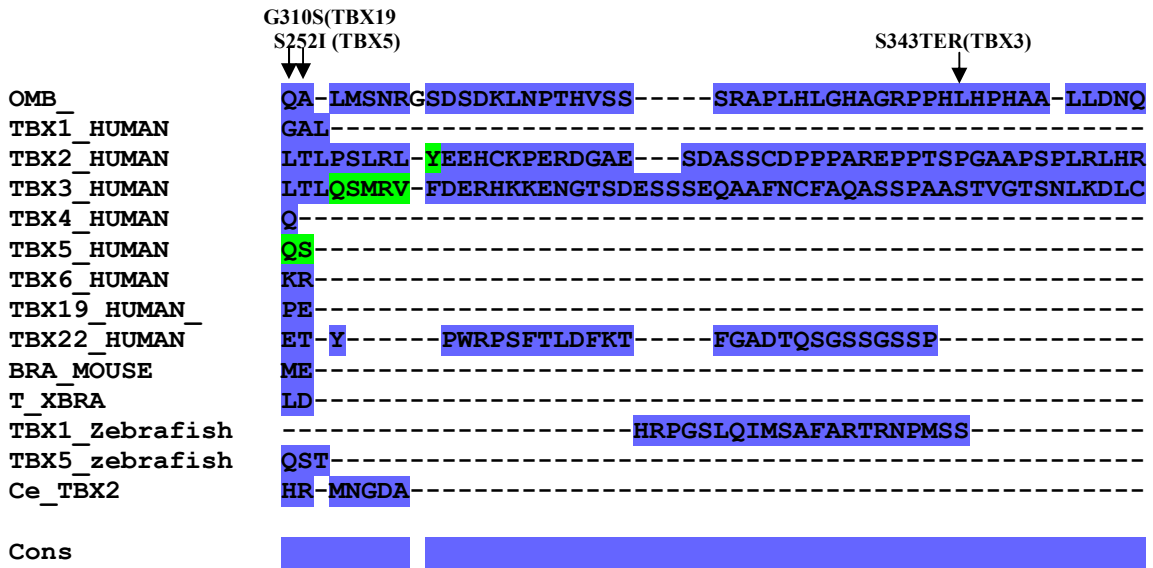
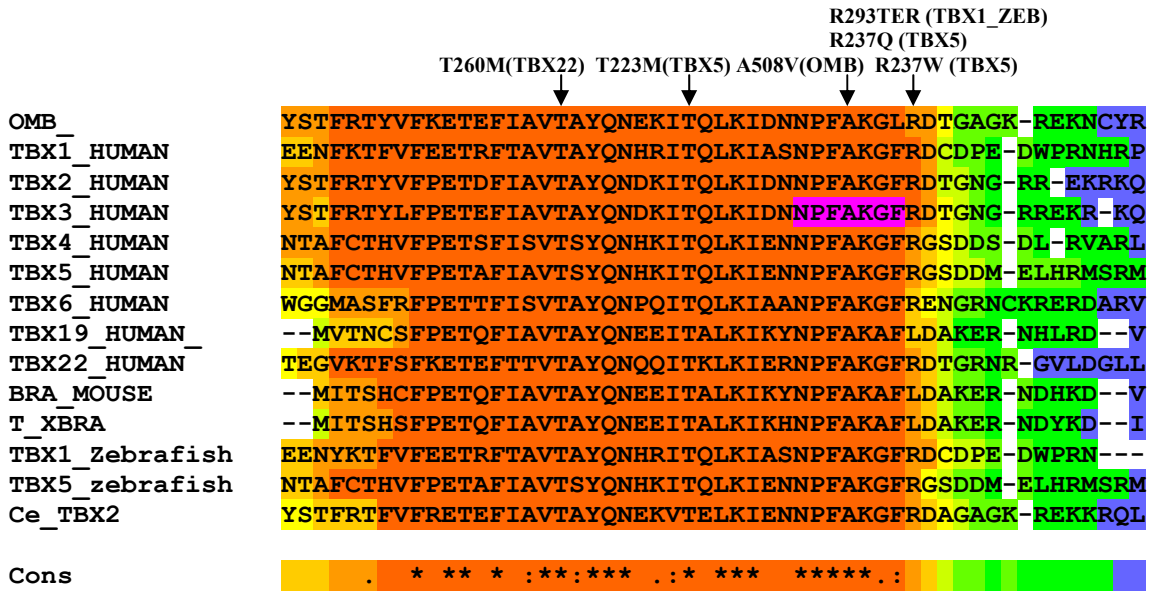
T_XBRA DPVSE^{ins S}FSK^{K164D/R}V^{K164D/R}KL^{K164D/R}TNK--MNGGGQI--MLNSLHKYEPRIHIVRVGG--TQR--

TBX1_Zebrafish QIVSE^{ins S}FDK^{K164D/R}LKLTNNLLDDNGHI--ILNSMHRYQPRFHVVYDPR--KDSEKYA

TBX5_zebrafish QLVSE^{ins S}FQKLKLTNNHLD^{K164D/R}PFGHI--ILNSMHKYQPRIHIVKAD--E--NNGFGSK

Ce_TB^{ins S}X2 KGANF^{ins S}HKLKLTNNISDKHGYT--ILNSMHKYQPRLHVRC--ADRHNL^{G195A}M

Cons * : : * * * * . : * : * : * : * : * : * : * : * : * : * : * : * :



```

                ↓                ↓
OMB_          SEHAAAAANASAEALRRRLQADADVERDGS DSSCSSESV-----GGSTG
TBX1_HUMAN   -----EKDA-----AEARREFQRDAG---GPAVLGD-----
TBX2_HUMAN   SPERGKEPAESGGDGPFLGRSLEKERA EARRKDEGRKEAAEGKEQ-----
TBX3_HUMAN   DSGRLDKAS PDSRHSPATISSSTRGLGAEERRSPVREGTAPAKVEEARALPGKE
TBX4_HUMAN   -----DVGP---LLGTHQALQHYQHENG AHSQLAEPQDL-----
TBX5_HUMAN   -----ESRA---LSTSSNLGSQYQCENGVSG---PSQDLLP-----
TBX6_HUMAN   -----DTPGGPCDSTLGGDI-----
TBX19_HUMAN  -----PLPAPHTHHGCEHYSGL-----
TBX22_HUMAN  -----VTSS-----GGA-----
BRA_MOUSE   -----SLPSTHGCERYPAL-----
T_XBRA      -----SLSSPHGCERYSSL-----
TBX1_Zebrafish -----
TBX5_zebrafish -----DVQG---LSATGAISSQYSCENS VSS---TSQDLLP-----
Ce_TBX2     -----SESN-----SEDDE-----

```

Cons

```

316TER(TBX5)  Q316TER(TBX5_ZEB)  R286TER(TBX19)  P396L(TBX1)
                ↓                ↓                ↓                ↓
OMB_          GAFRPTSTGSPKEA-VGAAAAA---AAGLNPGGGSYPSPNIS---VGPPIHPS
TBX1_HUMAN   PAHP---PQLLA---RVLSPSLPG-AGGAGGLVPLPGAPGGRPSPP-NPELRLE
TBX2_HUMAN   GLAPLVVQTDASAP-LGAGHLPGL--AFSSHLH---GQOFFGPLGAGQPLFLH
TBX3_HUMAN   AFAPLTVQTDAAAAHLAQQPLPGL--GFAPGLAG---QOFFNGHPLFLH
TBX4_HUMAN   PLSTFPTQRDSS---LFYHCLKRR--DGTRHLDLPCKRSYLEAPSSVGEDHYFR
TBX5_HUMAN   PPNPYPLPQEHS---QIYHCTKRK-EEECSTTDHPYK KPYMETS P S-EEDSFYR
TBX6_HUMAN   -----RESDPEQAPAP-GEATAA-PAPLCGG
TBX19_HUMAN  -----RGHRQAPYPSAYMHRNHS-PSVNLIE
TBX22_HUMAN  -----PSPLNS---LLSPLCFS
BRA_MOUSE   -----RNHRSSPYSPYAHNRNS-PT-YA-D
T_XBRA      -----RNHRSA PYSPYTHRNS- PNNLA-D
TBX1_Zebrafish -----SGNPLHSD
TBX5_zebrafish QSSSY---HEHT---QDYHCIKR KVEDECPAGEHPYK KPYVE SSSS-EDDHYYR
Ce_TBX2     PTLKKCKPEPSQTP-TTSSLSTS--TTPTLSAHHPLRSPQFC---IPPIDMM

```

Cons

```

OMB_          PHLLP-----YLYPHGLYPPPHLGLLHNPA AAAAMS PAGLNPGLLFNAQLAL
TBX1_HUMAN   -----A-PGASEPLH---HHPYKYPAAAYDHYLG-----
TBX2_HUMAN   PGQFTMGPGA-FSAM---GMGILLASVAGGGNGG-----
TBX3_HUMAN   PSQFAMG-----GAFSSMAA-----
TBX4_HUMAN   -----SPPPYD-QQML---SPSYCSEVTPREACMY-----
TBX5_HUMAN   -----S-SYPQQQGL---GASYRTESAQRQACMY-----
TBX6_HUMAN   PSAE-AYLLHPAAFHGAPSHLPTRSPSFPEAPD-----
TBX19_HUMAN  SSSN-NLQVFSGPDSWTSLSSTPHASILSVPH-----
TBX22_HUMAN  PMF-----HLPTSSLGMPCPEAYLPNVNLP L CYKICPTN---FWQQQPL
BRA_MOUSE   NSSA-CLSMLQSHDNWSSLGVPGH TSMLPVSHN-----
T_XBRA      NSSA-CLSMLQSHDNWSTLQMPAHTGMLPMSHS-----
TBX1_Zebrafish PTHQLMS-----RVLSPAL-----
TBX5_zebrafish -----PLSYSQSLGLSGGAPYRPESSQRQACMY-----
Ce_TBX2     YQNMPMDLL--AHWQMATLFPQFSMA-LNSPAAAASLLSK-----

```

Cons

```

OMB_          AAQHPALFGHAYAAAGHTPVSP LQGLKSHRFS P YSLPGSLGSAF DAVTPGSNAN
TBX1_HUMAN   AKS-RPAPYPLPGLRG-----H
TBX2_HUMAN   GGG-PGTAAGLDAGGLG---AASAASTAAPFPFHL-----SQH---M
TBX3_HUMAN   AGM-GPLLATVSGAST-GVSGLDSTAMASAAAQGLSGASAATLPFHLOQH---V

```

```

TBX4_HUMAN      SGS-GPEIAGVSGVDDLPPPPLSCNMWTSVSPYTSYS-----VQT--M
TBX5_HUMAN      ASS-APPSEFVPSLEDI-----SCNTWPSMPSYSSCTVTT-----VQP--M
TBX6_HUMAN      SGR-SAPYS--AAFLDV-----PHGSGGS-----GYP--A
TBX19_HUMAN     NGPINPGSPYPCLWTI-----SNGAGGP-----SGP--G
TBX22_HUMAN     VLPAPERLASSNSSQSLAPLMMEVPMSSLGVTNSKSGSSEDSSDQYLQAPNST
BRA_MOUSE      ASP-PTGSSQYPSLWSV-----SNGTITP-----GSQ--T
T_XBRA         TGT-PPPSSQYPSLWSV-----SNSAITP-----VSQ--S
TBX1_Zebrafish -----PVLGGI-----HAVPLTAGPRSPHELRLD--G
TBX5_zebrafish ASA-PQPPEPVPSLEDI-----S--WPGVPPYS-----VPQ--M
Ce_TBX2       -----

```

Cons

```

OMB_           RS---GDPPGGGGGLGGGVVENGPRSLSSSPRR-----
TBX1_HUMAN     GYHPHAHPHHH-----HHPVS--PAAAAAAAAAAAA
TBX2_HUMAN     LASQGIPTFTGGFLFY---PYTYMAAAAAAASALPATSAAAAAAAAAGSLRS
TBX3_HUMAN     LASQGLAMSPFGSLFY---PYTYMAAAAAAASS-----AASSSVHRH
TBX4_HUMAN     ETVPYQFPPTH-----FTATTMPRLPTLSAQSSQP
TBX5_HUMAN     DRLPYQHFAH-----FTSGPLVPRLAGMANHGSPQ
TBX6_HUMAN     APPAVPFAPHFLOGGPF-----PLPYTAPGGYLDVGSKP
TBX19_HUMAN    PEVHASTPGAFLLGNPA---VTSPPSVLSTQAPT--SAGVE-----
TBX22_HUMAN    NQMLYGLQSPGNIFLNSIT---PEALSCSFHPSYDFY-----
BRA_MOUSE      AGVSNGLGAQFFRGSFA---HYTPLTHTVSAATSSSSGSP
T_XBRA        GGITNGISSQYLLGSTP---HYSSLHAVP---SPSTGSP
TBX1_Zebrafish HPQPPDTLHHHPYKYPA---TYEHYLGAKTRPS-----PYPSPSIRGH
TBX5_zebrafish ERLPYQHHSFA-----HFASRQMPEAHGMYASSVSH
Ce_TBX2       -----

```

Cons

```

OMB_           -----PASHSPTRPIISMSP'TT PPSLMKQPRGGGAGVAQ---SQHS
TBX1_HUMAN     A-----AANMYSSA-----
TBX2_HUMAN     PFLG--SARPRLRFSPYQIPVTI---PPSTSLLT'TGLASEGSKAA--GGNSREP
TBX3_HUMAN     PFLNLNLTMRPRLRYSPYSIPVPV---PDGSSLLT'TALPSMAAAG--PLDGKVA
TBX4_HUMAN     P-----GNAHFSVY-----NQLS--QSQVRER
TBX5_HUMAN     L-----GEGMFQHQ-----TSVAHQPVVRQC
TBX6_HUMAN     -----
TBX19_HUMAN    -----
TBX22_HUMAN    -----RYNFS--MPSRL--ISGSNHLKVNDSDQVSFGE--GKCN
BRA_MOUSE      -----
T_XBRA        -----
TBX1_Zebrafish GYHPHMNP'TTANMYSATSAPTNY---DYGPR-----
TBX5_zebrafish Q-----CSPSGGIQ-----SPSA-----
Ce_TBX2       -----

```

Cons

```

OMB_           PSELKSMEKMVNGLEVQHNGSAAAAAAAAALQLAEFAAQHHHHTQAHHQQQHQSH
TBX1_HUMAN     -----G--AAPP-----G
TBX2_HUMAN     SPLPELAL-----RKVGAPSRG--ALSPSGSAKE--AA-----N
TBX3_HUMAN     ALAASPASVAVDSGSELNSRSSTLSSSSMSLSPKLCAEKEAAT-----S
TBX4_HUMAN     GPSASFP-----RERGLPQGC--ERKPPSPHLN--AA-----N
TBX5_HUMAN     GP-----QTGLQSPG--TLQP-----P
TBX6_HUMAN     -----
TBX19_HUMAN    -----
TBX22_HUMAN    HVHWYPA-----
BRA_MOUSE      -----

```

```

T_XBRA -----
TBX1_Zebrafish -----
TBX5_zebrafish -----GLQG-----N
Ce_TBX2 -----HLAKASSECKVEATSEDEEAEKPEVKKEQKSVTPPKKG

Cons -----

OMB -----
TBX1_HUMAN -----
TBX2_HUMAN -----
TBX3_HUMAN -----
TBX4_HUMAN -----
TBX5_HUMAN -----
TBX6_HUMAN -----
TBX19_HUMAN -----
TBX22_HUMAN -----
BRA_MOUSE -----
T_XBRA -----
TBX1_Zebrafish -----
TBX5_zebrafish -----
Ce_TBX2 -----

Cons -----

```


Appendix 10: Sequence of *omb* cDNA along with the translated sequence of protein. Exons are shown in alternate blue and red colour. Portion of amino acid sequence shown in green have homology with the T domain

1 AGTTAGTAAACGTCGACACTTCATATGAAACGAAGAGCGGAGATCACAGCGGAAAATCCAGG
 63 GGTCAATGAAACATGAATTTTTTTGAAACAACAAGAAGAGAAATAAAGTGTACAAGTCAG
 123 TGAGTGTCCCAAACAAAAGTTTTTAAAAAAAAGAAAACAAAACAAGTACCTGTAGAACA
 183 AAAACAAAATAAAGCATCTAAAAATTTCAAAAGTCAAAC TAGAGAGATCCCTTTTTTTGGA
 243 GAGATCGCCGTGGGAAACCCTTTCTGCATGACGCAC TTGGTTGTTTGAACGGTTATGTG

1 MetArgTyrAspValGlnGluLeuLeuLeuHisGlnSerAlaGluAspPropheAlaArg
 303 ATGAGATACGACGTCCAGGAGCTGCTACTTCATCAGTCTGCTGAGGATCCATTCGCCAGG

21 PheAlaAsnGlyMetAlaTyrHisProPheLeuGlnLeuThrGlnArgProThrAspPhe
 363 TTCGCCAATGGGATGGCATATCATCCATTTCTGCAGCTAACGCAACGACCCACTGACTTC

41 SerValSerSerLeuLeuThrAlaGlySerAsnAsnAsnAsnSerGlyAsnThrAsnSer
 423 AGCGTTTCCTCGCTGTTGACGGCGGGTAGCAACAATAACAACAGCGGCAACACCAACAGC

61 GlyAsnAsnAsnSerAsnSerAsnAsnAsnThrAsnSerAsnThrAsnAsnThrAsnAsn
 483 GGAAACAACAAC TCCAAT TCCAACAACAACACCAAT TCAAACACCAATAACACCAACAAT

81 LeuValAlaValSerProThrGlyGlyGlyAlaGlnLeuSerProGlnSerAsnHisSer
 543 CTCGTGGCCGTTTCACCAACGGGTGGTGGTGCAGTTATCGCCGCAAAGCAACCACAGC

101 SerSerAsnThrThrThrThrSerAsnThrAsnAsnSerSerSerAsnAsnAsnAsnAsn
 603 AGCAGCAACACCACCACCACCAGCAACACCAACAAC TCCAGTTCCAATAACAACAATAAT

121 AsnSerThrHisAsnAsnAsnAsnAsnHisThrAsnAsnAsnAsnAsnAsnAsnAsnAsn
 663 AACAGTACCATAATAATAACAACAACCACACGAATAACAACAACAATAATAATAATAAC

141 ThrSerGlnLysGlnGlyHisHisLeuSerThrThrGluGluProProSerProAlaGly
 723 ACAAGTCAAAGCAAGGACACCAC TTGAGCACCACCGAGGAACCGCCATCGCCCGCTGGC

161 ThrProProProThrIleValGlyLeuProProIleProProProAsnAsnAsnSerSer
 783 ACACCACCGCCCACAAT TGT TGGTCTACCGCCAATACCACCGCCCAACAACAACAGCAGT

181 SerSerSerSerAsnAsnSerAlaSerAlaAlaAlaHisProSerHisHisProThrAla
 843 AGCAGCAGCAGCAACAAC TCACTCAGCCGCGCCATCCGTGCGACCACCCAACCGCC

201 AlaHisHisSerProSerThrGlyAlaAlaAlaProProAlaGlyProThrGlyLeuPro
 903 GCACATCACTCACCAGTACGGGTGCCGCCGACCGCCCGCGGCCCCACAGGC TTGCCG

221 ProProThrProProHisHisLeuGlnGlnGlnGlnGlnGlnGlnGlnHisProAlaPro
 963 CCACCACACCGCCGACCACCTGCAACAACAACAGCAGCAACAACAGCACC CGGCCCA

241 ProProProProTyrPheProAlaAlaAlaLeuAlaAlaLeuAlaGlySerProAlaGly
 1023 CCACCACACCGTACTTTCCAGTGC GGCAC TGGCCGCTCTAGCTGGAAGTCCGGCCGGA

261 ProHisProGlyLeuTyrProGlyGlyGlyLeuArgPheProProHisHisProGlyAla
 1083 CCGCATCCGGGTCTGTATCCGGCGGTGGATTGCGCTTCCCGCCGACCAACCAGGTGCC

281 HisProHisAlaHisHisLeuGlySerAlaTyrThrThrAlaGluAspValValLeuAla
 1143 CATCCGACGCCCATCATCTGGGCAGCGCCTATACTACCGCCGAGGACGTCGTCTTGCC

301 SerAlaValAlaHisGlnLeuHisProAlaMetArgProLeuArgAlaLeuGlnProGlu
 1203 TCGCCGTCGCCATCAGCTGCATCCGGCGATGCGACCGCTGCGGGCGCTTCAGCCCGAG

321 AspAspGlyValValAspAspProLysValThrLeuGluGlyLysAspLeuTrpGluLys
1263 GACGATGGCGTCGTCGATGATCCCAAGGTCACGCTGGAGGGCAAGGACCTGTGGGAGAAG

341 PheHisLysLeuGlyThrGluMetValIleThrLysSerGlyArgGlnMetPheProGln
1323 TTCCACAAACTGGGCACGGAAATGGTCAATCACCAGAGCGGCAGACAAATGTTTCCGCAA

361 MetLysPheArgValSerGlyLeuAspAlaLysAlaLysTyrIleLeuLeuLeuAspIle
1383 ATGAAATTTTCGTGTTTCGGGACTGGATGCCAAGGCTAAATACATCTTGCTACTGGACATT

381 ValAlaAlaAspAspTyrArgTyrLysPheHisAsnSerArgTrpMetValAlaGlyLys
1443 GTGGCGCGGACGATTATCGTTATAAAATTTTCATAATAGTCGCTGGATGGTGGCTGGCAA

401 AlaAspProGluMetProLysArgMetTyrIleHisProAspSerProThrThrGlyGlu
1503 GCGGATCCCGAGATGCCAAAACGCATGTATATCCATCCAGATTCGCCACAACGGGTGAG

421 GlnTrpMetGlnLysValValSerPheHisLysLeuLysLeuThrAsnAsnIleSerAsp
1563 CAATGGATGCAGAAAGTTGTTTCATTTCCACAAATTAATAATGACCAACAATATTAGTGAT

441 LysHisGlyPheValSerThrThrIleLeuAsnSerMetHisLysTyrGlnProArgPhe
1623 AAACATGGATTTGTAAGTACTACGATCCTGAACTCGATGCACAAGTACCAGCCGCGTTC

461 HisLeuValArgAlaAsnAspIleLeuLysLeuProTyrSerThrPheArgThrTyrVal
1683 CACCTGGTGCAGCCAATGACATCCTGAAGCTGCCGTACTCCACGTTTCGCACGTACGTC

481 PheLysGluThrGluPheIleAlaValThrAlaTyrGlnAsnGluLysIleThrGlnLeu
1743 TTCAAGGAGACCGAGTTTCATCGCCGTCACAGCATATCAAATGAGAAGATAACTCAATTG

501 LysIleAspAsnAsnProPheAlaLysGlyLeuArgAspThrGlyAlaGlyLysArgGlu
1803 AAAATCGATAACAATCCGTTTGGCAAGGGCTTGCGTGATAC'TGGTGCCGGAAGCGGGAA

521 LysAsnCysTyrArgGlnAlaLeuMetSerAsnArgGlySerAspSerAspLysLeuAsn
1863 AAGAA'TTGT'TACAGGCAGGCAC'TGATGT'CGA'ACCGAGGGTCCGATTCGGACAAGTTGAAT

541 ProThrHisValSerSerSerArgAlaProLeuHisLeuGlyHisAlaGlyArgProPro
1923 CCGACGCATGTGAGCAGCTCGCGGGCACCGCTCCACCTGGGCCACGCCGGCCGTCCGCT

561 HisLeuHisProHisAlaAlaLeuLeuAspAsnGlnGlnAspAspAspLysLeuLeu
1983 CATCTGCATCCCCATGCCGCCCTGCTTGATAATCAGCAGGACGACGACGACAAGCTCCTG

581 AspValValGlyProProGlnSerProLeuLeuProLeuSerHisSerLeuGlnGlnMet
2043 GACGTGGTGGGTCCGCCACAGAGTCCGCTACTCCGCTCAGCCACTCGTGCAGCAGATG

601 HisAlaHisGlnHisSerAlaAlaLeuAlaAlaTrpPheAsnHisLeuAlaGlyAlaGly
2103 CACGCCACCAGCACTCCG'CAGCTCTGGCTGCCTGGT'TTAATCACT'TGGCTGGCGCTGGA

621 AlaGlyAlaSerGluHisAlaAlaAlaAlaAlaAlaAsnAlaSerAlaGluAspAlaLeu
2163 GCCGGAGCCTCCGAACATGCAGCTGCGGGCGGCGCCAATGCCAGTGC GGAGGATGCAC'TG

641 ArgArgArgLeuGlnAlaAspAlaAspValGluArgAspGlySerAspSerSerCysSer
2223 CGTCGTCGCTTGCAGGCGGACGCGGATGTGGAGCGGGATGGCAGCGATTCGAGTTGCTCG

661 GluSerValGlyGlySerThrGlyGlyAlaPheArgProThrSerThrGlySerProLys
2283 GAAAGCGTCGGCGGCAGTACCGGCGGTGCC'TTAGGCCACCTCGACGGGCAGTCCCAAG

681 GluAlaValGlyAlaAlaAlaAlaAlaAlaAlaAlaGlyLeuAsnProGlyGlyGlySer
2343 GAGGCGGTGGGCGCGGCTGCAGCTGCCGCAGCGGCTGGCTTGAATCCCGTGGCGGTAGC

701 TyrProSerProAsnIleSerValGlyProProIleHisProSerProHisLeuLeuPro
2403 TATCCGTCACCGAATATATCGGTGGGTCCGCCATTCACCCGTCGCCGCA'TTGTGTCCT

721 TyrLeuTyrProHisGlyLeuTyrProProProHisLeuGlyLeuLeuHisAsnProAla
2463 TACCTGTATCCACATGGCCTGTATCCACCGCCGCATCTGGGCTGCTGCACAATCCCCT

741 AlaAlaAlaAlaMetSerProAlaGlyLeuAsnProGlyLeuLeuPheAsnAlaGlnLeu
2523 GCAGCGGCGGCCATGAGTCCGGCTGGCTGAATCCGGTCTGCTCTTCAATGCCAACCTG

761 AlaLeuAlaAlaGlnHisProAlaLeuPheGlyHisAlaTyrAlaAlaAlaGlyHisThr
2583 GCGCTGGCCGCCAGCATCCGGCTTTGTTTGGCCACGCCCTACGCGGCGGCGGGTCACACA

781 ProValSerProLeuGlnGlyLeuLysSerHisArgPheSerProTyrSerLeuProGly
2643 CCGGTATCACCATTACAAGGCTGAAGAGCCATCGCTTTTCGCCGTACAGTTTGGCCGGC

801 SerLeuGlySerAlaPheAspAlaValThrProGlySerAsnAlaAsnArgSerGlyAsp
2703 AGTTTGGGCTCCGCCTTCGATGCAGTGACTCCTGGATCGAACGCAAATCGCTCGGGAGAT

821 ProProGlyGlyGlyGlyGlyLeuGlyGlyGlyValValGluAsnGlyProArgSerLeu
2763 CCTCAGGCGGCGGCGGCGGCTGGGTGGTGGTGTGTGGAGAATGGTCCCAGGAGTCTG

841 SerSerSerProArgProArgProAlaSerHisSerProProThrArgProIleSerMet
2823 AGTTCAGCCCTCGACCCCGACCTGCCCTCCACTCGCCGCCACTCGACCGATTTTCGATG

861 SerProThrThrProProSerLeuMetLysGlnProArgGlyGlyGlyAlaGlyAlaGly
2883 TCACCCACAACGCCGCCATCCCTGATGAAGCAACCACGTGGCGGTGGTGTGGCGCCGGT

881 ValAlaGlnSerGlnHisSerProSerGluLeuLysSerMetGluLysMetValAsnGly
2943 GTGGCCCAATCGCAGCACTCGCCTTCGGAACCTAAGAGCATGGAGAAGATGGTCAACGGA

901 LeuGluValGlnHisAsnGlySerAlaAlaAlaAlaAlaAlaAlaLeuGlnLeuAlaGlu
3003 CTGGAGGTTCAACACAATGGCAGTGGCGGCGCAGCAGCGGCGGCTCTTCAGCTGGCCGAG

921 GluAlaAlaGlnHisHisHisHisThrGlnAlaHisHisGlnGlnGlnGlnHisGlnSer
3063 GAAGCTGCCCAGCATCATCATCACACCCAGGCGCACACCAGCAGCAGCAGCATCAGTCG

941 HisHisGlnGlnGlnHisHisGlnGlnProAlaGlnProHisProHisHisGlnThrHis
3123 CACCACCAGCAACAGCACCACCAGCAACCGGCACAACCACATCCGCACCACCAGACCCAT

961 LeuHisSerHisHisGlyAlaThrThrGlyGlyThrAspGlnEND
3183 CTACACTCGCACCATGGGGCGACAACGGGCGGTACGGATCAGTGACAATTACTGGACGGC

3243 CGCTCCGATTGTGAGGATGCCGGTCTCGAATTGGAAC TAGAGTTGGAGGAGGATGTTCGAG
3303 GATCTGGATCAGGATCCGGATGAGCAGGACGAGGATCGCAGCTCGGTTCATCGATCTTGAT
3363 CTGGACGTCGACGCTTGACCCGGAACGGATCAGCGACATTCCTCTAGCCTCTGAAC TAC
3423 ACGGCCACCGTCTTTGTGGTTTAGCGTAGTGTATATGTACATATATATATCGGACGATTT
3483 GGACCC TAGACTATAGGCATTTGTAGCATATAGTGTGTATTCCTCTCTCGTTGCCG AAC
3543 TCACTCTGCCGTTTATCGCCAGTGTAAAGTAACATCTTTTTTTTTTTTTTTGTCTCGTTTCT
3603 AAGCAAAGCCTAGCCCTAGAAATCGCTGGCGATTTCGCTGGCAAAGTGATGGAGAGGTCT
3663 AATTGAAGACAGAAGGTAGCAAAAACAGAAGAAAAAAAAAAAAAAAAAATAACAAAAAAGGAA
3723 ACAAAAAACAGGAAAAAGTTAAGGGGACGTGGCAAGAGAAATCGTCGTAAC TTTTAGCGCC
3783 TTGAAGGTTCCAGACTTCAAGATCTTTTCAGACGGAAATAAAAATGAGAAGTAAGGGCAAG
3843 GGGCTATCCTCAGACAAAATTTATGTATCACCCATATATGTATATTTGATTTGGATTGAAAAT
3903 AGCAACATCAAAGATGGCGCCTCTTTATATACATCTAGAACACGCATATATATATATAAA
3963 TATATATATATATAGTATATATAGAAAGCTGGTATATATACAGAATGTAACCTTAGTAAAA
4023 CATAACAAGAAAAACAAAGAAAAACAAAACCCATAAAAAAAAAAAAAA

Erklärung

Versicherung gemäß Paragraph 11, Absatz 3d, der Promotionsordnung

- a. Ich habe die jetzt als Dissertation vorgelegte Arbeit selbst angefertigt und alle benutzten Hilfsmittel (Literatur, Geräte, Materialien) in der Arbeit angegeben.
- b. Die vorliegende Arbeit wurde nicht als Prüfungsarbeit für eine staatliche oder andere wissenschaftliche Prüfung eingereicht.
- c. Ich habe werde die jetzt als Dissertation vorliegende Arbeit, noch Teile einer Abhandlung davon, bei einer anderen Fakultät bzw. einem anderen Fachbereich als Dissertation eingereicht.

Mainz, den 09 Januar 2006

Aditya Sen